THE UNIVERSITY OF THE WEST INDIES

MASc. (Engineering)

Department of Electrical and Computer Engineering

ECNG 6021 – MASc Project

Analysis of the Impact of Uncoordinated Level 1&2 Electric Vehicle Charging to the San Juan 12kV Distribution Network

Progress Report

Andrew Balgobin
807002832

May 17th, 2019

Project Supervisor: Dr. Sanjay Bahadoorsingh

STATEMENT OF ACADEMIC HONESTY

For the purpose of this declaration form the following Faculty Regulations apply:

Rule 32 , *The Faculty of Engineering: Undergraduate Regulations 2008-2009,* states*:*

“ Cheating, Plagiarism and Collusion are serious offences under University Regulations.

a) Cheating is any attempt to benefit one's self or another by deceit or fraud.

b) Plagiarism is the unauthorised and/or unacknowledged use of another person's intellectual efforts and creations howsoever recorded, including whether formally published or in manuscript or in typescript or other printed or electronically presented form and includes taking passages, ideas or structures from another work or author without proper and unequivocal attribution of such source(s), using the conventions for attributions or citing used in this University. Plagiarism is a form of cheating.

c) For the purposes of these Regulations, ‘collusion’ shall mean the unauthorized or unlawful collaboration or agreement between two or more students in the preparation, writing or production of a course assignment for examination and assessment, to the extent that they have produced the same or substantially the same paper, project report, as the case may be, as if it were their separate and individual efforts, in circumstances where they knew or had reason to know that the assignment or a part thereof was not intended to be a group project, but was rather to be the product of each student’s individual efforts. Where two or more students have produced the same or substantially the same assignment for examination and assessment in circumstances that the assignment was to be the product of each student’s individual efforts, they shall receive a failing grade in the course. ”

I…………………………………………………..(insert name in BLOCK LETTERS), …………………………(student identification number) declare that the material submitted for assessment in my MASc final project report is my own work and does not involve plagiarism and collusion.

…………………………………………… …………………………………..

Student’s Signature with Date

TABLE OF CONTENTS

LIST OF FIGURES

LIST OF TABLES

INTRODUCTION

From the early years of the automotive industry, the evolution of electric vehicle (EV) technology has been outpaced by internal combustion engine (ICE) technology. The latter, being able to solve their problems faster, dominated the market and became the leading technology until the present times. At the turn of the 21st century, due to technical advancements, environmental concerns, and the foreseeable shortage and increased prices of fossil fuels, the EV industry is starting to emerge.

The electrification of the transportation sector is regarded as the most viable solution for greater vehicle efficiency and lower emissions of greenhouse gases (GHGs) and other air pollutants. ‘Electromobility’ comes with environmental, energy security and even electric system stability benefits.

The most commonly cited advantage of the adoption of EVs is the absence of tailpipe emissions. Due to the global warming problematic, governments support this change as a means of decarbonizing the economy. A report from the EPA in 2010 puts worldwide GHG emissions from transportation energy use at 14 percent of the total. Therefore, EVs have the potential to impact these GHGs emissions significantly. It is important to note that electromobility only represents a shift in air emissions upstream the transportation sector to the electricity generation one. Therefore, this transition can only be well succeeded by the simultaneous and proportional increase of low or non-carbon emitting power generation technologies, ideally from renewable energy sources (RES). There is also the issue of emission attributable to the manufacture of EV batteries. Regardless, particularly for dense urban areas, EVs can significantly improve the air quality.

EVs also have a significant potential to reduce a country's dependence on oil by shifting transportation energy from oil based fuel to electricity thereby saving money on the importation of a diminishing and finite resource.

In addition to the environmental and energy security benefits, EVs are capable of providing electricity grid support services. This support can be generally defined as capacity, energy and ancillary services made possible by the vehicle to grid (V2G) concept, where grid connected EVs can absorb and store electricity as well as inject it in the grid. By serving as a capacity and energy storage device, EVs can help balance the electric system thereby performing load smoothing on the system demand which serves to improve voltage levels and reduce congestions in lines and transformers. As a storage device, EVs can also compensate for the intermittent nature of RES generation to prevent curtailment which makes its large scale integration on the grid more economically feasible (Garcia-Valle and Lopes 2012, 3-5). As it is a faster ramping resource, it is better suited to provide ancillary services to alleviate short term voltage and frequency fluctuations. Although discussed widely, this concept is not yet realized on a large scale due to the complex controls and communications architecture required.

From the vehicle owner's perspective, although EVs are not yet capable of perfectly replacing conventional gasoline and diesel powered vehicles in terms of range and cost, they are inherently more efficient, hence reducing transportation costs, and can be conveniently refueled at home. EV policies can also be focused to offset these high costs and usability limitations through rebates, tax incentives etc. The usability of EVs depend heavily on how and when they are charged. The charge time and convenience, as well as electricity costs all contribute to its attractiveness to customers.

In what regards the electricity grid's operation and management, the integration of EVs at a particular penetration level would provoke some considerable impacts. If considered as a static, uncontrollable load, it would represent a significant additional power demand on the network which will inevitably lead to voltage drops and phase imbalances predominantly in radial distribution feeders, congestion problems lines and transformer leading to degradation, increased peak load demand, energy losses and harmonic distortion. To accommodate EV integration while preventing these violations, the utility can either, reinforce and modify their existing infrastructure to cater for this additional load or, employ charge management strategies capable of controlling the charging of EVs to satisfy the grid's limitations as well as the owner's requirements. This can be done through the use of EV policies, as well as technically, where EV charging can be controlled where the batteries are considered as variable, dispersed energy storage devices instead of static loads. Prerequisite to either these approaches, studies must first be done on the particular existing grid to assess the penetration level it can support without exhibiting any violations.

This study investigates and analyses the effects of the integration of EVs on select low voltage (LV) distribution networks in Trinidad and Tobago to accurately assess the penetration level these networks can safely and reliably support. It also serves to offer recommendations to alleviate any problems that are realised from said analyses.

The objectives of this study are as follows:

1. Perform a literature review on Electric Vehicles (EVs) and electric vehicle charging and infrastructure which includes suitable standards, best practices, latest developments, battery management systems (BMS) and emerging trends

2. Perform a technical power flow assessment of the T&TEC 12kV network utilizing the Newton-Raphson method.

3. Perform a data analysis and comparison on NREL Household EV profiles and T&TEC 12kV feeder data utilizing MATLAB

4. Perform a data mapping with the NREL Household EV Profiles and the T&TEC 12kV feeder data that include constraints and timings.

5. Perform basic transient and steady state analysis with EMTP-RV utilizing basic RLC networks alongside the exportation of data for use in MATLAB.

6. Build and perform a steady state and transient analysis of the T&TEC 12kV network in EMTP RV.

7. Build and test suitable models for EV batteries and chargers (L1/L2) in EMTP-RV.

8. Combine the network 12kV grid and the EV battery and charger in EMTP-RV along with the data mapping for a single phase and three phase analysis of the impact of uncoordinated charging on the 12kV network.

9. Discuss the impacts of this on future EV penetration, growth and steps to alleviate any problems.

LITERATURE REVIEW

The literature survey on EVs naturally focuses on those components and systems that are directly related to and interact with the electrical grid, i.e. when charging. From the grid's perspective, a plug-in EV is simply a load which can be connected at any point, independent of the vehicle's architecture. A plug-in EV can be generally defined as any vehicle fully or partially powered by an electric motor which, in turn, is powered by an onboard battery capable of being charged via the electricity grid. These comprise battery electric vehicles (BEVs), which depend on onboard batteries as their sole energy source, and plug-in hybrid electric vehicles (PHEVs), which utilize both batteries and liquid fuels as their energy sources. This study only considers light-duty passenger BEVs, which is predicted to be the majority of electric vehicles that will initially be adopted in Trinidad and Tobago and hence connected to its grid.

The BEV comprises of three subsystems; the energy propulsion, energy source and auxiliary subsystems.

The BEV system can be divided into three (3) subsystems as listed below (Un-Noor 2017, 9-10).

1. Electric Propulsion Subsystem (EPS) - this includes the controller, electric motor power converter; transmission system, and wheels.
2. Energy Source Subsystem (ESS) - this includes the source, its power supply unit and energy management unit.
3. Auxiliary Subsystem (AS) - this includes but is not limited to an auxiliary power supply, temperature control unit and power steering unit.

Figure 1 shows an overview of the aforementioned BEV subsystems and their interconnections.

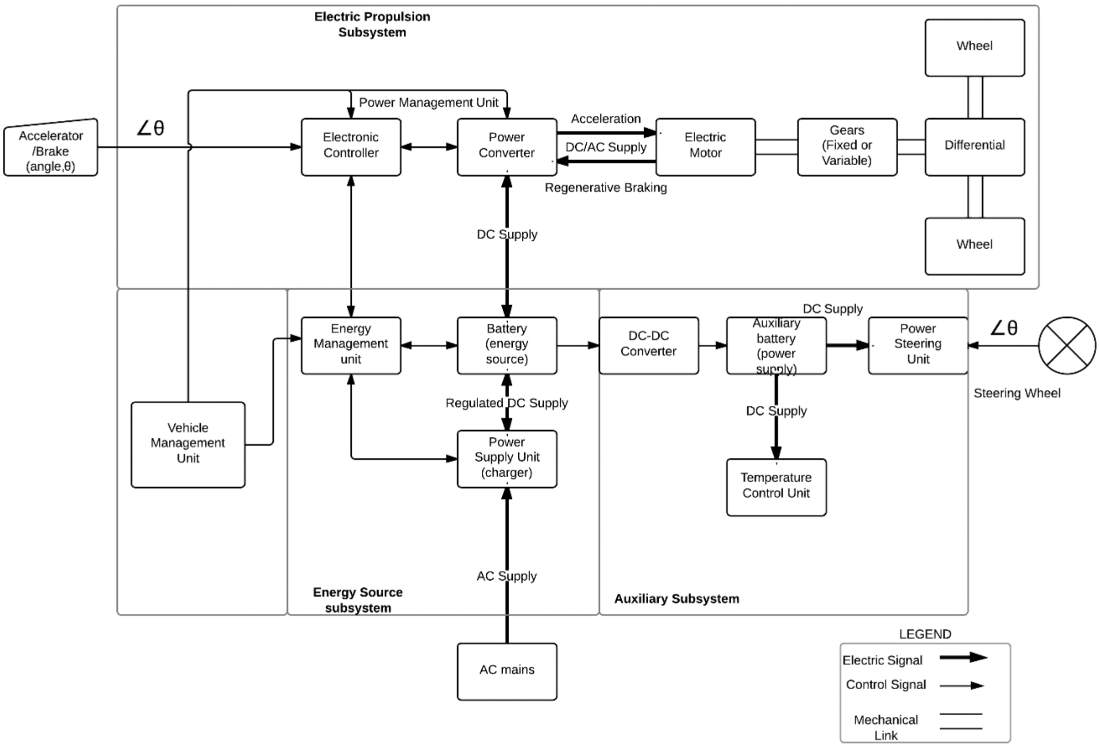

FIGURE 1: OVERVIEW OF BEV SUBSYSTEMS

For vehicle-grid interaction, the component of interest of the BEVs is evidently the battery pack where the energy is stored (or supplied). The power supply unit and battery management unit are responsible for safe and efficient grid coupling and charge control of the battery. Therefore, the ESS is the only subsystem of the three that is considered for grid integration studies. The battery, power supply unit (charger) and applicable functions of the battery (energy) management unit must be modelled to accurately simulate the effects BEVs has on the grid when connected and charging. Each of these subcomponents will be reviewed individually in detail, addressing suitable standards, best practices, latest developments and emerging trends. Following this, past integration studies and EV related studies in small islands grids will be surveyed to examine the component modelling and load determination techniques taken and outcomes of their analyses based on these choices.

The complete review will then serve to inform on the choices of models and load determination for the current case study in the software of choice to obtain the most accurate results for analysis purposes.

BATTERY

BATTERY TECHNOLOGIES

Several different types of battery technologies exist on the current market. These include conventional batteries such as lead acid, nickel cadmium (Ni-Cd) and nickel metal hydride (Ni-MH) as well as the latest and advanced lithium ion (Li-ion) battery types. Table 1 summarizes the performance comparison for all battery types using the typical key performance indicators.

TABLE 1: PERFORMANCE COMPARISON OF POPULAR BATTERY TYPES

Battery Type	Lead Acid (Spanos et al. 2015, 78-94)	Ni-Cd (Garcia-Plaza 2015, 595-604)	Ni-MH (Zhu et al. 2016, 6-9)	Zn-Br Lai et al. 2013, 1-4)	Fe-Cr (Fotouhi et al. 2016, 8-21)	Li-ion (Lu et al. 2013, 272-288)
Energy Density (Wh/kg)	30-50	45-80	60-120	35-54	20-35	110-160
Power Density (W/kg)	180	150	250-1000	-	70-100	1800
Nominal Voltage (V)	2	1.25	1.25	1.67	1.18	3.6
Operating Temperature (°C)	-20-60	-40-60	-20-60	-20-60	-40-60	-20-60
Cycle Life	200-300	1500	300-500	>2000	-	500-1000
Charge Efficiency%	79	-	-	-	-	100
Energy Efficiency%	70	60-90	75	80	66	80
Voltage Efficiency	-	-	-	-	82	-
Overcharge Tolerance	High	Moderate	Low	High	Moderate	Very low
Self-Discharge	Low	Moderate	High	Low	High	Very low
Thermal Stability	Very unstable	Very unstable	Very unstable	Very unstable	Stable	Very stable

From this extensive review it is clear that Li-ion batteries are superior as it regards power and energy density making them smaller in size and weight compared to different types of comparable capacities. Additionally, Li-ion batteries provide a greater cell voltage and charge efficiency along with a comparable temperature range of operation and long cycle life. Complete with a low self-discharge rate and high thermal stability, it is widely used in consumer electronic products (Grosjean et al. 2012, 35). Fig. 2 shows the significant differences in battery technologies according to size and weight (Xiong et al. 2017, 370).

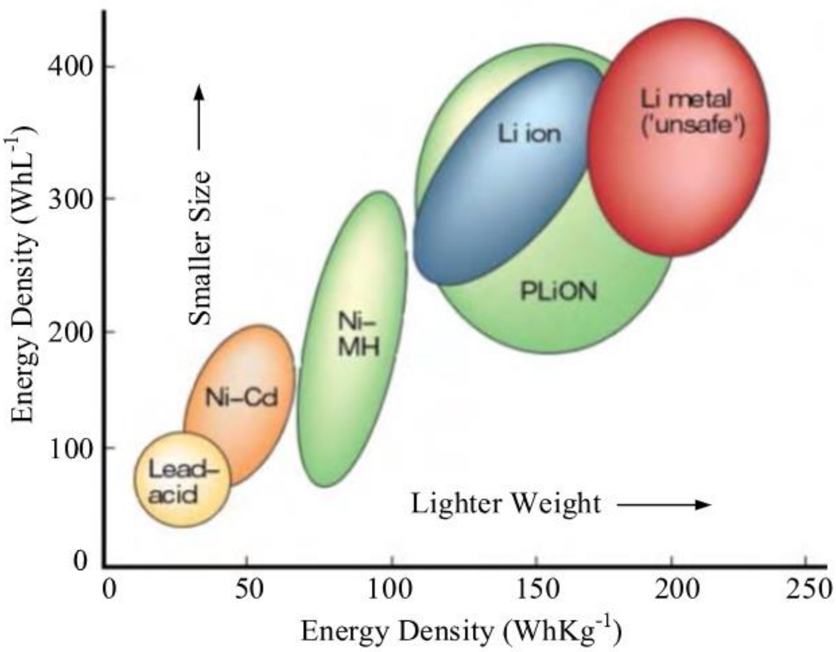

FIGURE 2: BATTERY TECHNOLOGIES ENERGY DENSITY PER SIZE VS PER WEIGHT

Therefore, it can be concluded that Li-ion batteries are the best technology due to its high energy density compared to its reduced size and weight which makes it the most suitable option for vehicle applications (Zhou, Li and Cheng 2014, 31). However, they are relatively expensive to manufacture and to avoid damage and failure, they need to be rigorously tested and protected during production and use due to their flammable electrolyte.

There are several Li-ion types due to the different electrodes chemistries. Further comparisons among the 5 principle Li-ion battery technologies are given in Table 2, detailing the advantages, disadvantages and applications and in Figure 3 using performance indicators in indexed values (Hannan et al. 2018, 19368-19369). The characteristics of lithium manganese oxide ($LiMn_2O_4$), lithium iron phosphate ($LiFePO_4$), lithium nickel manganese cobalt oxide ($LiNiMnCoO_2$) and lithium nickel cobalt aluminum oxide ($LiNiCoAlO_2$) make them suitable for EV use.

TABLE 2: CHARACTERISTICS AND APPLICATIONS OF LI-ION BATTERY TYPES

Types of Li-ion Batteries	**Advantages**	**Disadvantages**	**Applications**
$LiCoO_2$ (Omar et al. 2010, 1-6)	High specific energy	Short life span, limited load capacity and safety	Cellphones, laptops, digital cameras, medical, HEVs.
$LiMn_2O_4$ (Kennedy, Patterson, and Camilleri 2000, 56-62)	Specific power, life span, good safety	Moderate overall performance	Medical, EVs, HEVs.
$LiFePO_4$ (Zhao, Yin, and MA 2016, 89-93)	Good thermal stability, abuse tolerance, high current rating long life span, excellent safety	Moderate specific energy, relatively low voltage, high cost	Power tool, portable devices, EVs
$LiNiMnCoO_2$ (Omar et al. 2010, 2-5)	Good overall performance, excellent specific energy	High cost	Power tools, EVs, energy storages
$LiNiCoAlO_2$ (Omar et al. 2010, 3-5)	High energy and power density, good life span	High cost and marginal safety	EVs and power trains
$Li_4Ti_5OI_2$ (Liu et al. 2013)	98% recharge efficiency, 3000-7000 cycle life, high safety and stability, charges quicker	Small cell voltage 2.4V, low energy density, difficult to manufacture	Advanced nanotechnology applications

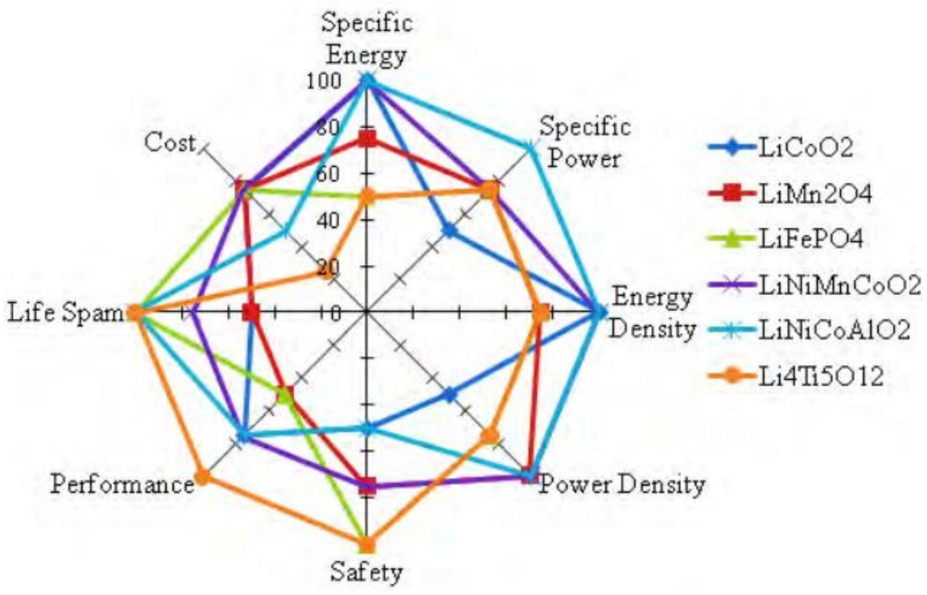

FIGURE 3: COMPARISON OF LI-ION BATTERY TYPES USING INDEXED VALUES

BATTERY MODELING

Modeling is an effective tool for the proper design and control of EV batteries. It is necessary to accurately capture the battery's key parameters for design and battery management functions since proper model development is prerequisite to the development of system identification and state estimation algorithms. The key parameters determined by a battery model includes information on charging/discharging cycle, its behavior to transient loads and its health status as a function of various stress factors, including temperature and charge/discharge rate (Samadani 2015, 7).

Researchers, in the past, have developed a wide variety of battery models with different degrees of complexity for different intended purposes. In search of the most suitable battery model for integration studies, the most common modeling approaches have been surveyed. These models can be classified into three distinct categories; electrochemical models, mathematical models, and equivalent circuit models (ECMs).

Electrochemical models are the most detailed and accurate since they simulate the battery cells at the microscopic level to investigate the complex electrochemical processes that occur inside the battery. Some of these include physical models that employ finite element analysis and computational fluid dynamics to model the effects of heat transfer and fluid flow in the battery (Samolyk and Sobczak 2013). Since they are developed using a system of coupled time-variant spatial partial differential equations, they can be computationally time consuming. As such, these models are suitable for the optimization of physical design aspects of the battery, but are considered inappropriate for dynamic simulations studies over long periods of time (Garcia-Valle and Lopes 2013, 36). Moreover, most of them are static and the model parameters require extensive investigation as they are not provided by the manufacturers. Electrochemical models, therefore, are deemed unsuitable for vehicular and grid integration applications.

Battery models have also been developed through the use of empirical equations or other mathematical methods such as stochastic approaches for battery characterization in terms of capacity, efficiency and runtime (Gomadam et al. 2002, 267-75). However, these mathematical models have proven to be inaccurate with a 5-20% error. Moreover, they cannot be used to obtain the IV characteristics of the battery which make them useless in circuit simulation software where grid integration studies are conducted (Chen and Rincon-Mora 2006, 2).

Equivalent circuit models (ECMs), on the other hand, generally use lumped parameters to model the electrical characteristics of the battery and are therefore the most intuitive and preferred for use in circuit design and simulation studies. Unlike electrochemical models, they do not require an extensive knowledge of the electrochemistry of the cell and is capable of capturing the dynamic behavior of the battery (Samadani 2015, 19). They employ relatively simple empirical equations to model the battery and, as such, requires limited processing power (Scott 2015, 11). An ECM consists of three main subcomponents (Jiang 2013, 23):

i. a static part that represents the thermodynamic properties of electrochemical processes in battery;
ii. a dynamic part that models the kinetics of the cell internal impedance;
iii. and a source or load for respective charge or discharge schemes

ECMs can be widely varied in complexity based on the degree of detail and precision required while maintaining their relative simplicity (Samolyk and Sobczak 2013). These models are further classified into Thevenin based; impedance based and runtime based.

Thevenin based models, as the name indicates, use a constant open circuit voltage source and a series resistor to represent the battery along with parallel RC networks to model its transient response (Liaw et al. 2004, 2) as shown in Figure 4. The predicted battery response to transient loads can be more accurately modelled by increasing the amount of parallel networks but only at a particular state of charge (SOC) and temperature. This approach alone is unsuitable for dynamic scenarios since the parameters are assumed constant. Moreover, their dependence on temperature and cycle number can lead to prediction errors for estimating SOC and runtime. (Chen and Rincon-Mora 2006, 3).

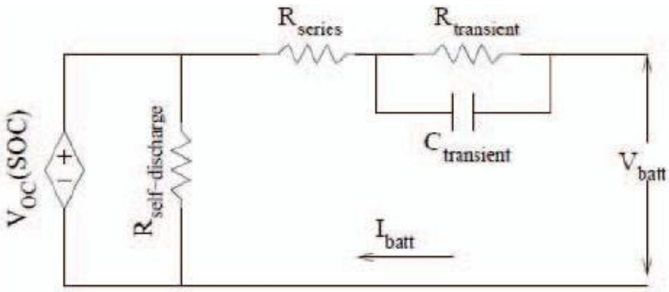

FIGURE 4: THEVENIN EQUIVALENT BATTERY MODEL

Several dynamic models have been developed in order to model specific battery types based on their individual charge equations. The improvement in this model is to account for the non-linearity in both the open-circuit voltage and the internal resistance due to varying states of charge and temperatures. The charge equation of lithium-ion type batteries is given in Liaw et al. (2004).

To validate the time constants obtained in the Thevenin's model, impedance based models utilize impedance spectroscopy to reduce and fit the battery's complex network to a measured equivalent AC impedance spectra in the frequency domain (Kroeze and Krein 2008, 2). However, this fitting process is complex, difficult and non-intuitive. Figure 5 shows this model which comprises a combination of a series resistance and inductance to account for the internal impedance of the battery and the impedance Z_{ac} to model the electrochemical equivalent of the battery (Buller et al. 2003, 3). These models are also only accurate for fixed SOC and temperature, limiting their ability to predict DC response and runtime.

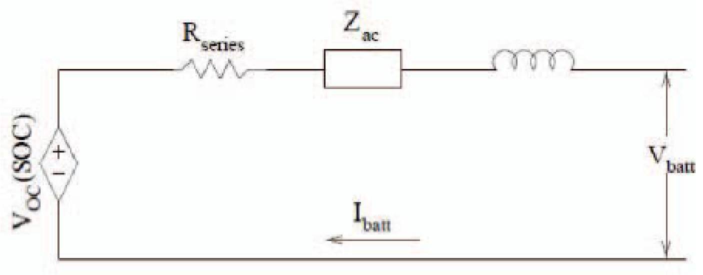

FIGURE 5: IMPEDANCED BASED BATTERY MODEL

Runtime based electrical models employ continuous or discrete time implementations through complex networks in order to accurately predict battery runtime and to obtain a DC voltage response in circuit simulation software for constant discharge currents. It allows for the accurate modelling of transients, self-discharge resistances and voltage drops due to internal losses. An example of the multiple circuit model is presented in Figure 6. However, varying load currents lead to increased inaccuracies in runtime and DC voltage response estimates (Gold 1997, 5).

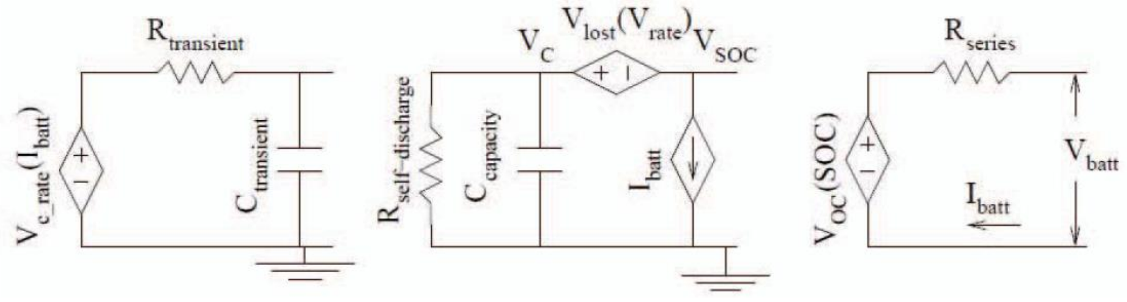

FIGURE 6: RUNTIME BASED BATTERY MODEL

Combinations of these different types of equivalent circuit models are often used to predict the desired parameters of the battery. Chen and Rincon-Mora (2006) presented a model for predicting both I-V characteristics and battery runtime and in 2016. The model is shown in Figure 7, where the capacitor $C_{capacity}$ and current source model the capacity, SOC and the run-time of the battery and the RC network ($R_{transient}$ and $C_{transient}$) models the transient response. A voltage controlled voltage source is used in order to relate the SOC with the open-circuit voltage. Hence, this model can accurately represent the transient response of the battery and other dynamic electrical characteristics like open circuit voltage and useable capacity.

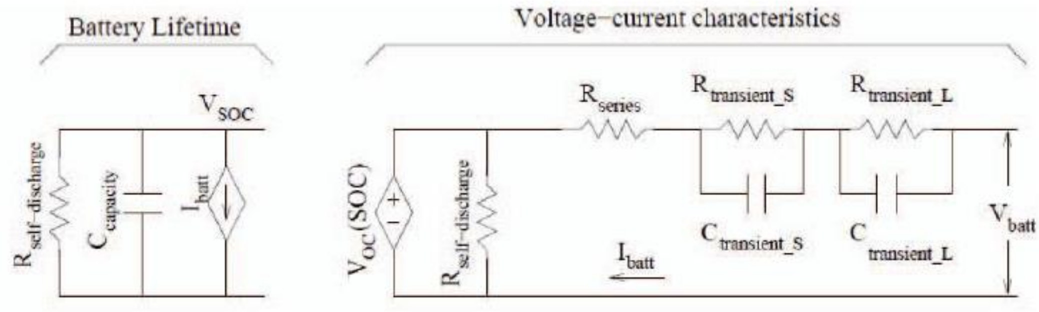

FIGURE 7: COMBINATION BATTERY MODEL

However, it is not accurate in predicting the transient response of short duration loads and hence cannot accurately predict the SOC throughout EV drive cycles. Another drawback of this model is it neglects the effects of temperature and capacity fading. Kroeze and Krein (2008) improved on this model by including rate factor to accurately determine discharge capacity during drive cycles as a function of temperature, discharge rate and cycle number. Further improvements were also done by Erdinc et al. (2009) to account for temperature and capacity fading.

For the purpose of EV-grid integration studies, lumped parameter models are most suitable and often used. In these studies, the battery terminal and other general parameters such as battery voltage, charge/discharge current and SOC are of more interest than those of the specific electrochemical reactions within the battery (Garcia-Valle and Lopes 2013, 36). Capacity fading or degradation due to the effects of temperature and cycle number are not of immediate importance since these simulations only seek to evaluate the impact of one charging cycle of the battery on the grid. It is not necessary to account for battery run time and state of health due to prolonged and/or multiple charge and discharge cycles. Therefore, a dynamic impedance based model would be optimal for use in this study in order to accurately predict I-V characteristics and the transient behavior of the battery. A simple but accurate method of estimating the SOC during the charging cycle is also required. This is one of the functions performed by the battery management unit.

Battery Management Systems

To enhance the performance, ensure the safe operation and extend the lifetime of lithium-ion batteries in EVs, battery management systems are vital. They serve to manage all the monitoring, management and control functions pertaining to the storage and transfer of energy in aforementioned EV sub-systems. These include the many functions which are presented in Figure 8 below (Affani et al. 2005; Xing et al. 2011; and Lu et al. 2013).

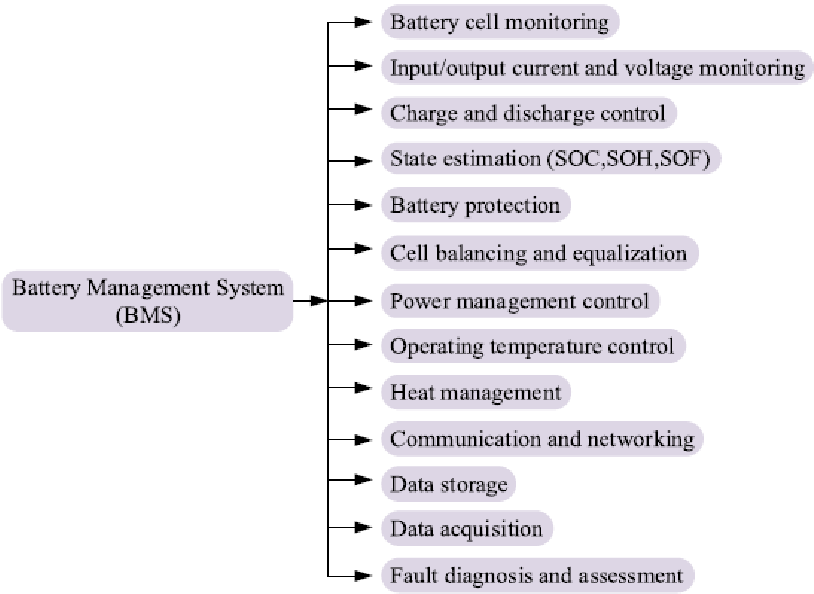

FIGURE 8: BATTERY MANAGEMENT SYSTEM FUNCTIONS

As it pertains to EV-grid integration studies, the relevant functions are limited to input current and voltage monitoring, charge control and SOC estimation. These particular functions will be reviewed in more detail than the others, as they would have to be implemented for the study.

Monitoring

The individual cells in the EV battery pack have various parameters that need to be constantly monitored as a prerequisite for certain management, control and optimization functions performed by the BMS. Parameters including voltage, charge and temperature would indicate the necessity of multiple functions of the BMS such as charge/discharge control, battery protection, cell levelling and heat management.

The monitoring of the cell input/output voltage and current levels are also important for protecting the cells from over or under voltage/current operations which may cause system failure (Hoque, Hannan and Mohammed 2016, 6). These parameters are also very important in the estimation of the status of battery capacity which can, in turn, be used to inform on further actions. Proper monitoring is the basis of all the functions performed by the BMS and is usually done utilizing sensors. In this study these parameters can simply be measured from the battery model in the software.

Charge/Discharge Control

The performance, safety and durability of a battery heavily depends on the method in which it is charged and discharged. If this is efficiently and optimally controlled, it can significantly extend the lifetime of the battery. There are three common charging methods specific to EV batteries (Dhameja 2002, 83-89).

1. Constant current (CC) charge control – for this charging method, a constant current is applied to the battery. This current is maintained by controlling the input voltage to the battery as the internal impedance changes throughout the charge cycle. For this method, the SOC increases linearly with time during charging and as such, it is difficult to estimate the completeness of charge to determine the cut-off time. Another drawback of this method is that application of an initial high current may result in sudden transients which can damage the battery.
2. Constant voltage (CV) charge control – for this simple charging scheme, a constant voltage is applied to the battery and so the charging current varies during the charging process. Because of the difference in charging and terminal voltage, the initial current can be high at the beginning of charge cycle and will gradually reduce to zero as the battery is fully charged. This large power requirement at the start of the cycle presents a worst case scenario for the electrical grid.

3. Constant current, constant voltage (CC/CV) charge control – this is combination of the previous two methods used to eliminate both drawbacks. In the initial stages, a low constant current is applied to pre-charge the battery if needed. Then, at a certain threshold SOC, a higher, constant controlled current is applied. Once, the battery SOC reaches another threshold, it is then changed to the constant voltage mode where the current can slowly decrease to zero once fully charged. Figure 9 shows the charge profile for this method (Garcia-Valle and Lopes 2013, 23).

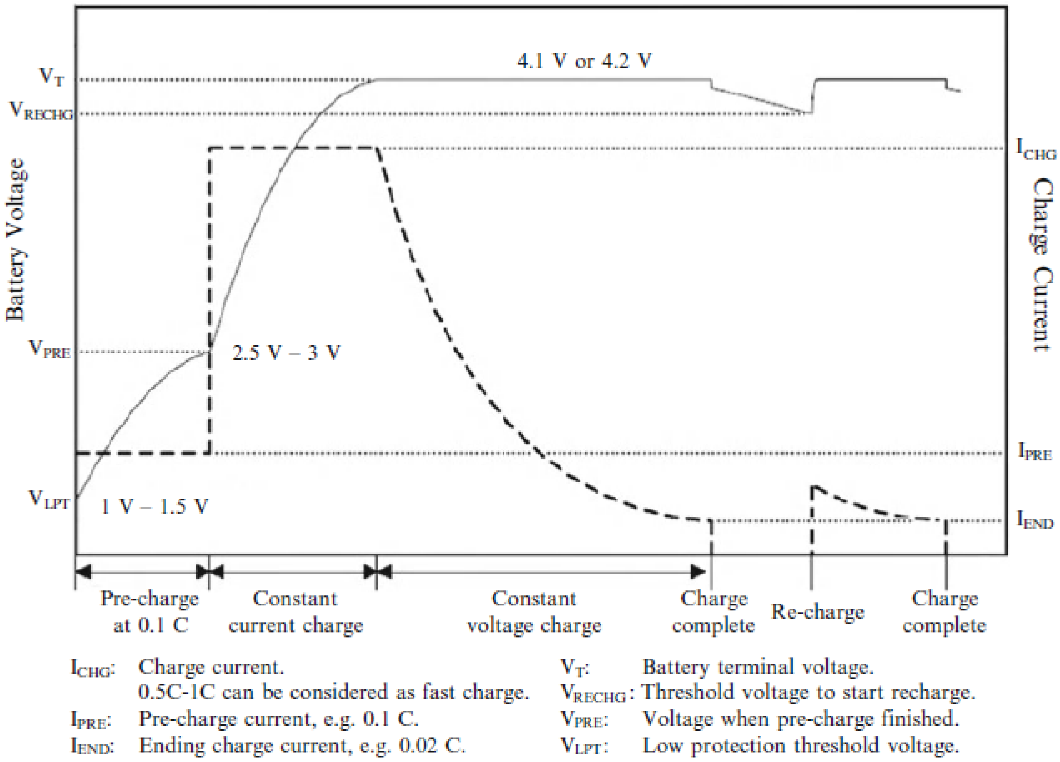

FIGURE 9: CONSTANT-CURRENT, CONSTANT VOLTAGE CHARGE PROFILE

The most optimal and recommended for Li-ion batteries is the CC-CV method (Hoque, Hannan and Mohamed 2016, 11) and will be implemented in this study using a PI (proportional-integral) controller.

The recommended discharge method for Li-ion batteries is by the discontinuous current mode (DCM) discharge control. This study will not analyze the EV battery when discharging and so these methods are not considered.

STATE ESTIMATION

The main states of the EV battery are the state of charge (SOC) and the state of health (SOH). These are very important capacity indicators of the battery which are required inputs for the management, control and optimization functions performed by the BMS.

The SOC is defined as the charge status of the battery with reference to the full charge capacity of the battery. It is also an indication of the discharge depth of the battery. It is particularly necessary to accurately estimate the SOC during the charging/discharging cycle to prevent the battery from overcharging and going into deep discharge as these conditions degrade battery life and may cause safety concerns (Eichi et al. 2013, 5). SOC estimation can be complicated as it is dependent on several factors including temperature, internal resistance and battery capacitance (Chiasson and Vairamohan 2005, 1). This state is determined using the monitored and modeled battery parameters and an estimation algorithm since it cannot be directly measured. These methods are reviewed as follows.

The discharge test method is the most elementary method to determine SOC. It involves discharging the battery and measuring the charge delivered to the load. It is then compared to a full discharge to determine the SOC. Since this method is evidently time consuming, must be done offline and modifies the current state of the battery, it is only suitable for the periodic maintenance of EV batteries.

The coulomb counting method is a simple online estimation technique that is relatively easy to implement. It simple integrates the battery charging/discharging current over time to determine the charged or discharged capacity. Equation 1 below defines this method.

$$\boldsymbol{SOC(t) = SOC(t-1) + \frac{I(t)}{Q_{rated}}\Delta t} \text{ .... (1)}$$

where SOC (t-1) is the previous SOC value, I(t) is charging/discharging current and Q_{rated} is rated charge capacity. However, this method does not account for the effects of temperature, battery history and cycle life on the SOC (Chang 2013, 4). Moreover, it requires accurate and costly current sensors and must be frequently recalibrated.

The open circuit voltage method uses the open circuit vs SOC characteristics of a particular battery to determine the SOC. It, therefore, determines the open circuit voltage during the charge/discharge cycle and then maps it using the characteristics. However, this is only possible to determine for EVs in the stop state and values take a long time to stabilize due to volatile currents (Wang et al. 2013, 2). Another drawback specific to Li-ion batteries using this method is its highly non-linear open circuit voltage characteristics which would make this method difficult to implement.

As previously mentioned, due to the non-linear nature of the EV battery behavior, mathematical models can be quite complex and cumbersome. Neural networks are self-learning and their non-linear mapping capabilities makes them highly applicable to SOC estimation. The neural network based model uses previous voltage, current and temperature values of the battery to estimate its SOC (Chang 2013, 4). They can be very accurate and efficient at SOC estimations depending on the available training data and methods for the networks (Wang et al. 2013, 3).

The Kalman filter algorithm is generally used to estimate the inner states of any dynamic system (Piller, Marion, and Andreas 2001, 1). When applied to the EV battery, it can be used to estimate the SOC. The algorithm employs a set of recursive formulae to calculate the estimation error and covariance matrix using several SOC estimates (Wang et al, 2013). The covariance matrix can then be used to determine the estimate error range. As such, both the SOC estimation and its error is obtained. Versions of the Kalman filter to this date includes the conventional, extended (Xiong et al. 2014), unscented (Yu et al. 2017) and adaptive cubature (Xiong et al. 2013). They most efficiently estimate SOC under dynamic conditions but require a suitable battery model for the determination of initial parameters and a large amount of computing power.

EV integration studies usually utilize the coulomb counting method for SOC estimation because it is gives a good compromise between complexity and accuracy. It is easy to implement, does not require a large amount of computing power and gives acceptably accurate results for low to medium SOCs.

The SOH is defined as the maximum charge capacity of an aged battery with reference to the maximum charge capacity when it was new. It is an indication of the extent of degradation and hence the remaining life. SOH is a measure of the battery current condition based on its internal impedance, power density, capacity and self-discharge rate (Hannan et al 2018, 19370).

A common SOH estimating technique is the durability model-based open-loop method which evaluates the SOH by the side reactions, Li-ion loss, capacity fade and internal resistance change. Another example is the model-based parameters identification closed-loop method that is implemented using estimated battery model parameters (Xiong et al 2013, 708). As stated earlier, the effects of battery degradation is only suitable for simulation of multiple cycles of both charging and discharging and is hence not applicable for integration studies.

Battery Protection and Cell balancing

The individual series connected cells in the EV battery pack may become imbalanced in terms of voltage and charge. These imbalances are caused by differences in their physical characteristics at the electrochemical level due to manufacturing, temperature and repeated charging and discharging. A charge imbalance among cells of the same battery pack can ultimately lead to overcharging and undercharging of certain cells. Both cases are undesirable since overcharging may lead to cell explosion and undercharging may damage the chemical properties of the cell, ultimately shortening the life of the battery (Hoque et al. 2017, 1367). The BMS protection will thus terminate overall charging/discharging to prevent these cells from being damaged. This leaves some cells not yet fully charged or discharged and will result in an overall capacity reduction of the battery.

It is for this reason, cell balancing and equalization is needed. This function serves to maintain the rated capacity of the battery while allowing the battery to be protected from unsafe conditions. Through proper SOC estimation of each cell, the charge equalization controller (CEC) can perform equalization. The equalization process involves the transfer of excess charge from the overcharged cell to a resistor or another cell/module/pack; or by transferring the required charge to the undercharged cell from other adjacent cell/module/packs such that the cells are equal in capacity or voltage level within an operating range (Hannan et al. 2018, 19371).

The available cell balancing techniques are generally categorized as passive and active. The passive cell balancing method dissipates the excess charge through a bleeding resistor and is very simple but inefficient. It requires a resistor and switch per cell and can be relatively slow at balancing. The active methods either transfer charge from cell to cell, module to cell or limit charges to cells via current switches. Although more efficient, these techniques are more complex and require advanced controls and switching networks.

Other Functions

The subsequent control and management facilities provided by the BMS shown in Figure such as battery protection, cell balancing and equalization, power management control, operating temperature control etc. are not relevant to integration studies and hence will not be covered in this scope.

The imbalances caused by differences in the cell physical characteristics at the electrochemical level due to manufacturing, temperature and repeated charging and discharging cycles are considered negligible. Therefore, cell balancing will not be implemented. There will also be no need for power management and control as the power distribution throughout the EV sub-systems is irrelevant. It will also be assumed that the Li-ion battery will operate within its prescribed operating temperature range. Similarly, no communications, networking or fault diagnostics need to be modelled for this study.

Charger Technologies

The power supply unit or charger can be identified as all hardware that couples the AC grid to the energy source whether integrated onboard the EV or not. This can also be referred to as the electric vehicle supply equipment (EVSE). It consists of mainly power converters with their associated microcontrollers, digital signal processors and integrated circuitry. It is responsible for the safe transfer of energy from the grid to the battery when depleted. The charging duration and even battery life is dependent on the characteristics of the charger.

Generally speaking a charger must be reliable and efficient with preferably high power density, low weight and volume and low cost (Yilamz and Krein 2013, 2152). It must ensure that the charging current from the grid is drawn with low distortion and at a high power factor. Design considerations must also be taken to limit the amount of DC current and harmonics injected into the grid. The design of its components and control strategies specific to its rating and complexity varies depending on the charging level and type and power flow direction considerations. These factors will be reviewed in this section.

Charging Levels

Charging levels define power requirement, charging duration and location, equipment, cost and hence, the effect on the electrical power system. The Electric Power Research Institute (EPRI) categorizes the available charging levels as follows.

1) Level 1 charging - this is typically uses a single phase 120V/15A outlet according to U.S. standards. Having the lowest power, it is the slowest method suitable for opportunity charging at home or even business places. It utilizes a power cord and onboard charging equipment and so no additional infrastructure is necessary.
2) Level 2 charging – this offers charging using a 208V or 240V single phase outlet which draws up to 80A. Due to its higher power and hence faster charging time, this level is considered optimal for private and public charging and V2G capability. Although it uses dedicated EVSE in both locations, most vehicles have the charging

infrastructure onboard to eliminate redundant power electronics and therefore only require the cord and power outlet. Separate circuitry and billing meter is common.

3) Level 3 charging – this typically uses a 480 V or higher three-phase supply. Intended for commercial and public use, it requires dedicated, off-board charging equipment due to its increased power rating to provide the option of fast charging in less than an hour. The vehicle connection for this level is direct DC to the battery.

The SAE J1772 U.S. charging standard (2009) suggests that the EVSE at Level 1 and Level 2 be located onboard the vehicle and Level 3 outside the vehicle at the energy supply interface (Mathoy 2008, 73). Table 3 summarizes the broader technical characteristics based on both the U.S SAE J1772 and the E.U. IEC 61851-1 charging standards.

TABLE 3: CHARGING LEVEL POWER CHARACTERISTICS

Power Level Types	**Voltage**	**Charger Location**	**Typical Use**	**Energy Supply Interface**	**Expected Power Level**	**Charging Time**	**Vehicle Technology**
Level 1 - Opportunity	120VAC (US) 230VAC (EU)	On-board 1phase	Home	Convenience outlet	1.4kW(12A) 1.9kW(20A)	4-11hrs 11-36hrs	PHEVs (5-15kWh) EVs (16-50kWh)
Level 2 - Primary	240VAC (US) 400VAC (EU)	On-board 1or 3phase	Private or public	Dedicated EVSE	4kW(17A) 8kW(32A) 19.2kW(80A)	1-4hrs 2-6hrs 2-3hrs	PHEVs (5-15kWh) EVs (16-30kWh) EVs (3-50kWh)
Level 3 – Fast	208-600 VAC or VDC	Off-board 3phase	Public	Dedicated EVSE	50kW 100kW	0.4-1hr 0.2-0.5hrs	EVs (20-50kWh)

Level 1 charging allows for the convenience of plugging in the vehicle at home or work using regular power outlets. If, however, several vehicles were to be plugged in during the same period of time (peak hours) in the same area, it will result in an increased load demand which will inevitably lead to voltage drops, congestion, imbalances between phases etc. on the distribution grid. For levels 2 and 3 charging, dedicated equipment may be needed for charging since the power level is much higher. Consequently, this can also lead to an unmanageable load demand which will cause similar violations on the distribution network. It is imperative that the utility provider is able to maintain a high quality electrical supply that is reliable. Therefore, it is essential that the limits for the integration of electric vehicles to the distribution grid be assessed to ensure that normal operation of the power system can be sustained and customers' needs can be fulfilled while allowing for the electric vehicles to be charged. For the purposes of this study, the impacts of only levels 1 and 2 charging of electric vehicles will be explored.

Charger Topologies

As previously mentioned, charger types are dependent on the charging level as well as their power flow capabilities. Electric vehicle chargers can be classified based on their location; either on board or off board, as well as their power flow capabilities; either unidirectional or bidirectional.

As the name suggests, on board chargers are those which are integrated into the vehicle and these have the disadvantage of limiting high power due to weight, space and cost constraints (Haghbin et al. 2010, 2; Grenier et al. 2010, 1). On board charging systems, can be conductive where direct contact is needed between the connector and charge inlet. They can also be inductive where the charger transfers power magnetically. The inductive on board charger has been explored in previous studies for use with levels 1 and 2 charging and may be either moving or stationary (Budhia et al. 2011, 614) Off board chargers on the other hand require external infrastructure and are less constrained by size and weight and would hence be more complex and of a higher power rating. Figure 10 details the on board or off board types according to charging level (Habib et al. 2018, 13870). The location of the charger relative to the EV is inconsequential to this project.

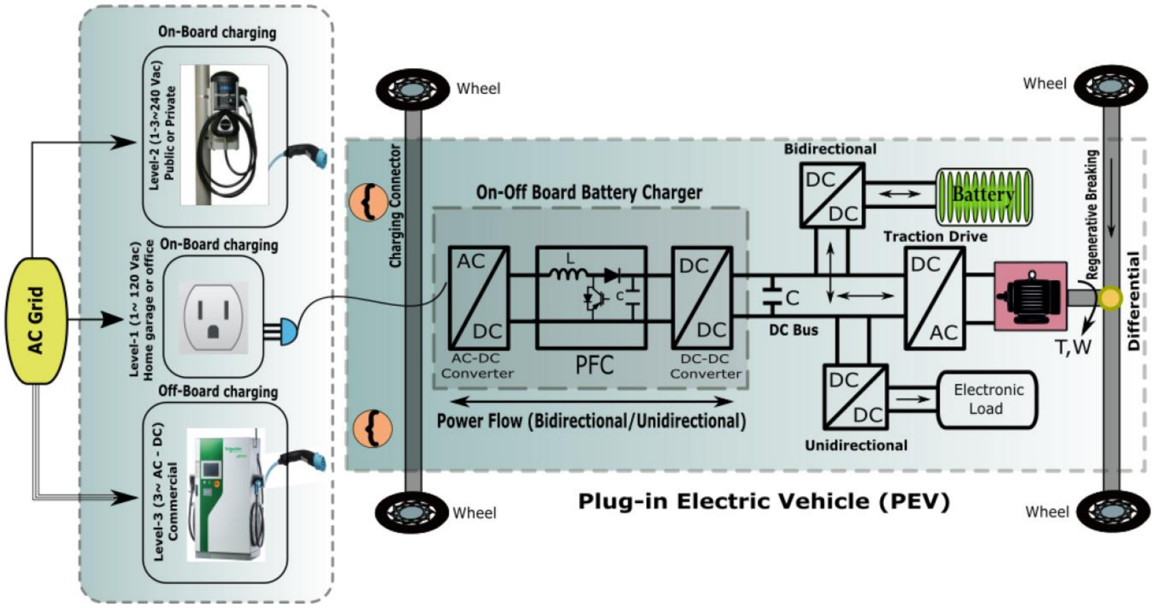

FIGURE 10: ON/OFF BOARD CHARGERS ACCORDING TO CHARGING LEVEL

EVs with unidirectional chargers, can only receive power from the grid. The benefits of unidirectional power flow are that the hardware requirements are limited, issues involving interconnection are minimal and the degradation of the electric vehicle battery is reduced compared to when bidirectional power flow is utilized. However, bidirectional power flow also has its advantages including its ability to facilitate both grid to vehicle (G2V) and vehicle to grid (V2G) power flow. This means that not only will the battery support charge from the grid, it is also capable of providing energy injections back into the power system. Bidirectional power flow also aids in power stabilization with sufficient energy conversion. This study is limited to the uncoordinated EV charging and as such, the modelling of a unidirectional charger will be sufficient.

EV chargers, when connected to the grid and implementing a non-linear charging regime as previously mentioned to optimally charge the vehicle battery may cause power quality issues. This non-linear characteristic of the EV load can cause harmonics in the network, a weak power factor and adversely affect the voltage profile of the network (Karmaker, Roy, and Ahmed 2019, 1). It causes a nonlinear voltage drop and a hence distorted voltage waveform. Additionally, harmonics can affect the performance of distribution transformers by causing excessive heating and increased power losses in the windings which reduces power output and life expectancy. Xu et al. (2014), conducted a harmonic analysis of EV charging loads on the IEEE 34 node test network. They concluded that EVs with a higher SOC cause less harmonic distortion. The SAE J2894/1 standard specifies power quality requirements for EV chargers in terms of harmonic injection.

Battery chargers, both on board and off board, can either be designed in a single stage or two-stage. Single stage chargers are insufficient for high power levels (Shi, Tang, and Khaligh 2017, 10901) and so the focus will be on two-stage chargers. The two stages includes an AC-DC converter for the rectification of the grid voltage and power factor correction (PFC), and then a DC-DC converter which converts the output DC voltage level of the first stage to the battery DC voltage level. Figure 11 shows the structure of a two-stage charger (including an EMI filter) along with unidirectional and bidirectional power flow directions (Yilamz and Krein 2013, 2155). These two stages will be reviewed separately.

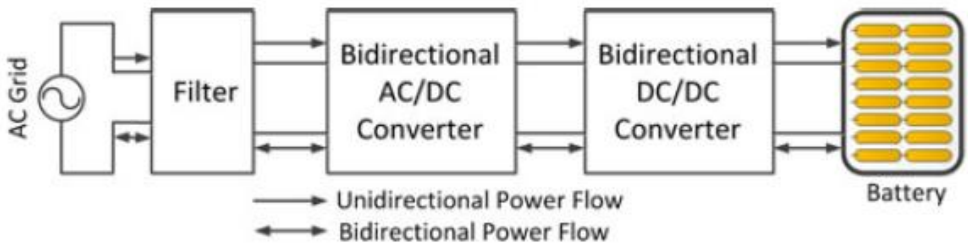

FIGURE 11: BLOCK DIAGRAM OF A TWO-STAGE EV CHARGER

AC/DC CONVERTERS

Selection of a proper AC-DC converter is important in achieving reduced current harmonic injections and power losses, proper regulation of output voltage and unity power factor correction. Several different topologies have been evolved for PFC implementation.

The conventional boost PFC topology shown in Figure 12 comprises a simple diode bridge rectifier and a boost PFC circuit. It suffers from high ripple output current and excessive diode losses for powers above 1kW (Musavi et al. 2011, 1837). The bridgeless boost PFC topology shown in Figure 13 maintains the classical boost PFC topology while avoiding the use of the rectifier input bridge. This solves the low efficiency problem but EMI increases due to the inductors (Jang and Jovanovic 2009).

The third topology shown in Figure 14 is the interleaved boost PFC topology which comprises two boost PFC in parallel. This topology decreases the EMI but still suffers with poor heat management (Janh and Jovanovic 2007). This problem is addressed in the bridgeless interleaved boost PFC topology given in Figure 15, which solves both the heat management problem and EMI problem. Although more complex, it is a suitable solution for power levels above 3.5kW (Musavi, Eberle, and Dunford 2011).

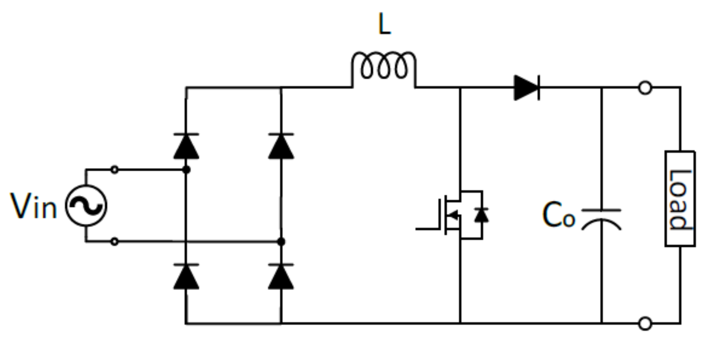

FIGURE 12: CONVENTIONAL BOOST PFC CIRCUIT TOPOLOGY

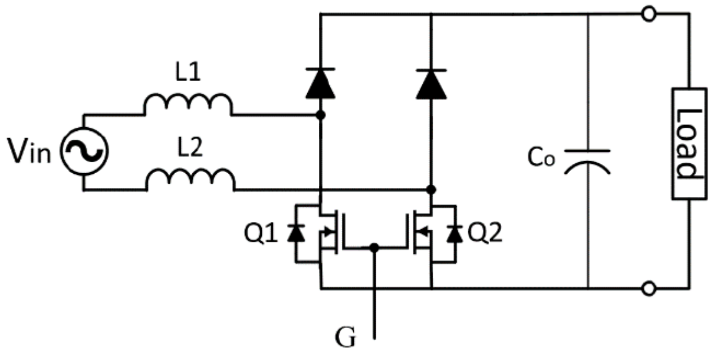

FIGURE 13: BRIDGELESS BOOST PFC CIRCUIT TOPOLOGY

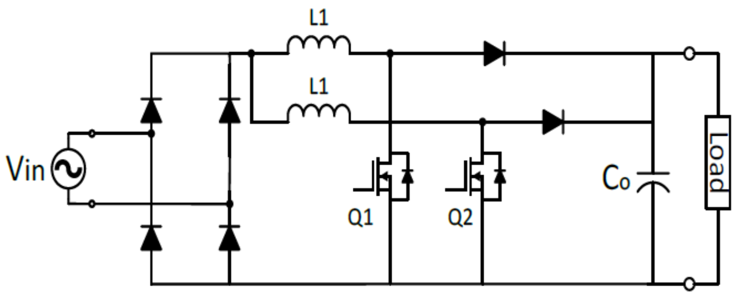

FIGURE 14: INTERLEAVED BOOST PFC CIRCUIT TOPOLOGY

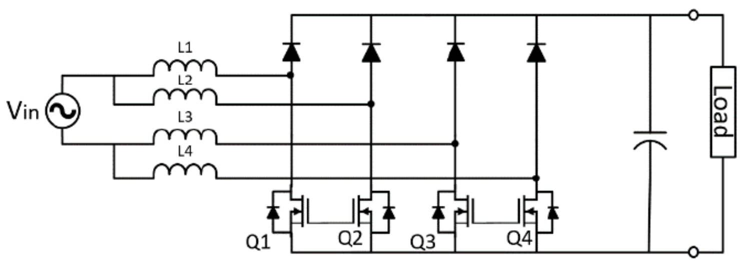

FIGURE 15: BRIDGELESS INTERLEAVED BOOST PFC CIRCUIT TOPOLOGY

DC/DC CONVERTERS

DC-DC converters specifically designed for EV chargers can be isolated or non-isolated. Each of these subgroups further divide into unidirectional and bidirectional types as defined earlier in this section.

Non-isolated DC-DC converters perform only DC regulation and hence have low cost, low active component number and high efficiency. However, without isolation, they are limited to low power systems and do not have any protection against high voltages and currents between the grid and battery (Marcos Pastor 2015, 43). Since they are suited for power levels of below 1kW, they were not included in this review.

Isolated DC-DC converters must perform inversion (DC-AC conversion) in order to be isolated by the transformer and then rectified again to the required battery voltage. Therefore, they are larger in size, comprise more active components and have less efficiency in low power applications due to higher switching losses compared to non-isolated converters. However, isolated converters have higher efficiencies at high power applications, the transformer provides protection between grid and battery and the turns ratio of the transformer also facilitates regulation of the battery voltage (Elankurisil and Dash 2011, 2).

The different unidirectional topologies are briefly reviewed as follows (Wan 2012, 42-59). The Flyback topology given in Figure 16 is the simplest as it is operated with a single switch and does not require an output inductor. As such, it is the easiest and cheapest to implement. However, this topology suffers from poor transformer utilization and requires extra additional capacitors at the input and output due to high current ripples. The push-pull topology shown in Figure 17 fully utilizes the transformer and it suitable for high power density applications. The primary switches, however, experience high voltage stresses during the off state.

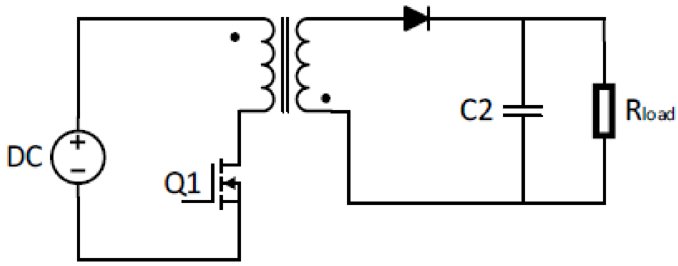

FIGURE 16: FLYBACK CIRCUIT TOPOLOGY

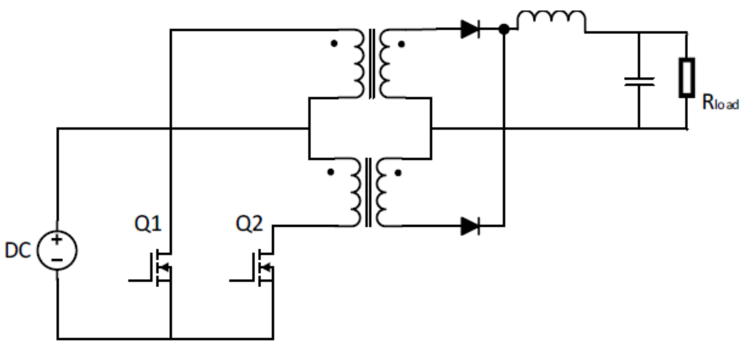

FIGURE 17: PUSH PULL CIRCUIT TOPOLOGY

As compared to the half bridge converters given in Figure 18, full bridge topologies gives a higher efficiency for higher power applications. This circuit, shown in Figure 19, contain more switches and is hence more costly to implement and requires a more complex control scheme. The Phase-shifted, full bridge converters are also suitable for high input voltage and power applications. It requires a different control methodology and has zero voltage stress on the primary switches. It, however, produces higher losses in the primary during the freewheeling time. This topology is presented in Figure 20.

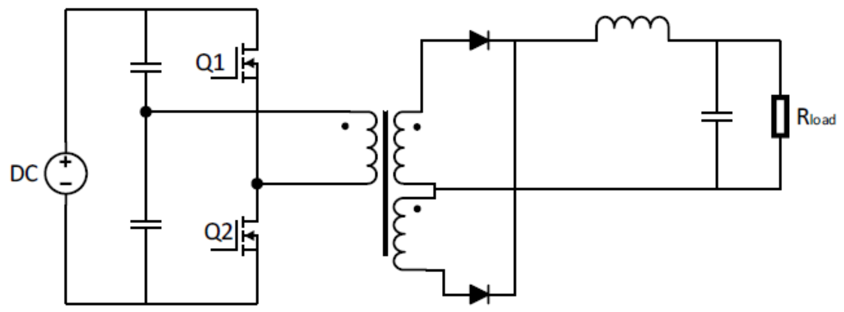

FIGURE 18: HALF BRIDGE CIRCUIT TOPOLOGY

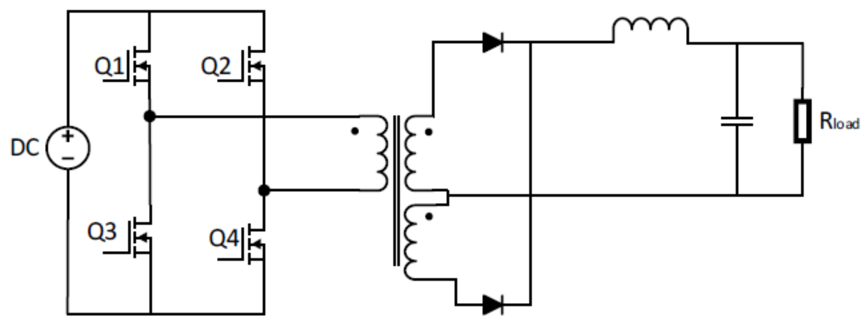

FIGURE 19: FULL BRIDGE CIRCUIT TOPOLOGY

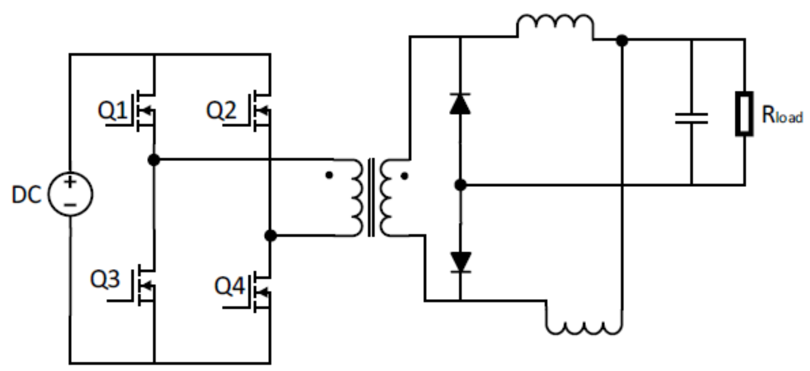

FIGURE 20: FULL BRIDGE, PHASE SHIFT CIRCUIT TOPOLOGY

The most popular topologies for bidirectional isolated converters in the reviewed literature is presented in the Figures 21 and 22. The half bridge converter is suitable for low power applications and costs less to implement compared to the full bridge topology which is more applicable for higher power demand. The efficiency of the full bridge is less because it utilizes more switches.

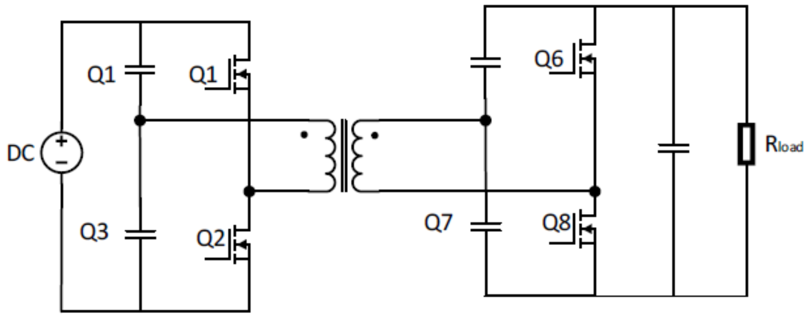

FIGURE 21: BIDIRECTIONAL HALF BRIDGE CIRCUIT TOPOLOGY

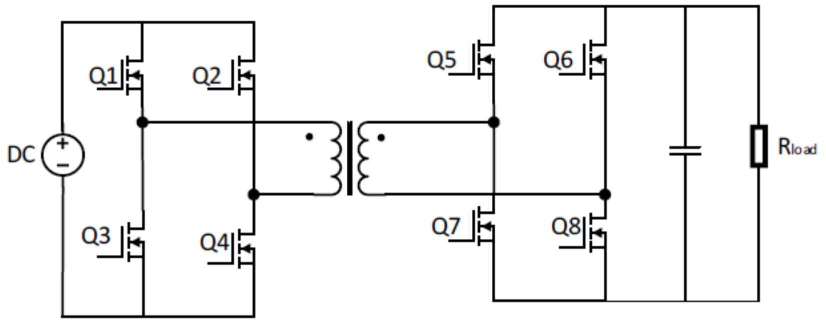

FIGURE 22: BIDIRECTIONAL FULL BRIDGE CIRCUIT TOPOLOGY

The performance comparison of the reviewed isolated unidirectional and bidirectional converter types in terms of power demand, efficiency, voltage stress, number of components and cost is summarized in Table 4.

TABLE 4: PERFORMANCE COMPARISON OF ISOLATED DC-DC CONVERTER TYPES

Converter Types		Optimal Power Demand	Efficiency	Voltage stress	Number of components	Cost
Uni-directional Isolated DC-DC Converters	Flyback	Low (<500W)	High	High	4	Low
	Half Bridge	Low (<1KW)	High	High	7	Medium
	Full bridge	High (>1KW)	Medium	Medium	9	High
	Push pull	High (>1KW)	High	High	8	High
	Full bridge phase shift	High (>1KW)	Low	Low	10	High
Bidirectional Isolated DC-DC Converters	Half bridge	Low (<1KW)	High	High	6	Low
	Full bridge	High (>1KW)	Low	Low	10	High

Since this review will be used to select a charger for simulation, the number of components and cost will not be relevant limiting factors. As mentioned in the 'Charging Levels' section of the report, a maximum of more than 1kW will be drawn by the charge. This eliminates any converters suited for low power applications. Therefore, the full bridge topologies are more favorable for both the unidirectional and bidirectional categories. A unidirectional converter would be optimal since this study only considers uncoordinated charging.

CHARGING INFRASTRUCTURE AND STANDARDS

According to the SAE J1772 charging standard, the major components of charging infrastructure or electric vehicle supply equipment (EVSE) include the EV charge cords, charge stands (private or public), attachment plugs, vehicle connectors, power outlets and protection systems. They are either in the form of a specialized cord set or a wall or pedestal mounted box. The specific configurations and designs vary widely depending on voltage, frequency, electrical grid connection and transmission standards. Several standards developed by key organizations address a wide range of issues relating to EVs such as batteries, charging, safety and infrastructure considerations. There are many duplications as well as inconsistencies across these standards. A merging of these standards is important to standardize charging technologies which will in turn encourage the mass adoption of EVs through customer comfort and reduced manufacturing costs. The standards related to EVSE are listed below.

- NFPA 70 National Electric Code: Article 625 covers the wires and equipment used to supply electricity for charging an electric vehicle.
- IEC 62196-1: Plugs, socket-outlets, vehicle connectors and vehicle inlets - Conductive charging of electric vehicles -Part 1: General requirements
- IEC 62196-2: Plugs, socket-outlets, vehicle connectors and vehicle inlets - Conductive charging of electric vehicles -Part 2: Dimensional compatibility and interchangeability requirements for a.c. pin and contact-tube accessories
- IEC 62196-3: Plugs, socket-outlets, vehicle connectors and vehicle inlets - Conductive charging of electric vehicles -Part 3: Dimensional compatibility and interchangeability requirements for d.c. and a.c./d.c. pin and contact-tube vehicle couplers

• UL 2202: Electric Vehicle (EV) Charging System Equipment

• UL NMX-J-678-ANCE/CSA C22.2 No. 282-13/UL 2251: Standard for Plugs, Receptacles, and Couplers for Electric Vehicles

• UL NMX-J-677-ANCE/CSA C22.2 NO. 280-13/UL 2594: Standard for Electric Vehicle Supply Equipment

In the absence of EVSE during the early adoption of EVs, such as the case in Trinidad and Tobago, customers would opt for vehicles with on board charging equipment. The availability of charging infrastructure however, would accompany a reduction of on-board energy storage requirements and costs. An in-depth review on different charging infrastructure was not done as it is not pertinent to this integration study. Specific connector types were recorded in Table 5 for typical EVs models some of which are available for purchase in Trinidad and Tobago from local dealers. All of them utilize the SAE J1772 connector for level 1 and 2 charging.

TABLE 5: CHARGING INFRASTRUCTURE AND CHARACTERISTICS OF SELECT EVS AT ALL CHARGING LEVELS

	Battery Type and Energy	All-Electric Range	Connector Type	Level 1 Charging		Level 2 Charging		DC Fast Charging	
				Demand	Charge Time	Demand	Charge Time	Demand	Charge Time
Toyota Prius PHEV(2012)	Li-Ion 4.4kWh	14 miles	SAE J1772	1.4kW (120V)	3 hours	3.8kW (240V)	2.5 hours	N/A	N/A
Chevrolet Volt PHEV	Li-Ion 16kWh	40 miles	SAE J1772	0.96–1.4 kW	5–8 hours	3.8kW	2–3 hours	N/A	N/A
Mitsubishi i-MiEV EV	Li-Ion 16kWh	96 miles	SAE J1772 JARI/TEPCO	1.5kW	7 hours	3kW	14 hours	50kW	30 minutes
Nissan Leaf EV	Li-Ion 24kWh	100 miles	SAE J1772 JARI/TEPCO	1.8kW	12–16 hours	3.3kW	6–8 hours	50 + kW	15-30 minutes
Tesla Roadster EV	Li-Ion 53kWh	245 miles	SAE J1772	1.8kW	30 + hours	9.6–16.8 kW	4–12 hours	N/A	N/A

EV Integration Impact Studies

Another literature review on past impact analyses from the grid perspective was performed in order to guide the methodology for this study. This review was done specific to the impact of uncoordinated charging on low-medium voltage distribution grids. For this charging scheme, often called dumb charging, EV owners have full control of when they connect and charge their vehicles, without any external control strategy, restrictions or incentives that manage the charging process. Therefore, charging starts immediately or after a fixed delay when they are plugged in and lasts until completely charged or when unplugged as defined by the user.

When EV charging is left uncontrolled, the charging times is highly dependent on the times EV users return after the last journey of the day. An increase in system load peak is expected for this charging scheme since home arrival also usually coincides with increased residential consumption. This may result in negative impacts to the local distribution network and the adoption of EV at some level will warrant grid reinforcement. The negative impacts on distribution grids due to the uncoordinated integration of EVs is captured in Figure 23 below (Un-Noor et al. 2017, 50).

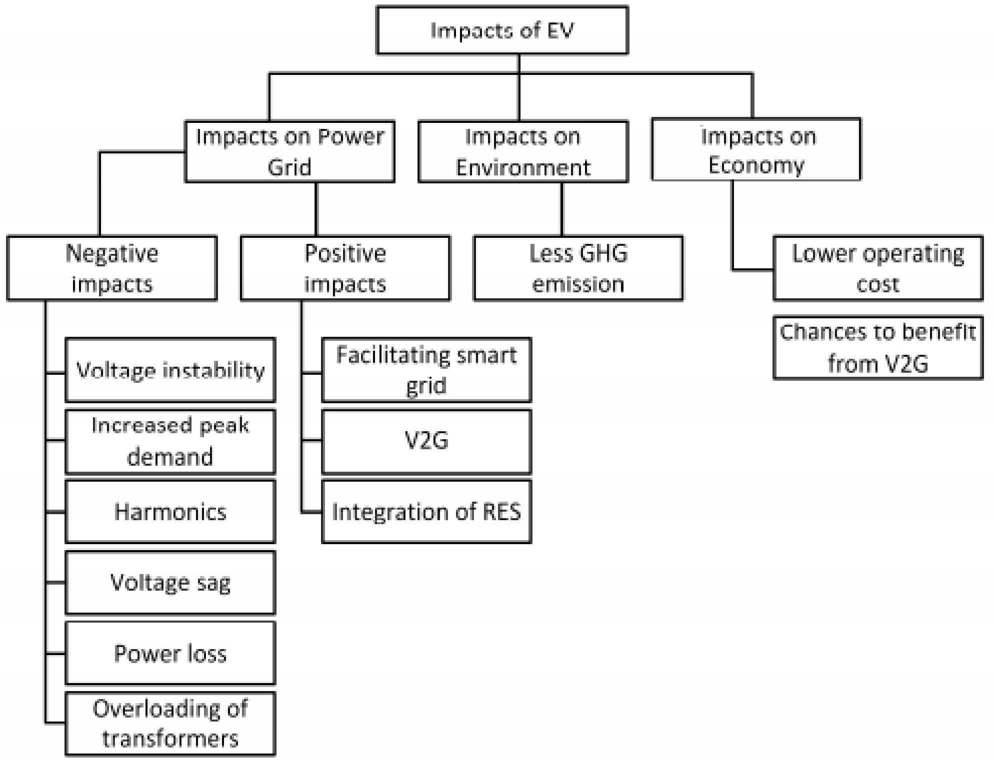

FIGURE 23: IMPACTS OF ELECTRIC VEHICLES

The accuracy of results of an impact study is obviously dependent on the extent to which the EV demand requirements is modeled. This additional demand on the grid for EV charging can be identified by considering several factors related to the EV technical specifications and the local driving patterns. The technical specifications of the vehicle were reviewed earlier in this section. The key parameters that defines the EV charging process are as follows (Garcia-Valle and Lopez 2013, 58-64):

1. EV Penetration Level – the number of vehicles expected to be connected to the grid expressed as a percentage of residential load, total market share etc. This is dependent on the forecasted EV sales for a particular country.
2. EV Technology – this includes technical parameters such as EV classification and model which would determine EV energy requirements; and then charging levels

and their respective infrastructure to determine charging power magnitude and duration of charging cycle.

3. Availability of Charging – the time and location the vehicles are available to charge. This would depend heavily on travel data and the availability of charging infrastructure.
4. Battery consumption – The amount of energy the EV battery consumes which reflects the SOC of the battery when charging is available and initiated. The amount of charging energy required can be estimated by defining the distance travelled. Therefore, this parameter is heavily dependent on travel data as well.
5. Charging Losses – the power conversion losses of all the EVSE between the grid connection and the battery. This can be quantified using the efficiency of the charging module.
6. Charging Strategy – this refers to the level of control implemented in the charging of electric vehicles on an electrical grid. It includes uncoordinated (dumb) charging, TOU tariffs, coordinated (smart) charging and vehicle to grid strategies.

Based on the availability of EV usage data specific to the case study, certain parameters have either been determined as constant based on assumptions or treated as probabilistic. Load determination approaches vary from applying static values to dynamic loads calculated from stochastic models and optimization equations.

Similar to the scope of this study, Akhavan-Rezai et al. (2012) examines Level 1 (slow) and Level 2 (fast) charging scenarios of EVs in terms of network performance. The method proposed applies a load flow analysis at both charging levels with an increasing penetration to examine the network voltage deviations and power losses on a real distribution system in Ontario, Canada. Using data obtained from the National Household Travel Survey (NHTS) for North America to select a vehicle type, vehicle number per household and charging time, static (constant power) loads were determined from this data and load flows were performed for penetrations of up to 30%. Therefore, the battery and charger was not modelled and it assumes a fixed state of charge of 0% when plugged in.

Several studies considering static load models were since conducted, such as by Neagoe-Stefana et al. (2014) and by Mahadeo, Bahadoorsignh and Sharma (2017). The latter was done on the island of Trinidad and assessed voltage deviations and line overloading on a local distribution feeder north of the island for Level 2 charging and penetrations of up to 20% of the peak residential load. Significant bus voltage violations were reported from as early as 10% penetration. This, however, represents a worst case scenario and hence overestimates the impact of EV charging on the feeder. The present study serves to further it through more accurate EV modelling.

A noteworthy and comprehensive EV integration study reviewed is the work of Almeida, Soars and Lopez (2012). Voltage level, line loading, energy losses and changes in the load duration curve were analyzed for the steady state simulations performed. The study also included a dynamic study for distributed primary and secondary frequency control.

In this critical study, various battery models and charging methods were evaluated, the most appropriate being implemented, and two methodologies were developed and employed. The three levels are charging were all considered for each. Methodology one is a deterministic one to distribute EVs along the network buses and determine EV loads during a day. Here, the EV load is a proportion of residential load at each node. The second method uses a stochastic method to simulate the expected movement of EV during one week. A Markov chain was employed to account for the variability of EV movement and then Monte Carlo simulations to generate their probable locations and power requirements based on this variability.

The impact analysis examined three scenarios; uncoordinated (dumb) charging, indirect controlled charging with multiple time of use (TOU) tariffs, and directly controlled (smart) charging. The smart charging function was formulated for both methods through optimizations problems to determine the appropriate charging levels and times to reduce deviations, prevent bus voltage and line overloading violations and flatten the load curve. The network used as a test case in this study resembles a typical semi-urban, radial, 15kV distribution grid. A daily load diagram for a typical, semi-urban MV grid was obtained by aggregating load profiles of different types of Portuguese consumers based on the proportion of installed power related with each type of consumer (residential, commercial and industrial).

Gruosso (2016) presented a study which shows how a constant penetration of electric vehicles would affect the performance of a test distribution grid in terms of voltage deviation, unbalance and losses. In each node of the network, the load is forecasted by means of a stochastic model. The model allows the determination of the spatial distribution of EV using a bottom up approach i.e. aggregating individual household load profile data. The vehicle consumption was determined by obtaining the technical specifications of typical vehicles in the small, middle and large classes and the average speed for standard drive cycles derived from real world driving data collected in Europe for rural, urban and highway trips. These were then used to estimate the energy consumption and hence the remaining SOC of the battery. Charging in this paper was done at a fixed level of 2.3 kW (230 V, 10A).

Another study with this approach was presented by Muratori (2018) where a similar behavioral model based on a bottom-up approach was used to quantify consumer energy-use behavior in the United States and capture the entire energy footprint of US households, including both residential and EV demand profiles for different penetration levels (vehicle market share percentage) and charging levels. Level 1 and Level 2 charging were assumed to operate at 1.92 kW and 6.6 kW respectively but was only applied to simple components and network cases.

The work of Wu et al. (2013) quantifies the power system components that will be overloaded at different EV penetration levels and EV charging scenarios on a 10kV distribution system in Bornholm Island, Denmark, and evaluates the cost of replacing those components. It analyses 5 different charging scenarios, three uncontrolled and two controlled. For the aggregator controlled charging schemes, they utilized an optimization problems to determine the charging rates and times. This study considers driving data from the Danish National Travel Survey, an EV battery specification of 23.3kWh, charging options at single phase (3.6kW) and three phase (11kW) and penetration levels of up to 50% to determine the EV load and performs a time series load flow analysis to assess component overload for the different charging scenarios. The current study will employ a similar time series load flow analysis for uncontrolled schemes.

A more recent, comprehensive impact study by Nour, Ramadan, Ali and Farkas (2019) was conducted on a benchmark LV distribution grid. The charging time and SOC of the EVs are considered to be variable and are modeled based on probability density functions from data presented by Leou et al. (2013). The study examined two charging scenarios, uncontrolled and indirect controlled charging via Time of Use (TOU) pricing, for 3 selected penetration levels of PEVs on separate residential, commercial and industrial feeders. The EV load was modeled using the 29.07kWh Nissan Altra lithium-ion battery and charge profile, a relatively constant power of 6.5kW for 5 hours. The network was modeled using DigSilent Power Factory and parameters such as the voltage profile and loading of feeders and distribution transformers were assessed.

Ramadan, Ali and Farkas (2019) then followed with a more practical case study that investigates the impacts of EVs on the low voltage distribution grid in Hungary. The grid was modeled on the same DigSilent Power Factory software using actual component data. The impacts on voltage deviation, feeder and transformer loading, and total system losses were evaluated for two charging scenarios, uncoordinated (peak) and delayed (off-peak) charging, with varying levels of EV penetration. They also use NHTS data to estimate charging time and a constant power charging profile based on the Nissan Leaf Li-ion battery. Like their previous study, a probability density function of the battery initial SOC was used based on Leou et al. (2013). For this study, this approach will be taken to determine the residential load at the nodes on the distribution network.

This study will take employ a similar methodology using EV demand data of 200 households in the Midwest region of the United States for a year obtained from National Renewable Energy Laboratory (NREL) (Muratori 2017) to derive probability density functions for charge time and duration. The duration can then be used to calculate a function for initial SOC.

Before the EV load can be quantified and connected to the distribution network, the key parameters that defines the charging process identified earlier in this section must be clearly defined. These are derived in the following section.

PROPOSED METHODOLOGY

ASSUMPTIONS

Before the models can be developed, several assumptions have to be declared that would hold for this project. These assumptions were guided by the scope of the project and the previous studies discussed in the Literature Review.

1. The only EV considered will be of the battery electric vehicle (BEV) type. This type of EV has the greatest power requirement from the utility compared to the other types of plug-in EVs.
2. A 24kWh Li-ion battery (Nissan Leaf) will be considered as the maximum capacity of a single BEV.
3. A maximum power demand of 1.44kW at level 1 and 7.68kW at level 2 will be used as per the SAE J1772 standard.
4. An average of 1 vehicle per household will be assumed due to the anticipated slow adoption and low availability of BEVs in Trinidad.
5. The project assumes that no charging infrastructure is available in public spaces due to the slow adoption of BEV. Therefore, Level 1 and 2 charging events will be restricted to household charging.
6. Due to lack of driving behaviour data for Trinidad, data acquired from NREL (Muratori, 2017) will be used as the base load data for BEV consumers. Therefore, BEV charging patterns in Trinidad are assumed to be the same as in the US. Probability density functions for charging time and duration will be derived to estimate initial SOC.
7. The number of charging events per day will be based on the NREL data mentioned in 6 above. The frequency of charge will also be derived from this sample load data.

8. Four (4) feeders of the local distribution system of the San Juan area will be modeled similar to the distribution system of a highly residential area using updated geographical and infrastructure data obtained from the utility.
9. BEV charging loads are added end-of-line to substation (Mahadeo 2017). In terms of voltage regulation, the voltage line drop is directly proportional to the distance from the source and the load. As such, the worst-case scenario can be obtained by initially adding the BEV load furthest from the source.
10. The inevitable overloading of pole-mounted distribution transformers based on their current rating is expected. This study will focus its analysis beyond the pole-mount transformer and will observe impacts of the feeder assuming that transformer overloading is already understood.
11. At present system infrastructure, the maximum level of penetration applied will be 20% based on results of the previous impact analysis conducted by Mahadeo et al. (2017).

Software

CYME Power Engineering Software

The CYME Power Engineering software includes a network editor, analysis modules and user-customizable model libraries. The modules available comprise a variety of advanced applications and extensive libraries for either transmission/industrial or distribution power network analysis. The software is suitable for steady state simulations including power flow and short circuit analyses at the power frequency mainly on balanced networks (CYME via Web 2019).

Being the program of choice by the country's utility, the Trinidad and Tobago Electricity Commission (TTEC), CYME was used by default as the entire electrical generation and transmission network for the country is already modelled. The system, however, was not modelled at the distribution level (12 kV and under) and hence the distribution network would have to be further modelled.

The requirements of this project is outside the capabilities of CYME in terms of the detailed modelling of the battery and charger and its single phase connection to the distribution feeder. The software is also incapable of transient simulations. For this reason, additional software would have to be used to create the feeder and EV models. The software was used only to find a network equivalent from the 33 kV distribution substation bus.

EMTP-RV Software

The Electromagnetic Transient Program (EMTP) have been one of the most widely used and most trusted tools by researchers and electric utilities particularly for the simulation and analyses of transient electromagnetic (EM) phenomena in power systems networks. ATP, an early version of the program, and ATPDraw, a graphical, mouse-driven preprocessor to the ATP version, is open source and has been popular for its liberal license policy. EMTP-RV is the latest 'restructured version' which offers more features including a new fast and powerful computational engine; a new graphical user interface (GUI), EMTPWorks; and an output processor for data display and analysis, ScopeView (EMTP via Web 2019).

The robust EMTP-RV engine offers load flow, steady state, time domain and frequency scan simulation options which are suitable for a wide range of steady state and transient network analyses involving load flow, insulation coordination, switching, protection, transient stability etc. The engine provides standard and built-in models in its libraries and also features a plug-in model interface, allowing users to add their own models. The GUI, EMTPWorks, provide top-level access to EMTP-RV simulation methods and models. The intuitive drawing interface as well as the ability to program device data allow a high level of customization of models and simulation options. The output processor, ScopeView, provides waveform visualization and analysis features that perform advanced mathematical post-processing capabilities (Powersys 2012).

The features of the software applicable to this study is the advanced three phase unbalanced load flow simulation capabilities for unbalanced distribution network studies. BEVs charged at Levels 1 and 2 represent a dynamic single phase load on the network and will inevitably lead to unbalancing. Transient analyses will also be performed to investigate the response of the system for the integration of the charger and battery components. Detailed modelling and implementation of the power electronics making up the charger and battery is of paramount importance for accurate transient simulation results.

MODELING

The 12kV Distributions System

The distribution system in Trinidad under study was created on the EMTP-RV software based on geographical and technical information acquired from the utility, T&TEC. This distribution system which services the entire San Juan area includes the San Juan distribution substation supplying four radial feeders; the Aranguez feeder, Santa Cruz feeder, East feeder and South Barataria feeder.

This particular distribution network is connected to the transmission level of the electrical grid via two step down transformers from 33 kV to 12 kV. Therefore, to adequately model the system, an equivalent of the entire network upstream the distribution station must be determined. This was done using the existing transmission network built in the CYME software made available by the utility.

NETWORK EQUIVALENT

The Thevenin's circuit equivalent of the Trinidad and Tobago network was determined by conducting simulations on the model provided in the CYME software. This software is currently used by T&TEC for simulation and analysis of the grid at the transmission level. Their model does not have the granularity required at the distribution level but can be used to obtain an equivalent representation (generator and impedance) of the system as seen from the 33kV distribution bus.

To obtain this network equivalent, a short circuit study was conducted at the San Juan 33kV bus. An estimate of the available fault current of the incoming utility feed to the bus was obtained in CYME. Figure 24, shows the results of said short circuit study. After the equivalent impedance was calculated, it was input into a standard three phase voltage source with impedance model in EMTP-RV.

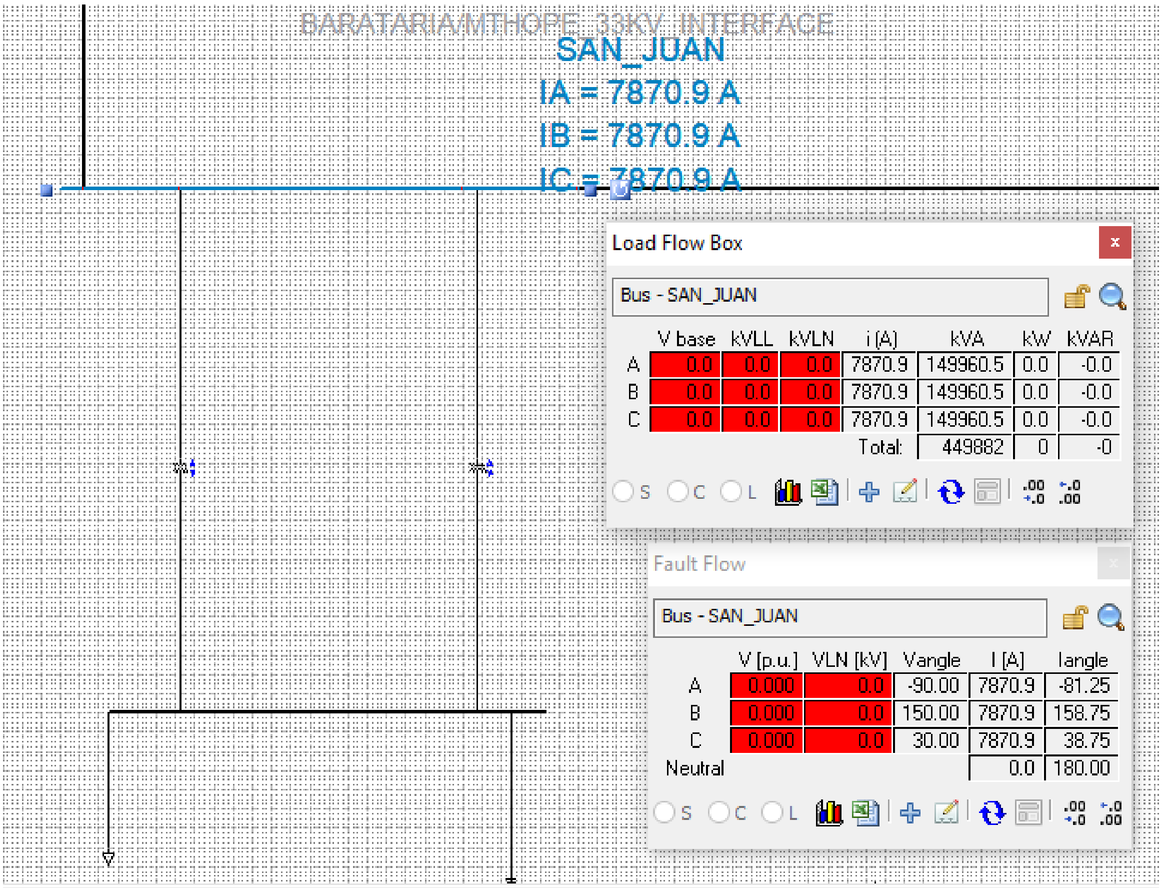

FIGURE 24: SHORT CIRCUIT STUDY RESULTS

From the results it can be seen that, at the distribution substation, the 33 kV side can supply a fault current of 7870.9A and a three-phase short circuit duty of approximately 450MVA. The circuit equivalent was then determined by the following calculations.

For a system base of 100MVA and nominal bus voltage at the San Juan 33kV bus,

$$I_{sc\_actual} = I_{sc\_pu} \times I_{base}$$

$$I_{base} = \frac{MVA}{\sqrt{3}kVA} = \frac{100 \times 10^6}{\sqrt{3} \times 33 \times 10^3} = 1749.5462A$$

$$I_{sc\_pu} = \frac{I_{sc\_actual}}{I_{base}} = \frac{7870.9}{1749.5462} = 4.4988\, p.u.$$

From the per unit theory,

$$Z_{eq\_pu} = \frac{V_{pu}}{I_{pu}} = \frac{1.0}{4.4988\angle -81.25°} = 0.2223\angle 81.25° = 0.03382 + j0.2197$$

where the base impedance Z_{base} is,

$$Z_{base} = \frac{{kV_{base}}^2}{\mathrm{MVA}_{base}} = \frac{33^2}{100} = 10.89\Omega$$

And the actual Thevenin's equivalent impedance is,

$$Z_{eq\_actual} = Z_{eq\_pu} \times Z_{base} = 0.2223\angle 81.25° \times 10.89 = 2.4206\angle 81.25°\Omega$$

$$= 0.3683 + j2.3927\Omega$$

Although this analysis could have been done at the 12kV side, the 33kV bus was selected so as to include the substation transformers in the distribution system. This gives the option of analysis of the impact on these assets for EV integration.

SUBSTATION

Modelling of the substation only involves that of the two power transformers. The transformers at this substation has online tap changers for automatic voltage regulation. This type of transformer control is not available in the standard EMTP libraries. As such, one would have to be modelled. Online tap control (OLTC) was implemented by modifying a model obtained from the EMTP application cases. The control setting and transformer vector group was manually modified within the sub circuit to match the CYME transformer model as closely as possible. Figures and shows the transformer and OLTC sub circuits modelled in EMTP.

The technical specifications of power and voltage ratings and impedance of these transformers were obtained from the utility via the CYME model where this data was also embedded. Using some fundamental calculations on the impedance data retrieved from the

CYME transformer model to satisfy the format in the EMTP transformer model, the impedances were entered. Simple tests were performed on both models (in CYME and EMTP) to validate the model developed in EMTP.

FEEDER CIRCUIT CHARACTERISTICS AND COMPONENTS

The characteristics of a typical distribution feeder in Trinidad and Tobago, according to the utility, is 3-phase, 4-wire, 12kV supply which can be a maximum of 25 kilometers long. Each feeder is protected by a circuit breaker at the substation and by fuses for each branch line.

The feeder conductor used is solely overhead lines. The topologies are modelled using Global Information Systems (GIS) data acquired from T&TEC for the four (4) 12kV feeders. This data is represented on geographical maps that show the exact route of the lines and the locations of each service transformer and metered customer. It does not, however, link the number and location of customers for each service transformer. This GIS data is shown in Appendix I.

The technical specifications for the electrical modelling of the overhead lines and service transformers will also be acquired from the utility. Specifics on the data obtained thus far and the modelling approaches are as follows.

OVERHEAD LINES

The conductors of the distribution system consist of overhead main feeder lines of a high capacity as well as overhead lines of a lower capacity that branch off the main lines. These capacities along with the specific conductor impedances used on the feeders under study have not yet been acquired from the utility. They, however, have provided some typical impedance data in the interim as shown in Table 6.

TABLE 6: TYPICAL 12KV FEEDER IMPEDANCE DATA USED BY TTEC

Phase Conductor	Neutral Conductor	Positive Sequence Impedance (Ohms/km)		Zero Sequence Impedance (Ohms/km)	
		R	X	R	X
Darien	Raven (1/0)	0.1417	0.3818	0.4875	1.3100
Canton	Raven (1/0)	0.2002	0.3949	0.5460	1.3240
Penguin (4/0)	Raven (1/0)	0.3729	0.4251	0.7216	1.3470
Raven (1/0)	Raven (1/0)	0.5339	0.4508	0.8802	1.3780

These are per length (km) impedances will introduce voltage drops and system losses as the feeder length increases. The conductors used for initial modelling were Penguin for the main feeder lines and Raven for the branch lines.

From inspection of the GIS data provided, the distances between each successive pole mounted transformers varied widely from being immediately adjacent to each other to as much as 100 meters apart. This would evidently be based on the density of customers in each particular area.

Due to the length and complexity of the feeders, they were not modelled in detail i.e. per pole mounted transformer. Instead, sections of feeder were modelled using a short PI line model in EMTP where all service transformers positioned along that section were lumped at the end of the line. This introduces minor errors as the voltage drops and line losses would be greater than actually realized. Using the GIS data, and online mapping of the area (GoogleMaps), distances were obtained for each section.

SERVICE TRANSFORMERS

A typical single feeder circuit from a distribution substation in Trinidad services thousands of metered customers. The distribution of customer type (residential, commercial, industrial etc.) varies with location. For the predominantly residential feeder of the San Juan area, it will be assumed that assume that the customers are 100% residential. As such, the study will be limited to only single phase pole mounted transformers.

As previously mentioned, the feeder model was developed in such a way that each lumped load represents several service transformers which in turn is loaded as per the demand of the connected metered customers. Since the number and location of customers for each service transformer was not indicated on the GIS mapping provided, the number of customers per pole mounted transformers would have to be estimated.

A typical pole mounted transformer used by the utility is rated at 50kVA, with smaller sizes being used in special cases which will not be considered in this study. Also, a standard 50kVA transformer loading varies widely from 10-25 metered customers due to the great differences in the demand of customers of different socio-economic privileges. For the San Juan area a typical value of 15 will be assumed as the number that corresponds to middle and upper class customers.

The phase selection per service transformer will be selected so as to balance the overall three phase loading of each feeder as this information was also not indicated on the GIS mapping. Typical to distributions systems, the overall three phase load will not be perfectly balanced especially when considering the dynamic load.

Similar to the overhead lines, the transformer impedances will contribute to voltage drop and system losses. Impedances, X/R ratios and all electrical characteristics of service transformers are yet to be acquired from the utility. They are modelled using the lossless single phase m-winding transformers EMTP-RV model in the interim.

BASE LOAD MODELING

All customers connected to the feeders are assumed to be residential customers due to a lack of utility data provided. In Trinidad and Tobago, the residential characteristic of supply is defined as, single-phase, AC, 60 Hz, 2-wire or 3-wire, at 115 V or 115/230 V respectively.

Metered load data at 15 minute intervals for the total load and of each of the four feeders at the San Juan substation was provided for the days of January and February of the year 2016. This, however, is not useful for an impact study which requires data at a more granular level. Sample load data at the customer level as recorded by the utility's Advanced Metering Infrastructure (AMI) has yet to be provided from the utility for different socio-economic residential customers. Once acquired, this data would be used as the basis for modelling the typical residential load for customers in the area.

For impact studies, residential and commercial demands are typically modeled as constant power loads. This study, however, intends to consider a dynamic load i.e. the load profile to more accurately assess what the voltage profile and loading on the feeder would vary during the 24 hour period. A typical daily load demand curve will be derived from the data which will be assumed to be the consumption of each household on the modelled system. This will be modelled using the standard dynamic load model available in the EMTP library. A time series load flow analysis will then be conducted for the residential load only (with 0% EV penetration). The results of this simulation will be used to establish a baseline or starting point for data analysis and trending for this EV integration impact study.

Battery Electric Vehicle Load Modeling

In this section, the BEV load refers to all EV related components connected to the electrical grid i.e. both the charger and the battery. According to the objectives of the project, both components are to be modelled in detail to represent the dynamic load of the BEV during the charging cycle. The characteristic of the battery charger affects the charge rate and time. The charger and its controls determine the current draw and hence power requirement from the grid. At this rate, the charging time is based, in turn, on the battery's initial SOC, capacity and unique charge cycle. Specifics on the modelling of these components are as follows.

Battery Modelling

As specified by the scope of this study, the battery of the BEV will be modelled in detail to represent its dynamic behavior on the system when charging. This behavior includes an accurate reflection of the battery voltage and SOC when charged at a certain uncoordinated rate as stipulated by the charger (charging level and infrastructure).

According to the literature review performed on existing battery models, a dynamic impedance based model would be optimal for use in this study in order to accurately predict I-V characteristics and the transient behavior of the battery. SOC estimation as performed by the BMU will also need to be done within this model. This is an important parameter for the charge control module, another function of the BMU, which also needs to be implemented to perform the constant current, constant voltage charge scheme. The model will also be capable of specifying initial SOC as an input to appropriately reflect the charge duration.

The equivalent circuit model of the battery to be used is presented in Figure 25 below. The battery output voltage is determined by using the relationship between the open circuit voltage V_{oc}, internal resistance, R_{series}, and the RC networks which models the short and long load transient responses.

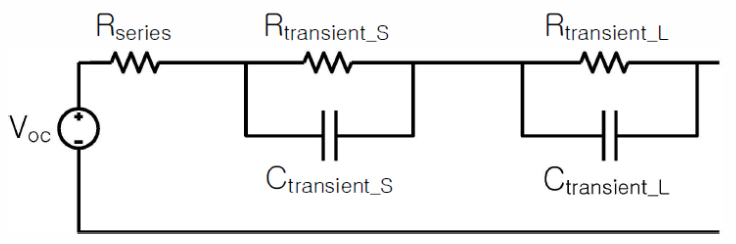

FIGURE 25: SELECTED EQUIVALENT CIRCUIT BATTERY MODEL

Each of the battery parameters shown in Figure 25 are dependent on the SOC for Li-ion batteries and are calculated from equations 2-7 given below (Chen and Rincon Mora 2006). They describe the general dynamic behavior of Li-ion batteries.

$$V_{OC}(SOC) = 1.031e^{-35SOC} + 3.685 + 0.2156SOC - 0.1178SOC^2 + 0.3201SOC^3 \ldots\ldots (2)$$

$$R_{series}(SOC) = 0.1562e^{-2437SOC} + 0.07446 \ldots\ldots\ldots (3)$$

$$R_{transient\_S}(SOC) = 0.3208e^{-29.14SOC} + 0.04669 \ldots\ldots\ldots (4)$$

$$C_{transient\_S}(SOC) = -752.9e^{-13.51SOC} + 703.6 \ldots\ldots\ldots (5)$$

$$R_{transient\_L}(SOC) = 6.603e^{-1552SOC} + 0.04984 \ldots\ldots\ldots (6)$$

$$C_{transient\_L}(SOC) = -6056e^{-27.12SOC} + 4475 \ldots\ldots\ldots (7)$$

To determine these dynamic internal parameters throughout the charging cycle, SOC needs to be estimated. After consideration of all the battery SOC estimation techniques reviewed, the coulomb method will be employed as the simpler, more direct and transparent method. This method determines the SOC by integrating the charging current as shown in the equation 8 below.

$$SOC = SOC_o + \int_{t_0}^{t} \frac{i}{Q_{rated}} dt \text{.... (8)}$$

where SOC_0 is the initial SOC, i is the charging current and Q_{rated} is the rated capacity of the battery. The charging current supplied from the charger is stipulated by the charge control. In the EMTP-RV software, trapezoidal integration which is well-known method for integration, will be used.

The entire parameter estimation process is summarized in the flowchart presented in Figure 26.

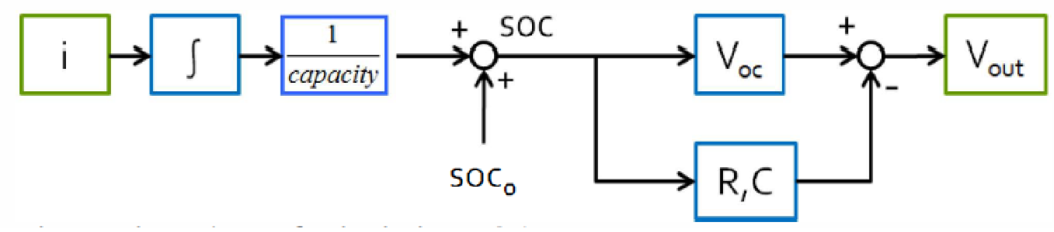

FIGURE 26: BATTERY PARAMETER ESTIMATION FLOWCHART

None of the standard libraries in EMTP-RV contain detailed battery models. However, one was located on the software's online exchange platform as part of a micro grid applications library. Therefore, before attempting to build the model from basic components in the EMTP-RV software, this model is being tested for suitability of use according to the specifications previously mentioned in this section.

The charging time and initial SOC of the BEVs connected on the network at any particular penetration level will be randomized based on probability density functions. These functions will be derived from actual sample EV demand data of US households in the Midwest region obtained from NREL as previously mentioned in the literature review. The randomization of these variables will be implemented using EMTP-RV's statistical simulation option. As the outputs of a parallel project in the University, the functions have yet to be provided.

CHARGING MODEL

CHARGING DEMANDS

The specific charging power requirements stated in the assumptions at both Level 1 and 2 can be determined by the maximum current allowed to be drawn by the charger. This maximum current will be assumed to be the current drawn from the grid (AC side) by the charger during the constant current portion of the charging cycle. The ratings of overcurrent devices on these charging circuitry give an indication of the maximum current. The power required by the battery during charging will then gradually drop from this maximum value during the constant voltage portion near the end of the charging cycle.

Level 1 charging does not require the installation of any specialized charging infrastructure. It is done via a standard dedicated, 120V AC power receptacle. The charging cord provided with the vehicle has a typical three pronged household plug (NEMA 5-15 connector) on the grid end and the standard SAE J1772 connector on the vehicle end. These standard household sub-circuits have an overcurrent rating of 15A or 20A (NEC, 2018). As per NEC 2018 Article 210 – Branch Circuits, Section 210.20 – Overcurrent Protection, part A – Continuous and Non-continuous Loads,

"*Where a branch circuit supplies continuous loads or any combination of continuous and noncontinuous loads, the rating of the overcurrent device shall not be less than the noncontinuous load plus 125 percent of the continuous load.*"

Conforming to this standard, and assuming the lower of the overprotective devices 15A, the maximum allowable current through the Level 1 charging circuit will be 80% of the overcurrent rating, i.e. 12A, and hence a maximum instantaneous apparent power demand of 1.44kVA on the grid. A full level 1 charging cycle general takes 8 -16 hours depending on the battery technology and as such will commonly be charged overnight at the vehicle owner's residence.

Level 2 charging, on the other hand, requires the installation of dedicated EVSE which has a rating of at least 40A. Level 2 charging cords utilizes the very same SAE J1772 vehicle connector used for Level 1 charging. Assuming an overcurrent device rating of 40A, the maximum allowable current drawn from the grid would be 32A (NEC, 2018) which corresponds to a maximum instantaneous apparent power demand of 7.68kVA. A full level 2 charging cycle general takes 4 -6 hours depending on the battery technology and as such will commonly found in both residential and commercial settings.

The assumed characteristics for both Level 1 and 2 charging is summarized in Table 7 below.

TABLE 7: EV CHARGING RATINGS FOR LEVEL 1 AND LEVEL 2 AC CHARGING

Charging Level	Voltage/ VAC	Current/ A	Assumed Power Factor	Power/ kVA
Level 1	120	12	0.8	1.44
Level 2	240	32	0.8	7.68

CHARGER MODEL

The charger comprises several power electronic circuits which serve different functions. In its completeness, it contains an electromagnetic (EMI) filter, rectifier (AC-DC converter), power factor correction circuit, inverter and isolator, and finally a DC-DC converter which then connects to the battery. Some applications do not have EMI filters or isolation transformers which removes need for the inverter.

As guided by the literature review on existing charger topologies, the designed battery charger should be of high efficiency and cause minimal disturbance on the network. The on-board, unidirectional full-bridge series resonant charger presented by Choe et al. (2010) was selected for modelling. The circuitry for this charger is given in Figure 27 below. It utilizes a conventional boost PFC topology and a full bridge DC-DC converter topology as guided by the literature review. This model was selected specifically for its application to onboard Level 1 and 2 AC uncoordinated charging.

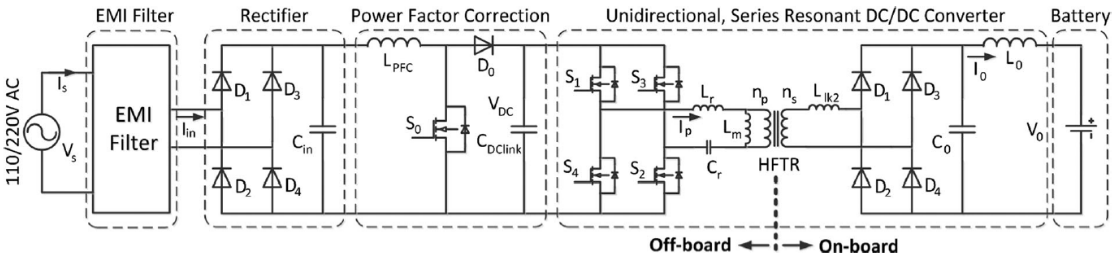

FIGURE 27: SELECTED BATTERY CHARGER MODEL

The EMI filter may be excluded from the design as it is not relevant to include this protective measure for simulation purposes. The charger and its controls including the PI control for the charging process has yet to be implemented and tested in EMTP.

The overall block diagram of the BEV component of the project is summarized in Figure 28.

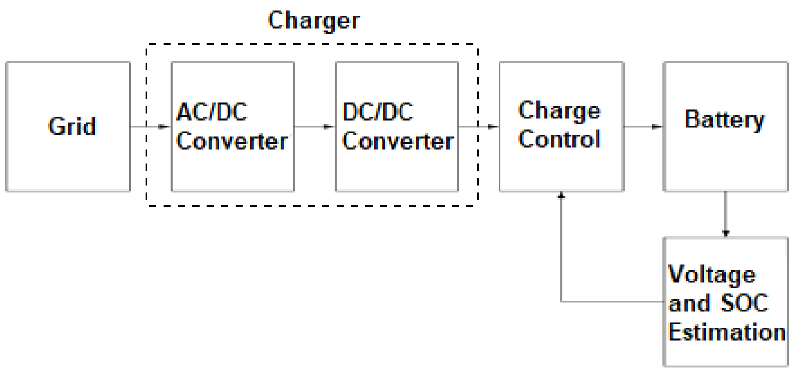

FIGURE 28: BLOCK DIAGRAM OF EV LOAD

Preliminary Results

Figure 29e 29 shows the EMTP-RV model of the San Juan distribution system that was created based on the utility data acquired and summarized in the preceding chapter. The network consists of the substation transformers and buses and four (4) radial feeders each of which contain branches at various points along the main feeder.

Figure 30 shows the power transformers sub circuit model where the DYN11 configuration was built and the OLTC for automatic voltage regulation was implemented. The tap settings of the EMTP-RV model were closely matched from the CYME transformer model as indicated in Figure 31.

The four (4) feeder models are presented in Figures 32-35. Each feeder node has a lumped load sub circuit connected, labelled “L”, which contain both the aggregated base residential load and EV the load.

Figure 36 shows the LV lumped load sub circuit model. This consists of the pole mounted transformers as well as the customers serviced by each. This is where the aggregated dynamic load model representing the residential load and the BEV load models (charger and battery) would be interfaced as clearly indicated in the diagram.

The EV load model has not yet been developed. However, Figure 37 illustrates the structure of the EV load sub circuit. It consists of a manual switch to toggle between Level 1 and Level 2 charging and sub circuits for both the charger and battery model. The charger and its control scheme has yet to be implemented. The battery model illustrated, as mentioned in the last section is the model acquired from the software’s online exchange platform. Its sub circuit is given in Figure 38. It is currently undergoing unit testing to assess its suitability for this project.

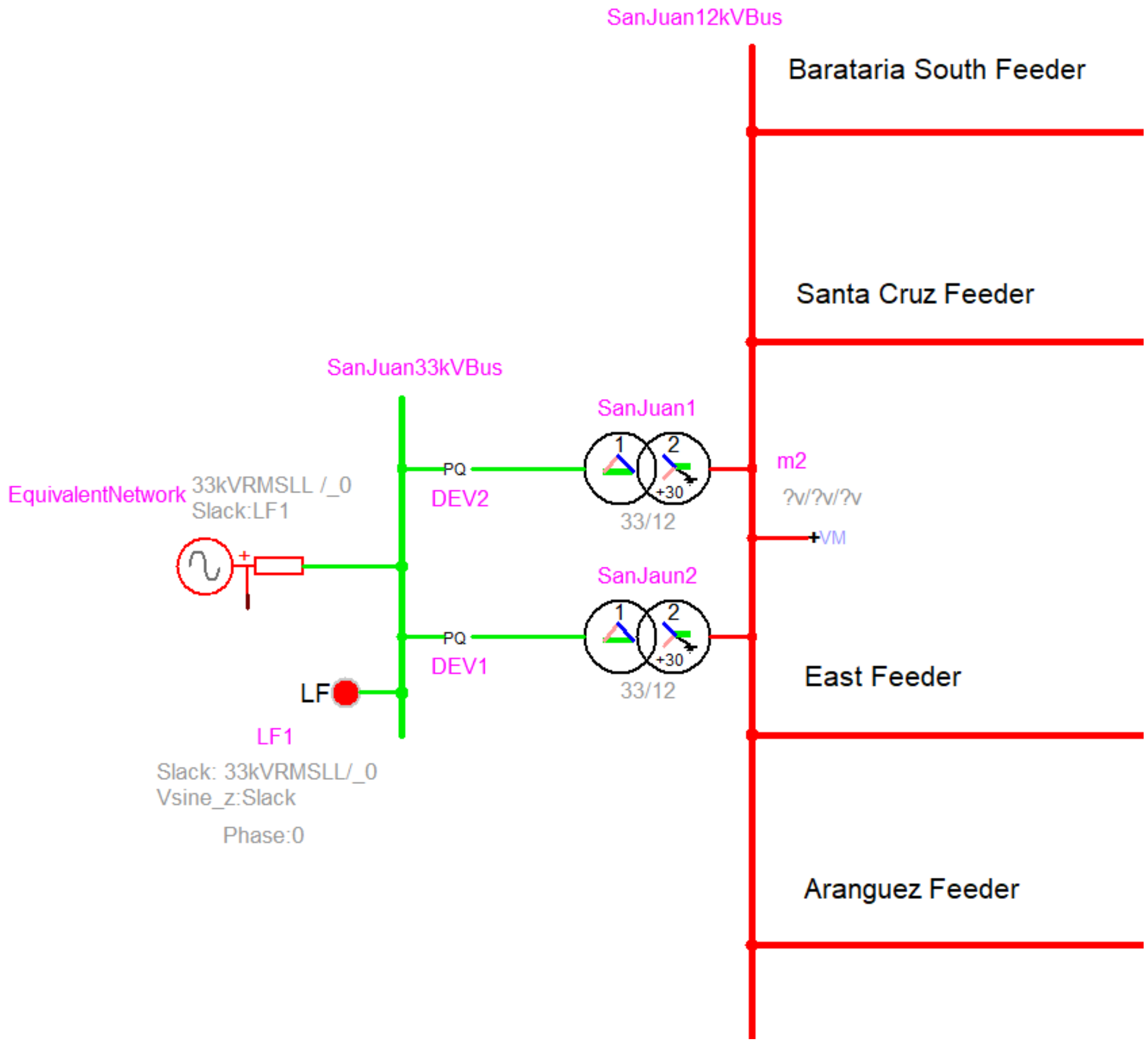

FIGURE 29 – EMTP BASED MODEL FOR SAN JUAN SUBSTATION

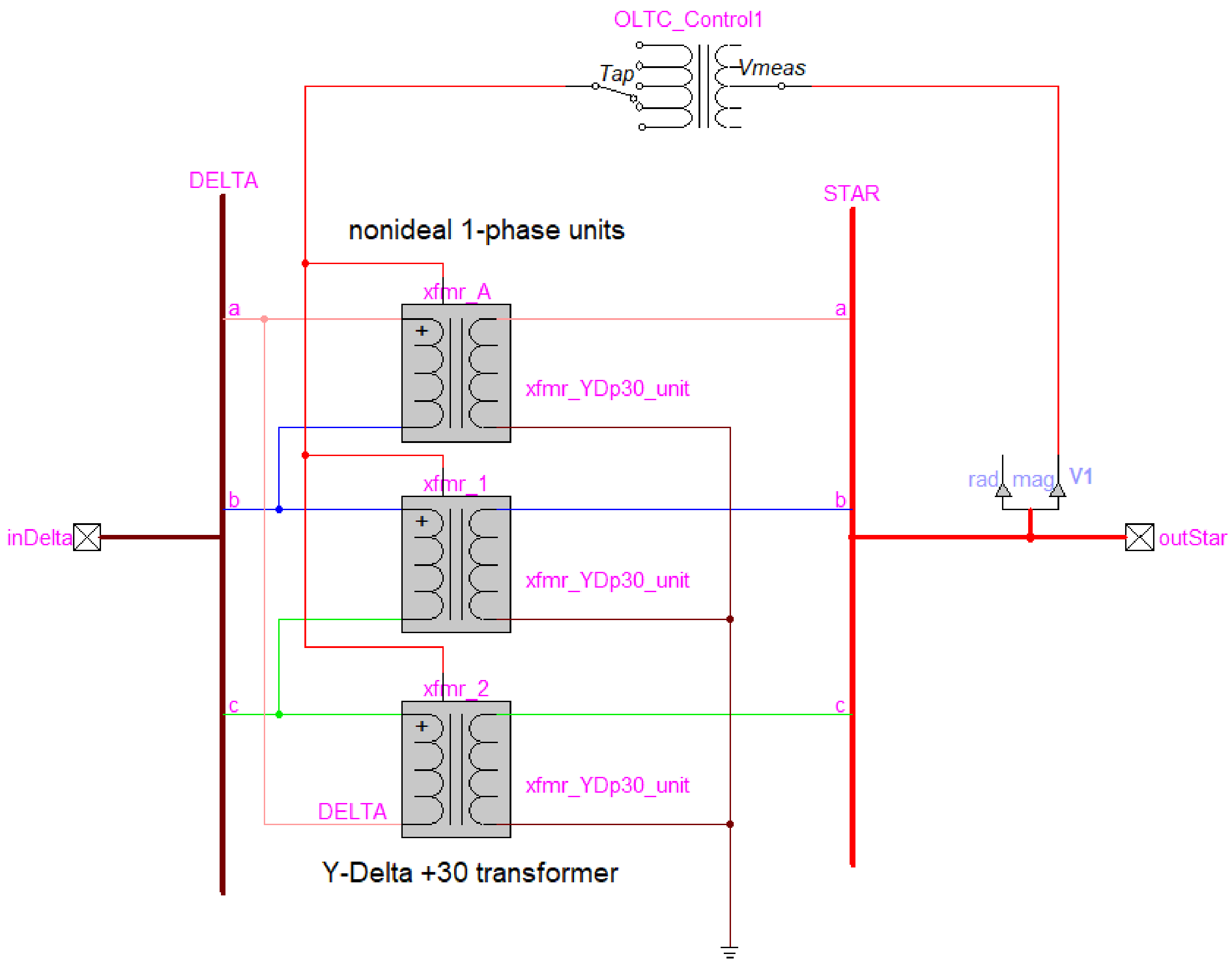

FIGURE 30: EMTP BASED MODEL FOR OLTC TRANSFORMER

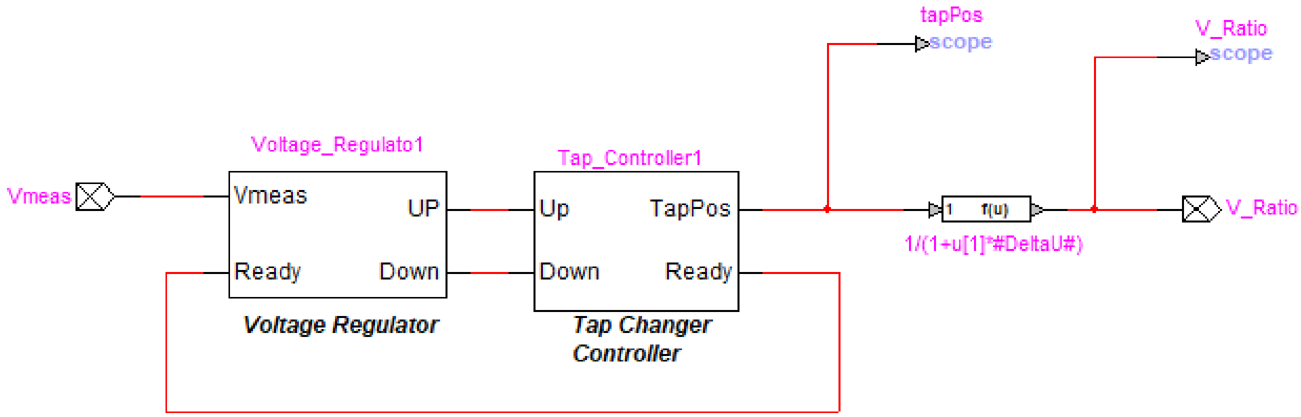

Initial Parameters-Values: Text mode input Disable ☐ Collapse

```
V_SS_LL        = 12         // Nominal LL Voltage in kV (regulated side)
NumberOfTaps   = 60            // Number of Taps: -NbTaps<=TapPos<=NbTaps
DeltaU         = 0.005      // Voltage step DeltaU per Tap (pu)
InitialTap     = 0              // initial Tap position
MecDelay       = 0.5              // Tap Mechanical Delay in second
//Voltage Regulator
RegOn            = 1          // 0 off , 1 On. If Off keep InitialTap
Vref_pu          = 1.03       // Desired Regulated Voltage in pu of V_SS_LL
DeadBand         = 0.015      // Dead Band limit in pu
Td0              = 15         // voltage regulator fix time delay
Td_select        = 2          // 1 fix, 2 inverse
Td_first         = 4;         // Time to first change
change_dur        = 0.5;          // minimum variation time in sec. to initiate a tap change
```

FIGURE 31: EMTP BASED MODEL FOR OLTC CONTROL AND SETTINGS

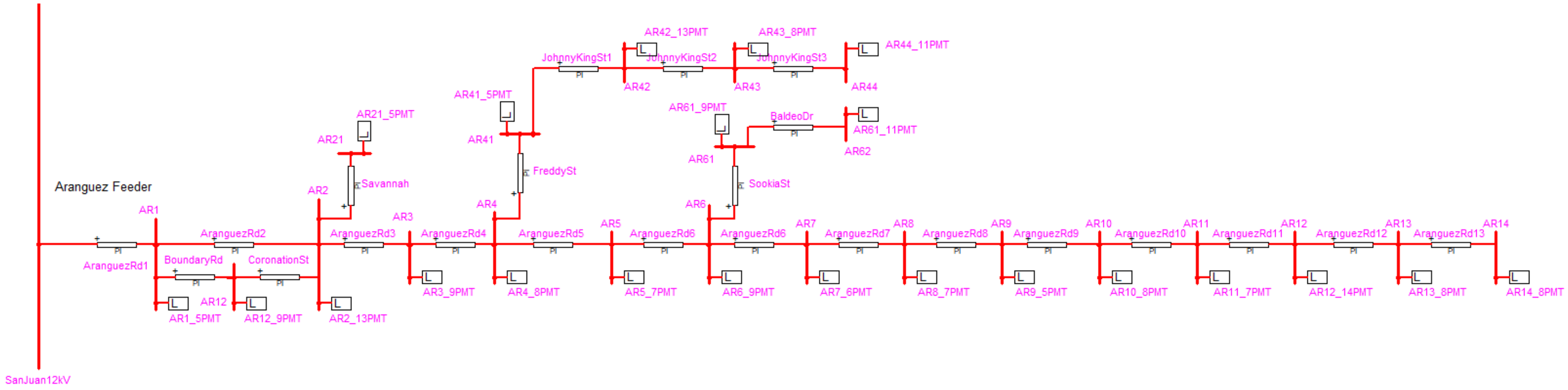

FIGURE 32: EMTP BASED MODEL FOR ARANGUEZ FEEDER

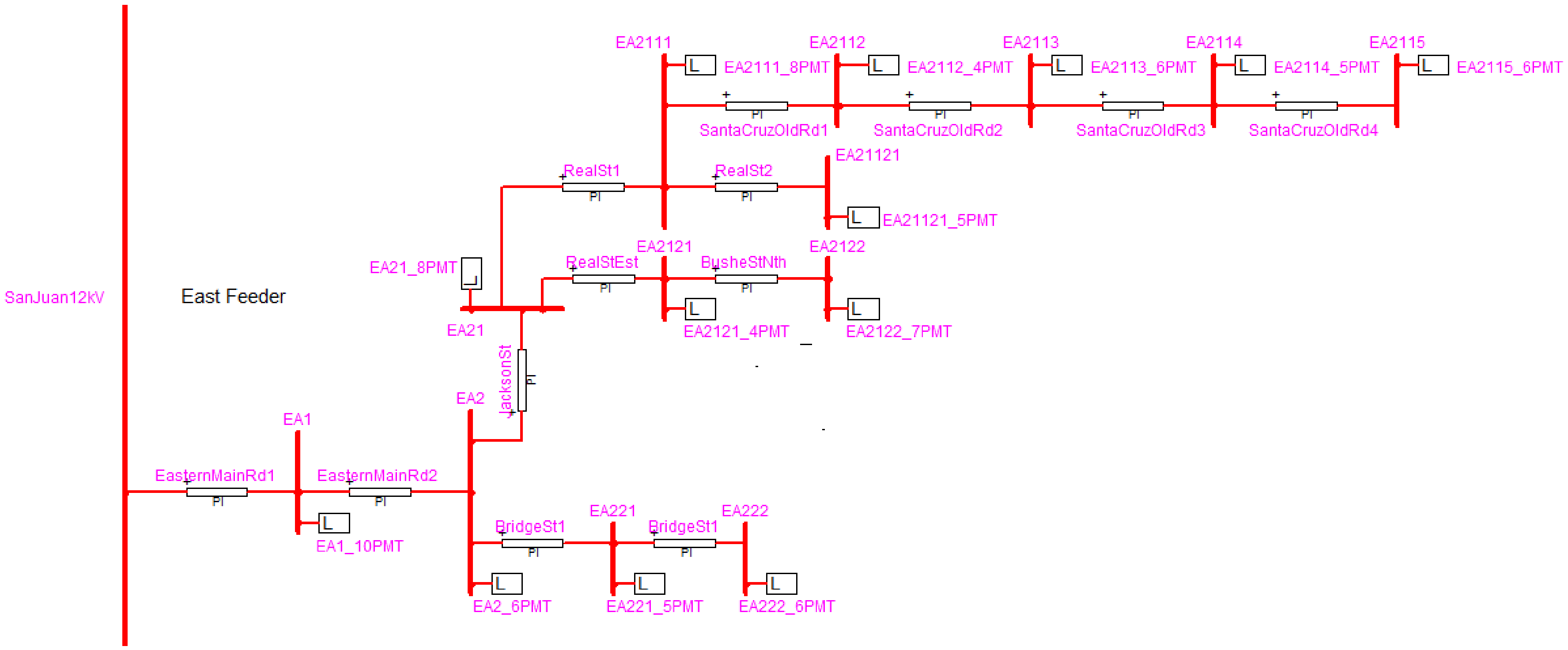

FIGURE 33: EMTP BASED MODEL FOR EAST FEEDER

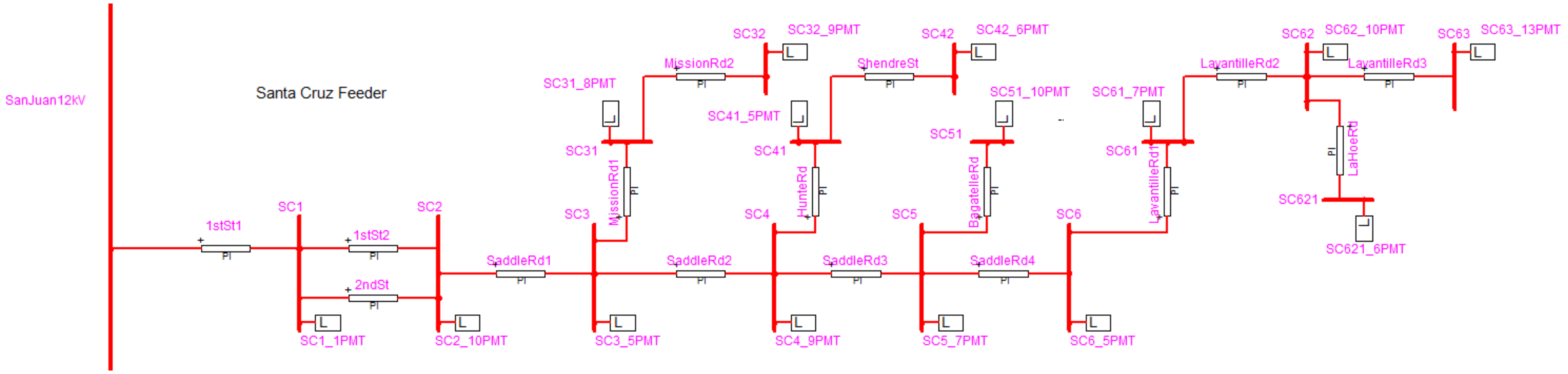

FIGURE 34: EMTP BASED MODEL FOR SANTA CRUZ FEEDER

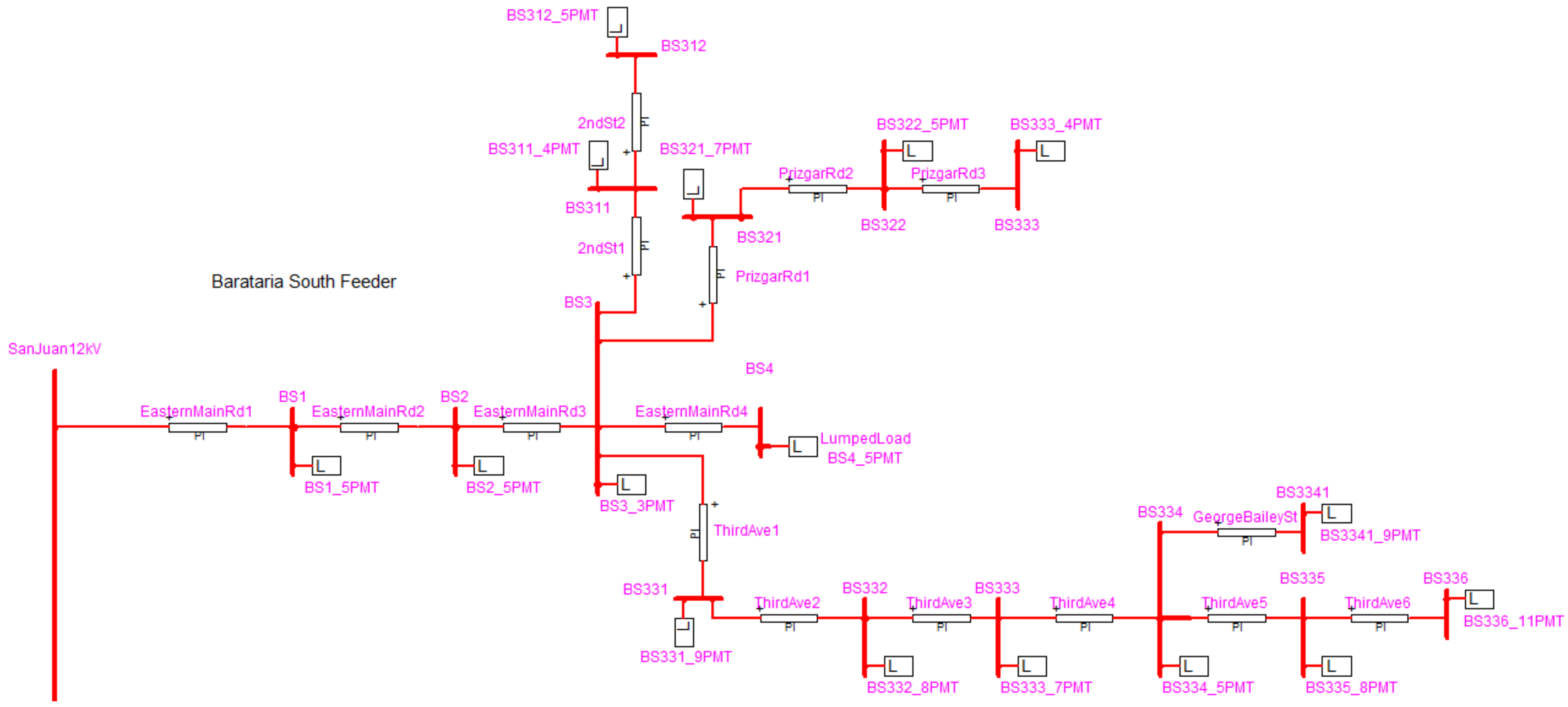

FIGURE 35: EMTP BASED MODEL FOR BARATARIA SOUTH FEEDER

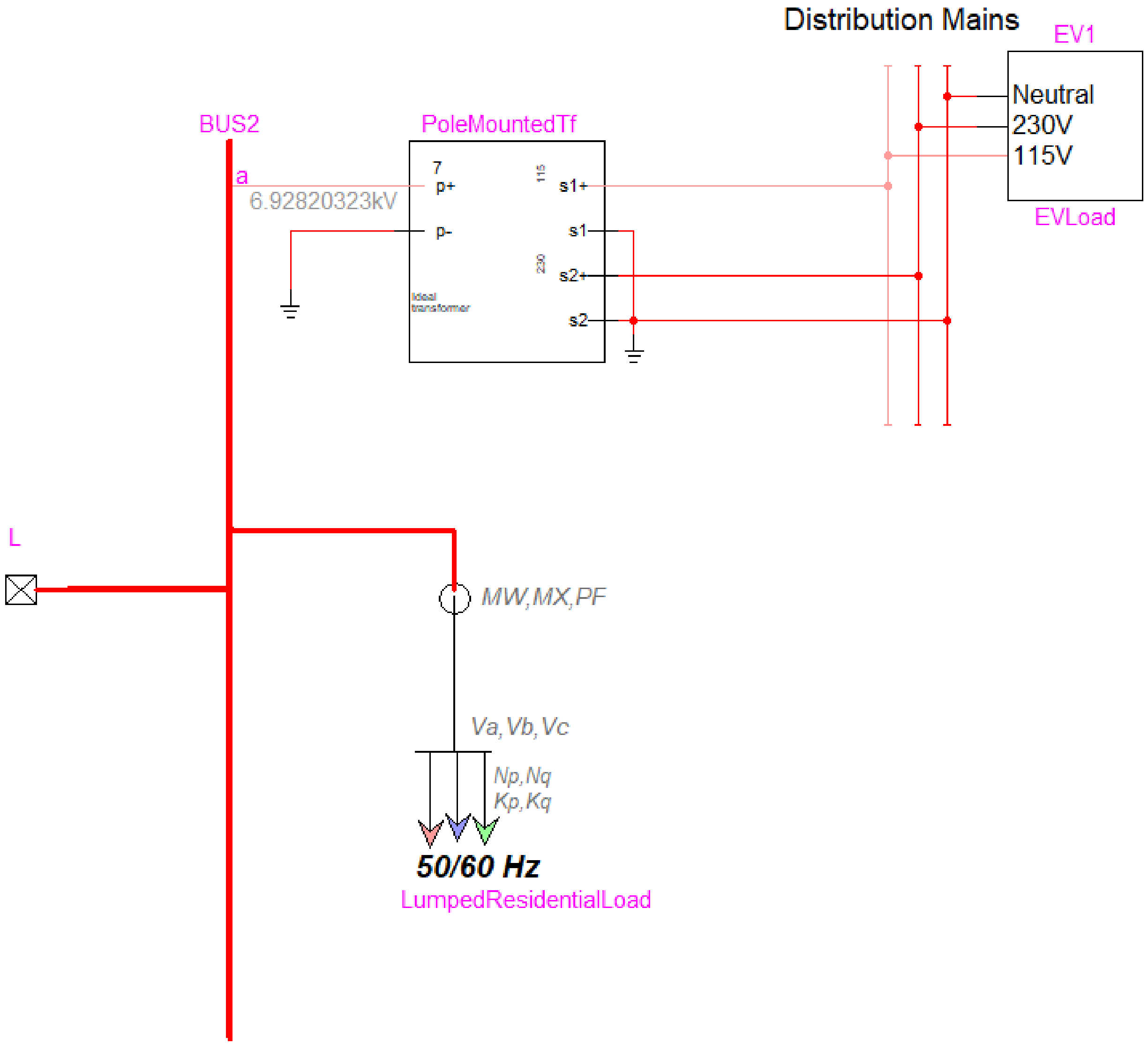

FIGURE 36: EMTP BASED LOAD SUBCIRCUIT

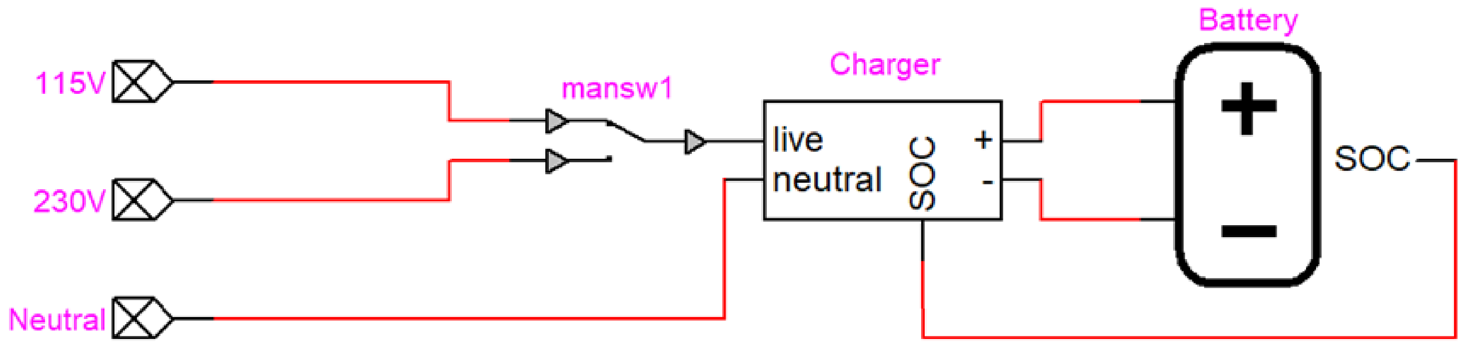

FIGURE 37: EMTP BASED EV LOAD SUBCIRCUIT

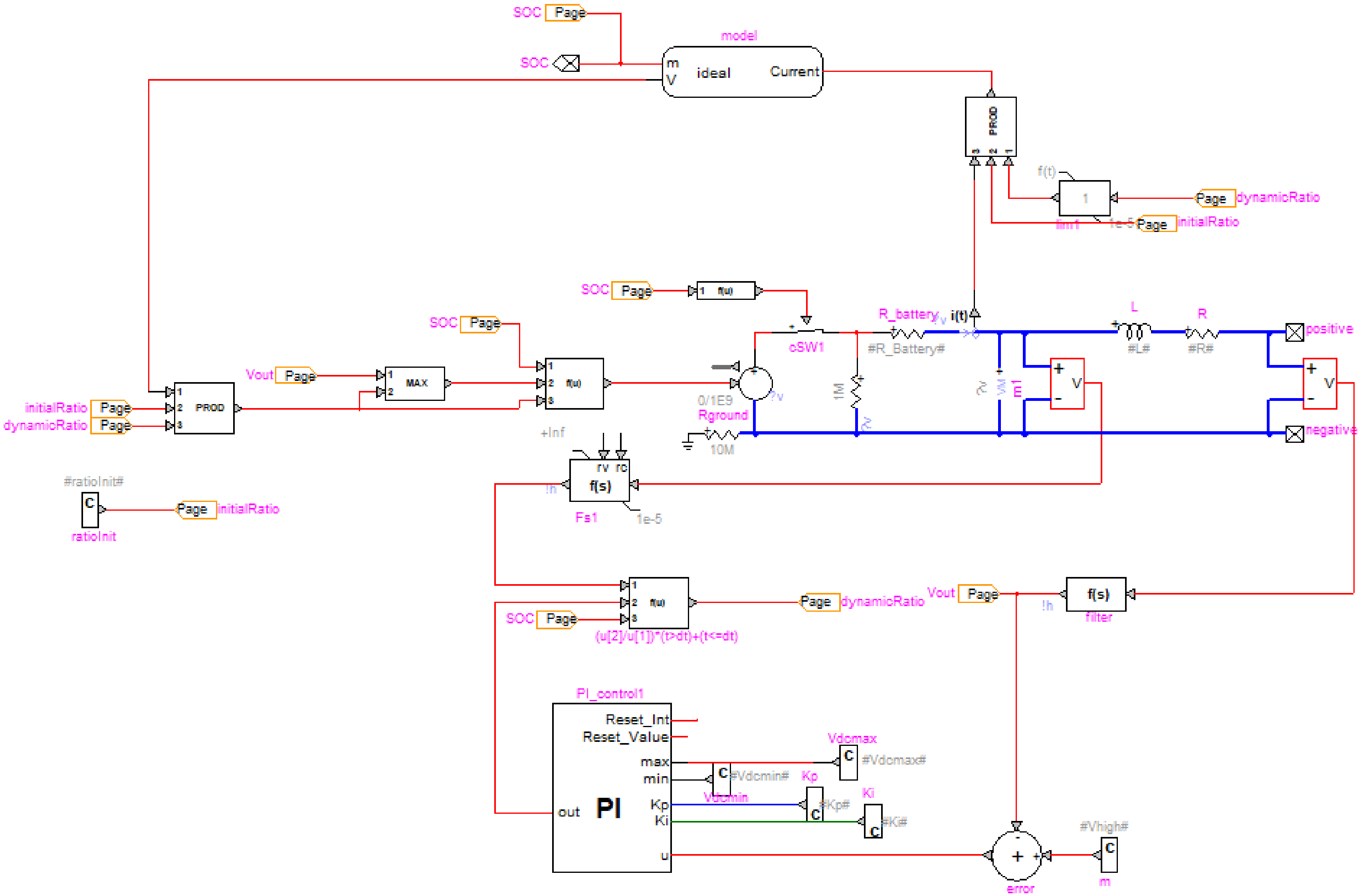

FIGURE 38: EMTP BASED BATTERY SUBCIRCUIT

PROJECT IMPLEMENTATION PLAN

The implementation of the project will continue with the construction and testing of the EV load models. The current model will be tested and if found unacceptable for the purposes of this study, detailed modelling of the battery will be conducted according to the proposed method stated. After accurate estimation of the battery parameters and SOC is achieved throughout the charging cycle, the charger circuit topology and associated controls will be implemented. The charger model selected and built will accurately perform the constant current, constant voltage charging regime at both Levels 1 and 2 based on the grid connection.

Unit testing of the entire EV load component will follow the successful modelling of the charger. This detailed modelling represents the most challenging aspect of the project and will therefore take the most time to complete. The sourcing and use of generic battery and charger models will be considered before attempts to model in detail. However, the transient analysis of EV load integration will not be accurately assessed if these components are not modelled in detail.

The statistical analysis and modelling of the dynamic residential load and EV probability density functions for charging time and duration will then be performed. This was chosen to be undertaken after the modelling of the network and EV load models so as to utilize the models for testing the statistical data inputs. Time was also given for the utility to acquire and provide the AMI data and component specifications still pending. If at this point no data is acquired, a generic residential load profile model will be developed and integrated with the completed system. Standard functions such as Gaussian etc. available in the EMTP-RV software will be used to randomize charging time and duration until the data is made available.

Subsequent to all component modelling, is integration and testing. Provided that the components integrate on the system without error, the impact analysis can be conducted at different charging and penetration levels. Collection of results, analysis of those results and conclusions would then follow.

All the aforementioned steps of the projected plan and their time budgets allocations are presented in the progressive Gantt chart shown in Figure 39.

EXPECTED RESULTS

Like any other EV integration impact study, the expected results would be the voltage each node, and loading and losses in each feeder line segment and transformer in the distribution network for the different charging and penetration levels considered. Harmonic injection will also be analyzed at different points in the network. These parameters would be compared against power quality thresholds and equipment ratings to identify the potential network violations.

As this project models the load dynamically, 24 hour profiles for these parameters will be obtained per case which would provide more detailed information not only on the violations at different EV loading scenarios, but the time at which they occur during the day. These results will give a more accurate indication of the limits of the network for EV integration.

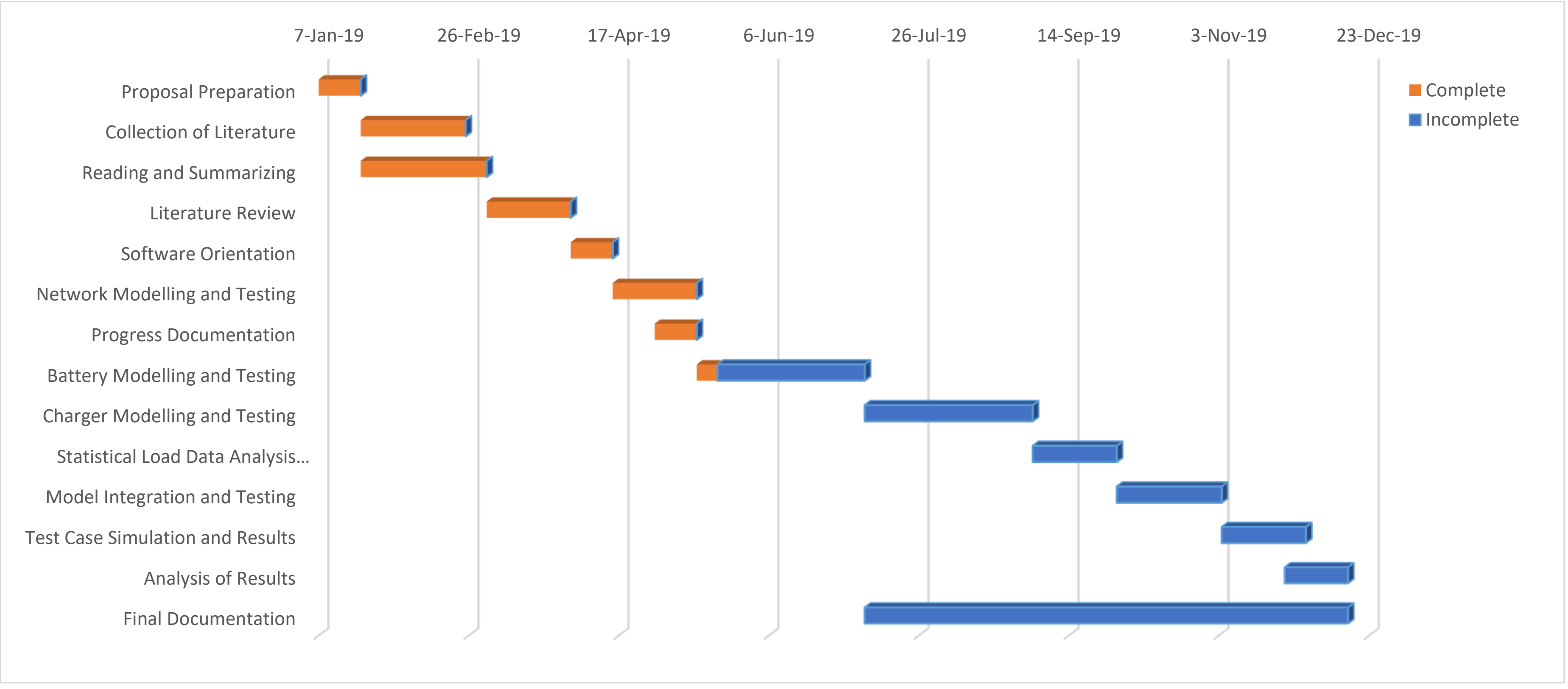

FIGURE 39: PROGRESSIVE GANTT CHART

References

Affanni, Antonio, Alberto Bellini, Giovanni Franceschini, Paolo Guglielmi, and Carla Tassoni. 2005. "Battery Choice and Management for New-Generation Electric Vehicles." *IEEE Transactions on Industrial Electronics* 52 (5):1343-1349.

Akhavan-Rezai, E, MF Shaaban, EF El-Saadany, and Aboelsood Zidan. 2012. "Uncoordinated Charging Impacts of Electric Vehicles on Electric Distribution Grids: Normal and Fast Charging Comparison." 2012 IEEE Power and Energy Society General Meeting.

Budhia, Mickel, Grant A Covic, John T Boys, and Chang-Yu Huang. 2011. "Development and Evaluation of Single Sided Flux Couplers for Contactless Electric Vehicle Charging." 2011 IEEE Energy Conversion Congress and Exposition.

Buller, Stephan, Marc Thele, Rik WAA De Doncker, and Eckhard Karden. 2005. "Impedance-Based Simulation Models of Supercapacitors and Li-Ion Batteries for Power Electronic Applications." *IEEE Transactions on Industry Applications* 41 (3):742-747.

Chang, Wen-Yeau. 2013. "The State of Charge Estimating Methods for Battery: A Review." *ISRN Applied Mathematics* 2013.

Chen, Min, and Gabriel A Rincon-Mora. 2006. "Accurate Electrical Battery Model Capable of Predicting Runtime and Iv Performance." *IEEE transactions on energy conversion* 21 (2):504-511.

Chiasson, John, and Baskar Vairamohan. 2003. "Estimating the State of Charge of a Battery." Proceedings of the 2003 American Control Conference, 2003.

Dhameja, Sandeep. 2001. *Electric Vehicle Battery Systems*: Elsevier.

Elankurisil, SA, and SS Dash. 2011. "Comparison of Isolated and Non-Isolated Bi-Directional Dc-Dc Converter for Dc Motor." *Journal of Electrical Engineering*:1-9.

Erdinc, Ozan, Bulent Vural, and Mehmet Uzunoglu. 2009. "A Dynamic Lithium-Ion Battery Model Considering the Effects of Temperature and Capacity Fading." 2009 International Conference on Clean Electrical Power.

Fotouhi, Abbas, Daniel J Auger, Karsten Propp, Stefano Longo, and Mark Wild. 2016. "A Review on Electric Vehicle Battery Modelling: From Lithium-Ion toward Lithium–Sulphur." *Renewable and Sustainable Energy Reviews* 56:1008-1021.

Fotouhi, Abbas, Daniel J Auger, Karsten Propp, Stefano Longo, and Mark Wild. 2016. "A Review on Electric Vehicle Battery Modelling: From Lithium-Ion toward Lithium–Sulphur." *Renewable and Sustainable Energy Reviews* 56:1008-1021.

García-Plaza, M, D Serrano-Jiménez, J Eloy-García Carrasco, and J Alonso-Martínez. 2015. "A Ni–Cd Battery Model Considering State of Charge and Hysteresis Effects." *Journal of Power Sources* 275:595-604.

Garcia-Valle, Rodrigo, and João A Peças Lopes. 2012. *Electric Vehicle Integration into Modern Power Networks*: Springer Science & Business Media.

Gold, Sean. 1997. "A Pspice Macromodel for Lithium-Ion Batteries." The twelfth annual battery conference on applications and advances.

Gomadam, Parthasarathy M, John W Weidner, Roger A Dougal, and Ralph E White. 2002. "Mathematical Modeling of Lithium-Ion and Nickel Battery Systems." *Journal of power sources* 110 (2):267-284.

Grenier, Mathieu, MG Hosseini Aghdam, and Torbjörn Thiringer. 2010. "Design of on-Board Charger for Plug-in Hybrid Electric Vehicle."

Grosjean, Camille, Pamela Herrera Miranda, Marion Perrin, and Philippe Poggi. 2012. "Assessment of World Lithium Resources and Consequences of Their Geographic Distribution on the Expected Development of the Electric Vehicle Industry." *Renewable and Sustainable Energy Reviews* 16 (3):1735-1744.

Grosjean, Camille, Pamela Herrera Miranda, Marion Perrin, and Philippe Poggi. 2012. "Assessment of World Lithium Resources and Consequences of Their Geographic Distribution on the Expected Development of the Electric Vehicle Industry." *Renewable and Sustainable Energy Reviews* 16 (3):1735-1744.

Gruosso, Giambattista. 2016. "Analysis of Impact of Electrical Vehicle Charging on Low Voltage Power Grid." 2016 International Conference on Electrical Systems for Aircraft, Railway, Ship Propulsion and Road Vehicles & International Transportation Electrification Conference (ESARS-ITEC).

Haghbin, Saeid, Kashif Khan, Sonja Lundmark, Mats Alaküla, Ola Carlson, Mats Leksell, and Oskar Wallmark. 2010. "Integrated Chargers for Ev's and Phev's: Examples and New Solutions." The XIX International Conference on Electrical Machines-ICEM 2010.

Hannan, Mahammad A, Md Murshadul Hoque, Aini Hussain, Yushaizad Yusof, and Pin Jern Ker. 2018. "State-of-the-Art and Energy Management System of Lithium-Ion Batteries in Electric Vehicle Applications: Issues and Recommendations." *Ieee Access* 6:19362-19378.

Hoque, MM, MA Hannan, and Azah Mohamed. 2016. "Voltage Equalization Control Algorithm for Monitoring and Balancing of Series Connected Lithium-Ion Battery." *Journal of Renewable and Sustainable Energy* 8 (2):025703.

Hoque, MM, MA Hannan, Azah Mohamed, and Afida Ayob. 2017. "Battery Charge Equalization Controller in Electric Vehicle Applications: A Review." *Renewable and Sustainable Energy Reviews* 75:1363-1385.

Jang, Yungtaek, and Milan M Jovanovic. 2007. "Interleaved Boost Converter with Intrinsic Voltage-Doubler Characteristic for Universal-Line Pfc Front End." *IEEE Transactions on Power Electronics* 22 (4):1394-1401.

Jang, Yungtaek, and Milan M Jovanovic. 2009. "A Bridgeless Pfc Boost Rectifier with Optimized Magnetic Utilization." *IEEE Transactions on Power Electronics* 24 (1):85-93.

Jiang, Bo. 2013. "From Electrode Materials to Dynamic Models of Li-Ion Cells." The Ohio State University.

Karmaker, Ashish Kumar, Sujit Roy, and Md Raiu Ahmed. 2019. "Analysis of the Impact of Electric Vehicle Charging Station on Power Quality Issues." 2019 International Conference on Electrical, Computer and Communication Engineering (ECCE).

Kennedy, B, D Patterson, and S Camilleri. 2000. "Use of Lithium-Ion Batteries in Electric Vehicles." *Journal of Power Sources* 90 (2):156-162.

Kennedy, B, D Patterson, and S Camilleri. 2000. "Use of Lithium-Ion Batteries in Electric Vehicles." *Journal of Power Sources* 90 (2):156-162.

Kroeze, Ryan C, and Philip T Krein. 2008. "Electrical Battery Model for Use in Dynamic Electric Vehicle Simulations." 2008 IEEE Power Electronics Specialists Conference.

Lai, Qinzhi, Huamin Zhang, Xianfeng Li, Liqun Zhang, and Yuanhui Cheng. 2013. "A Novel Single Flow Zinc–Bromine Battery with Improved Energy Density." *Journal of Power Sources* 235:1-4.

Lai, Qinzhi, Huamin Zhang, Xianfeng Li, Liqun Zhang, and Yuanhui Cheng. 2013. "A Novel Single Flow Zinc–Bromine Battery with Improved Energy Density." *Journal of Power Sources* 235:1-4.

Leou, Rong-Ceng, Chun-Lien Su, and Chan-Nan Lu. 2013. "Stochastic Analyses of Electric Vehicle Charging Impacts on Distribution Network." *IEEE Transactions on Power Systems* 29 (3):1055-1063.

Liaw, Bor Yann, Ganesan Nagasubramanian, Rudolph G Jungst, and Daniel H Doughty. 2004. "Modeling of Lithium Ion Cells—a Simple Equivalent-Circuit Model Approach." *Solid state ionics* 175 (1-4):835-839.

Liu, Wei, Yu Wang, Xiaolin Jia, and Baojia Xia. 2013. "The Characterization of Lithium Titanate Microspheres Synthesized by a Hydrothermal Method." *Journal of Chemistry* 2013.

Liu, Wei, Yu Wang, Xiaolin Jia, and Baojia Xia. 2013. "The Characterization of Lithium Titanate Microspheres Synthesized by a Hydrothermal Method." *Journal of Chemistry* 2013.

Lu, Languang, Xuebing Han, Jianqiu Li, Jianfeng Hua, and Minggao Ouyang. 2013. "A Review on the Key Issues for Lithium-Ion Battery Management in Electric Vehicles." *Journal of power sources* 226:272-288.

Lu, Languang, Xuebing Han, Jianqiu Li, Jianfeng Hua, and Minggao Ouyang. 2013. "A Review on the Key Issues for Lithium-Ion Battery Management in Electric Vehicles." *Journal of power sources* 226:272-288.

Marcos Pastor, Adrià. 2015. "Design and Control of a Battery Charger for Electric Vehicles." Universitat Rovira i Virgili.

Mathoy, Arno. 2008. "Definition and Implementation of a Global Ev Charging Infrastructure." *PDF). BRUSA Elektronik." SAE J1772-SAE Electric Vehicle*

Conductive Charger Coupler.

Muratori, Matteo. 2017. Impact of Uncoordinated Plug-in Electric Vehicle Charging on Residential Power Demand-Supplementary Data. National Renewable Energy Laboratory-Data (NREL-DATA), Golden, CO (United ….

Muratori, Matteo. 2018. "Impact of Uncoordinated Plug-in Electric Vehicle Charging on Residential Power Demand." *Nature Energy* 3 (3):193.

Musavi, Fariborz, Wilson Eberle, and William G Dunford. 2011. "A High-Performance Single-Phase Bridgeless Interleaved Pfc Converter for Plug-in Hybrid Electric Vehicle Battery Chargers." *IEEE Transactions on Industry Applications* 47 (4):1833-1843.

Musavi, Fariborz, Murray Edington, Wilson Eberle, and William G Dunford. 2012. "Evaluation and Efficiency Comparison of Front End Ac-Dc Plug-in Hybrid Charger Topologies." *IEEE Transactions on Smart Grid* 3 (1):413-421.

Nour, Morsy, Hassanien Ramadan, Abdelfatah Ali, and Csaba Farkas. 2018. "Impacts of Plug-in Electric Vehicles Charging on Low Voltage Distribution Network." 2018 International Conference on Innovative Trends in Computer Engineering (ITCE).

Omar, Noshin, Bavo Verbrugge, Grietus Mulder, Peter Van den Bossche, Joeri Van Mierlo, Mohamed Daowd, Miguel Dhaens, and Stijn Pauwels. 2010. "Evaluation of Performance Characteristics of Various Lithium-Ion Batteries for Use in Bev Application." 2010 IEEE Vehicle Power and Propulsion Conference.

Omar, Noshin, Bavo Verbrugge, Grietus Mulder, Peter Van den Bossche, Joeri Van Mierlo, Mohamed Daowd, Miguel Dhaens, and Stijn Pauwels. 2010. "Evaluation of Performance Characteristics of Various Lithium-Ion Batteries for Use in Bev Application." 2010 IEEE Vehicle Power and Propulsion Conference.

Piller, Sabine, Marion Perrin, and Andreas Jossen. 2001. "Methods for State-of-Charge Determination and Their Applications." *Journal of power sources* 96 (1):113-120.

Rahimi-Eichi, Habiballah, Unnati Ojha, Federico Baronti, and Mo-Yuen Chow. 2013. "Battery Management System: An Overview of Its Application in the Smart Grid and Electric Vehicles." *IEEE Industrial Electronics Magazine* 7 (2):4-16.

Ramadan, Hassanien, Abdelfatah Ali, and Csaba Farkas. 2018. "Assessment of Plug-in Electric Vehicles Charging Impacts on Residential Low Voltage Distribution Grid in Hungary." 2018 6th International Istanbul Smart Grids and Cities Congress and Fair (ICSG).

Samolyk, Mateusz, and Jakub Sobczak. 2013. Development of an Algorithm for Estimating Lead-Acid Battery State of Charge and State of Health.

Scott, William. 2015. "Impact of High Fidelity Battery Models for Vehicle Applications." University of Waterloo.

Seyed Ehsan, Samadani. 2015. "Modeling of Lithium-Ion Battery Performance and Thermal Behavior in Electrified Vehicles."

Shi, Chuan, Yichao Tang, and Alireza Khaligh. 2017. "A Single-Phase Integrated Onboard Battery Charger Using Propulsion System for Plug-in Electric Vehicles." *IEEE Transactions on Vehicular Technology* 66 (12):10899-10910.

Spanos, Constantine, Damon E Turney, and Vasilis Fthenakis. 2015. "Life-Cycle Analysis of Flow-Assisted Nickel Zinc-, Manganese Dioxide-, and Valve-Regulated Lead-Acid Batteries Designed for Demand-Charge Reduction." *Renewable and Sustainable Energy Reviews* 43:478-494.

Toepfer, C. 2009. "Sae Electric Vehicle Conductive Charge Coupler, Sae J1772." *Society of Automotive Engineers*.

Un-Noor, Fuad, Sanjeevikumar Padmanaban, Lucian Mihet-Popa, Mohammad Mollah, and Eklas Hossain. 2017. "A Comprehensive Study of Key Electric Vehicle (Ev) Components, Technologies, Challenges, Impacts, and Future Direction of Development." Energies 10 (8):1217.

Wan, Hongmei. 2012. "High Efficiency Dc-Dc Converter for Ev Battery Charger Using Hybrid Resonant and Pwm Technique." Virginia Tech.

Wang, Haiying, Yang Liu, Hang Fu, and Gechen Li. 2013. "Estimation of State of Charge of Batteries for Electric Vehicles." *International Journal of Control and Automation* 6 (2):185-194.

Wu, Qiuwei, Lin Cheng, Ulysse Pineau, Arne Hejde Nielsen, and Jacob Østergaard. 2013. "Impact and Cost Evaluation of Electric Vehicle Integration on Medium Voltage Distribution Networks." 2013 IEEE PES Asia-Pacific Power and Energy Engineering Conference (APPEEC).

Xing, Yinjiao, Eden WM Ma, Kwok L Tsui, and Michael Pecht. 2011. "Battery Management Systems in Electric and Hybrid Vehicles." *Energies* 4 (11):1840-1857.

Xiong, Rui, Fengchun Sun, Zheng Chen, and Hongwen He. 2014. "A Data-Driven Multi-Scale Extended Kalman Filtering Based Parameter and State Estimation Approach of Lithium-Ion Olymer Battery in Electric Vehicles." *Applied Energy* 113:463-476.

Xiong, Rui, Fengchun Sun, Xianzhi Gong, and Hongwen He. 2013. "Adaptive State of Charge Estimator for Lithium-Ion Cells Series Battery Pack in Electric Vehicles." *Journal of power sources* 242:699-713.

Xiong, Rui, Jinpeng Tian, Hao Mu, and Chun Wang. 2017. "A Systematic Model-Based Degradation Behavior Recognition and Health Monitoring Method for Lithium-Ion Batteries." *Applied energy* 207:372-383.

Xiong, Rui, Jinpeng Tian, Hao Mu, and Chun Wang. 2017. "A Systematic Model-Based Degradation Behavior Recognition and Health Monitoring Method for Lithium-Ion Batteries." *Applied energy* 207:372-383.

Xu, Yijun, Yunshan Xu, Zimin Chen, Fei Peng, and Mohammed Beshir. 2014. "Harmonic Analysis of Electric Vehicle Loadings on Distribution System." 2014 IEEE International Conference on Control Science and Systems Engineering.

Yilmaz, Murat, and Philip T Krein. 2013. "Review of Battery Charger Topologies, Charging Power Levels, and Infrastructure for Plug-in Electric and Hybrid Vehicles." *IEEE transactions on Power Electronics* 28 (5):2151-2169.

Yu, Quanqing, Rui Xiong, Cheng Lin, Weixiang Shen, and Junjun Deng. 2017. "Lithium-Ion Battery Parameters and State-of-Charge Joint Estimation Based on H-Infinity and Unscented Kalman Filters." *IEEE Transactions on Vehicular Technology* 66 (10):8693-8701.

Zhao, Chen, He Yin, and Chengbin Ma. 2016. "Quantitative Evaluation of Lifepo $ _4 $ Battery Cycle Life Improvement Using Ultracapacitors." *IEEE Transactions on Power Electronics* 31 (6):3989-3993.

Zhao, Chen, He Yin, and Chengbin Ma. 2016. "Quantitative Evaluation of Lifepo $ _4 $ Battery Cycle Life Improvement Using Ultracapacitors." *IEEE Transactions on Power Electronics* 31 (6):3989-3993.

Zhou, Guangmin, Feng Li, and Hui-Ming Cheng. 2014. "Progress in Flexible Lithium Batteries and Future Prospects." *Energy & Environmental Science* 7 (4):1307-1338.

Zhou, Guangmin, Feng Li, and Hui-Ming Cheng. 2014. "Progress in Flexible Lithium Batteries and Future Prospects." *Energy & Environmental Science* 7 (4):1307-1338.

Zhu, Ying, Wenhua H Zhu, Zenda Davis, and Bruce J Tatarchuk. 2016. "Simulation of Ni-Mh Batteries Via an Equivalent Circuit Model for Energy Storage Applications." *Advances in Physical Chemistry* 2016.

APPENDIX I – GIS DATA FOR SAN JUAN 12 KV FEEDERS

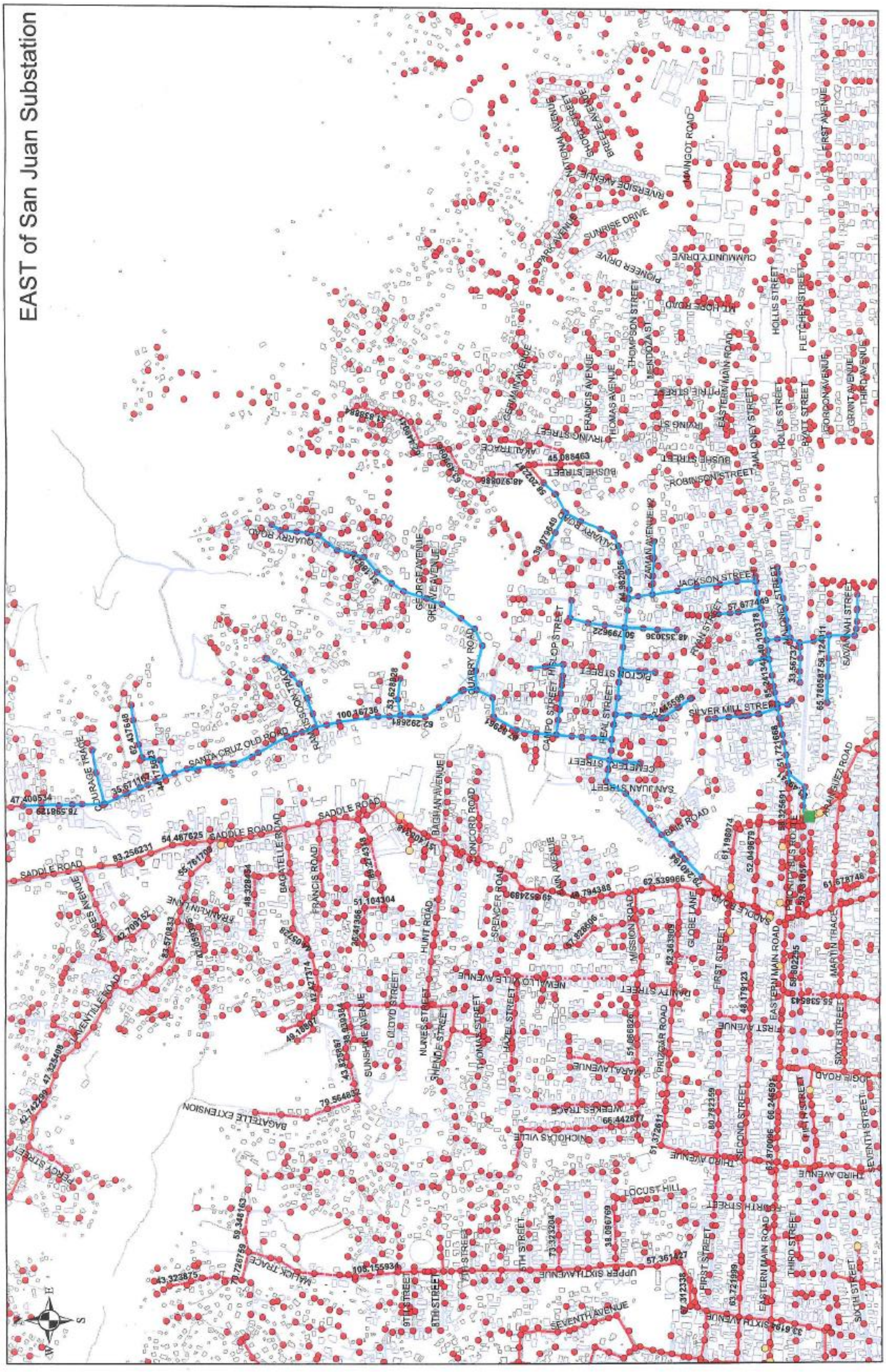

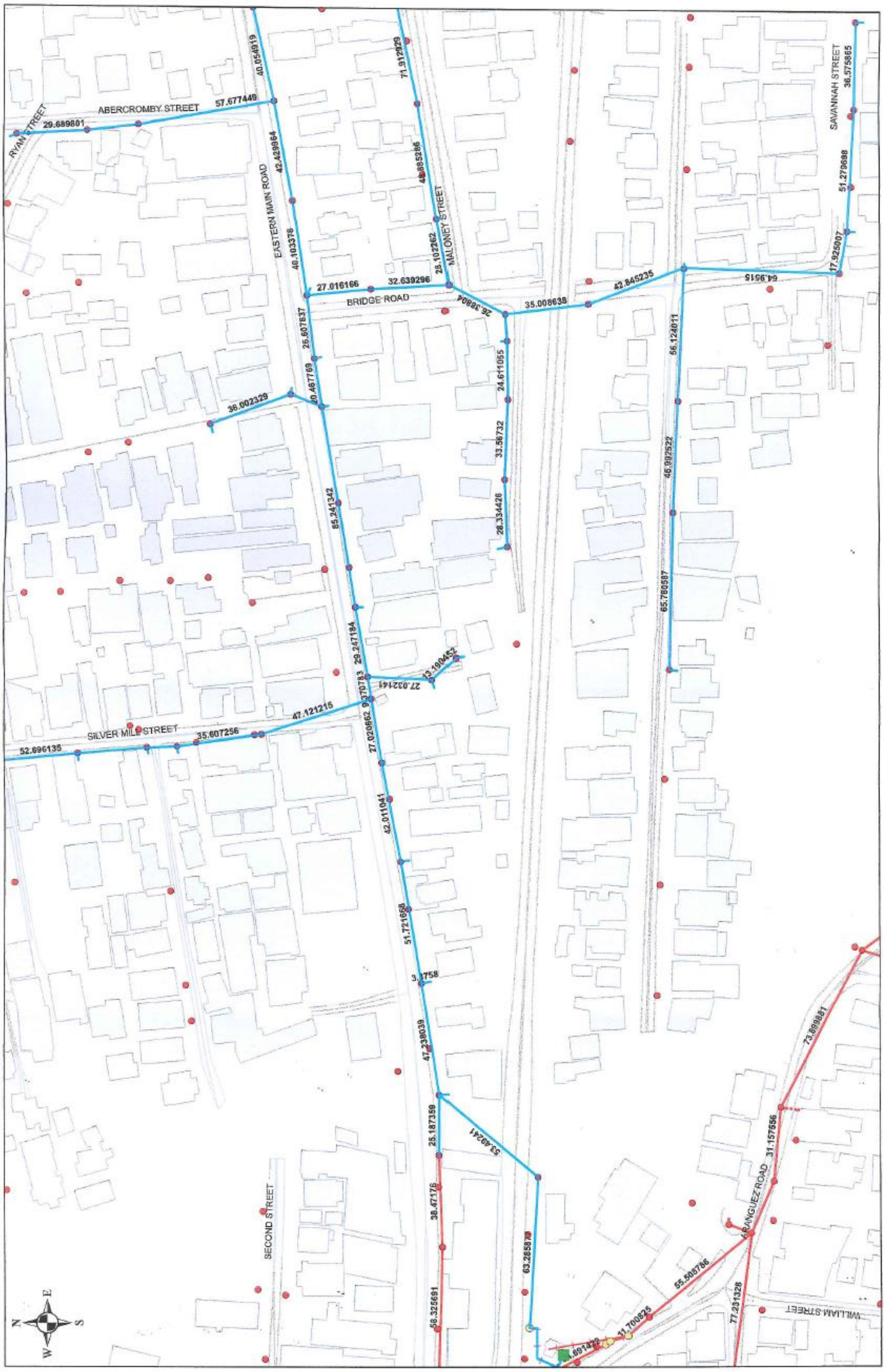
ABERCROMBY STREET
RYAN STREET
EASTERN MAIN ROAD
MALONEY STREET
BRIDGE ROAD
SILVER MILL STREET
SAVANNAH STREET
SECOND STREET
WILLIAM STREET
29.689801
57.677449
40.054919
71.912929
42.429964
40.103378
48.885286
28.102262
27.016166
32.639296
35.008638
42.845235
26.607837
24.611055
56.124011
36.002329
20.467769
33.56732
46.992522
85.241342
28.334426
65.780587
29.247184
13.190452
27.032141
47.121215
35.607256
52.696135
27.020662
42.011041
51.721668
47.238039
25.187359
38.47176
63.265879
55.508786
31.157556
73.899881
77.231328
11.700825
58.325691
51.279698
17.925007
36.575865
N
E
S
W


BUSHE STREET
EASTERN MAIN ROAD
ROBINSON STREET
MALONEY STREET
BROOME STREET
JACKSON STREET
ABERCROMBY STREET
RYAN STREET
BRIDGE ROAD
SAVANNAH STREET
13.412306
47.239817
35.459618
29.631822
11.912929
40.054919
57.677449
29.689801
42.429964
40.103378
28.102262
27.016166
32.639296
35.008638
42.845235
17.925007
51.279898
36.575865
26.607837
36.002329
85.241342
24.611055
33.58732
56.124011
46.992522
N
E
S
W

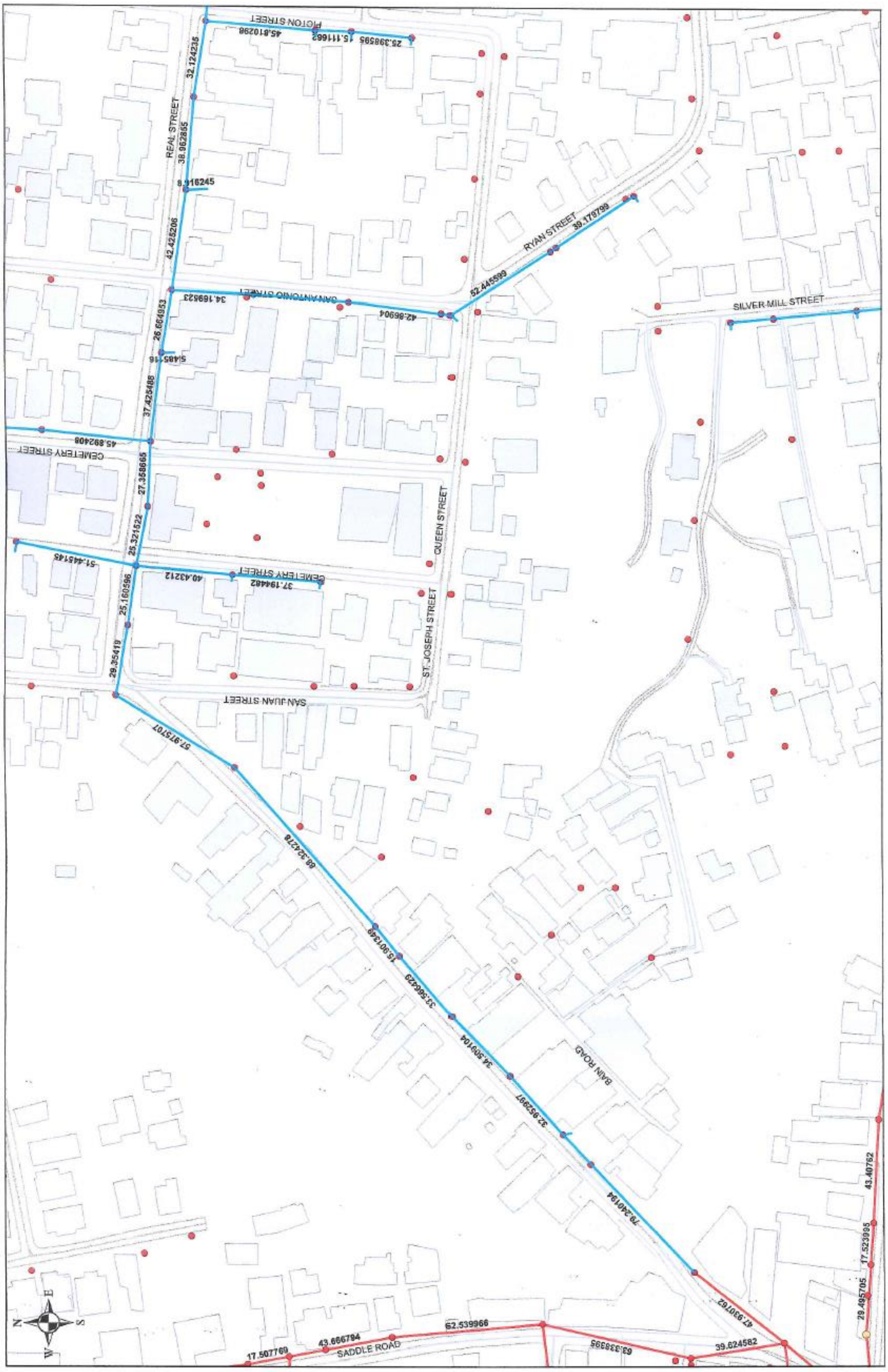
PICTON STREET
REAL STREET
SAN ANTONIO STREET
RYAN STREET
SILVER MILL STREET
CEMETERY STREET
QUEEN STREET
ST. JOSEPH STREET
SAN JUAN STREET
BAIN ROAD
SADDLE ROAD
N
E
S
W

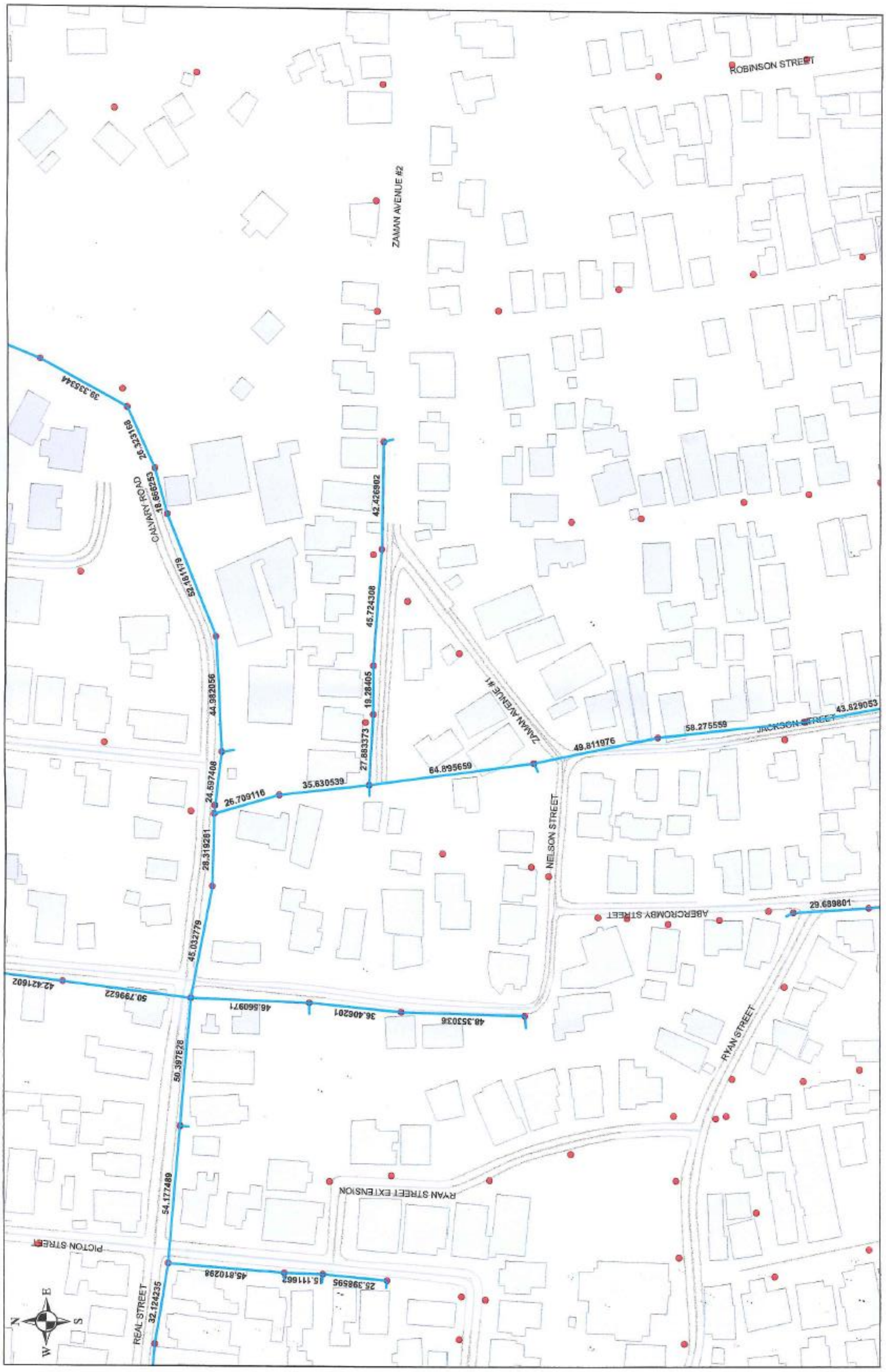

ROBINSON STREET
ZAMAN AVENUE #2
CALVARY ROAD
ZAMAN AVENUE #1
JACKSON STREET
NELSON STREET
ABERCROMBY STREET
RYAN STREET
RYAN STREET EXTENSION
PICTON STREET
REAL STREET

SUMMIT DRIVE
CALVARY ROAD
CAMPO STREET
HISLOP STREET
PICTON STREET

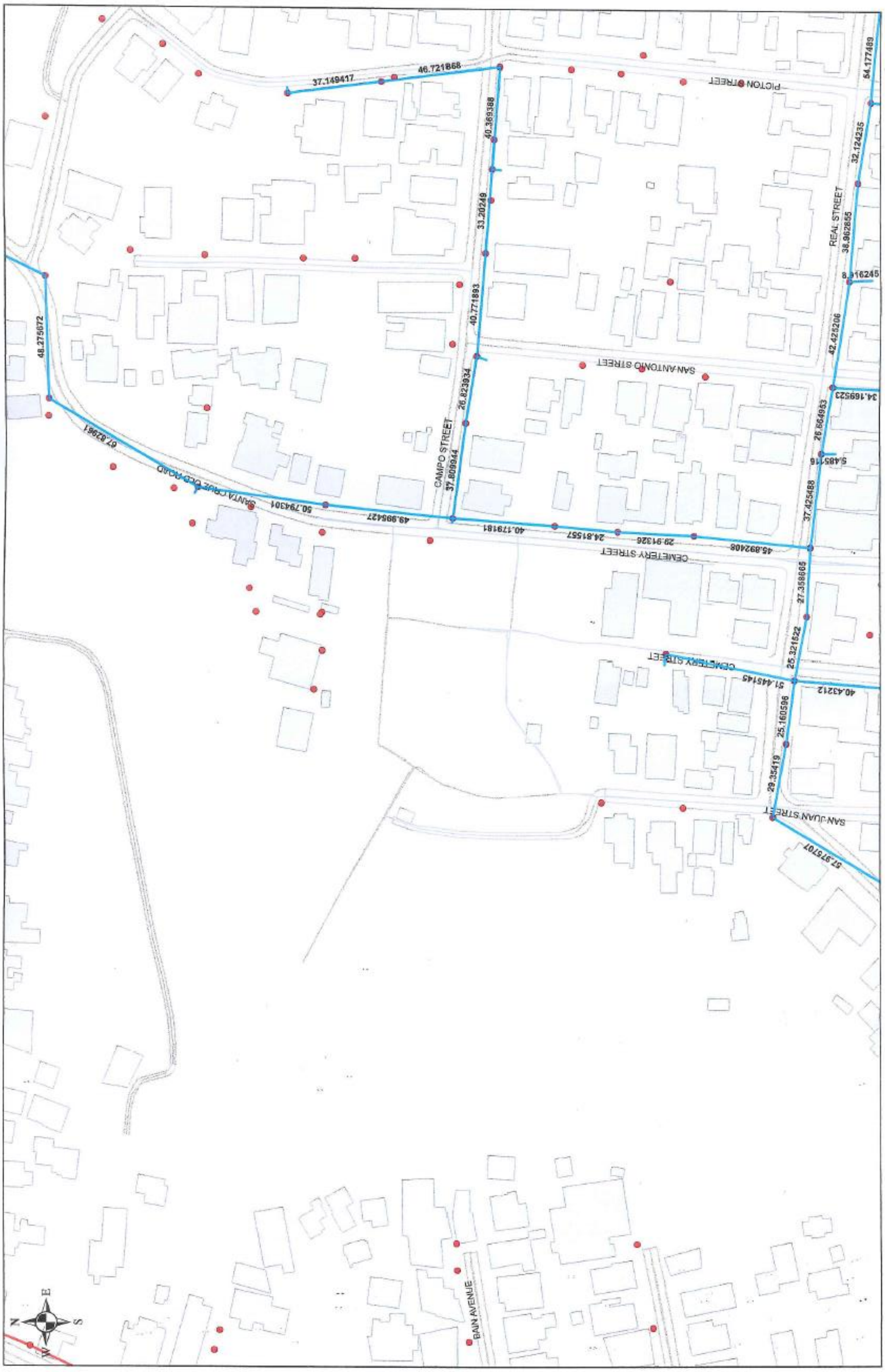
PICTON STREET
REAL STREET
CAMPO STREET
SAN-ANTONIO STREET
SANTA CRUZ OLD ROAD
CEMETERY STREET
SAN-JUAN STREET
BAIN AVENUE

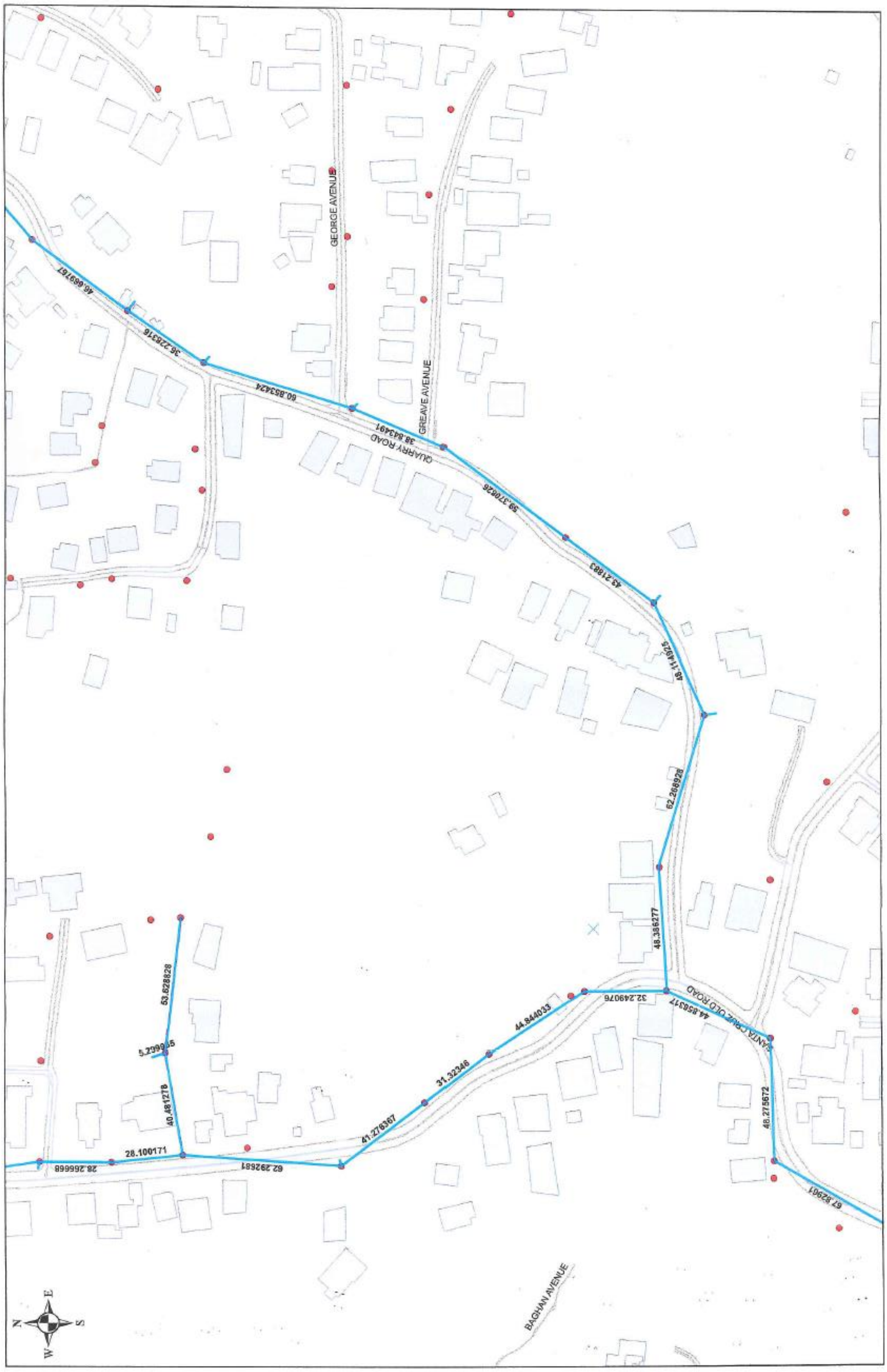
GEORGE AVENUE
GREAVE AVENUE
QUARRY ROAD
SANTA CRUZ OLD ROAD
BAGHAN AVENUE
46.669767
36.225316
60.853424
38.843491
59.370626
43.21883
48.114925
62.268926
48.386277
32.249076
44.844033
31.32346
41.276367
62.292681
28.100171
28.266668
40.481278
5.299955
53.628828
44.856517
48.275672
67.82961
N
E
S
W

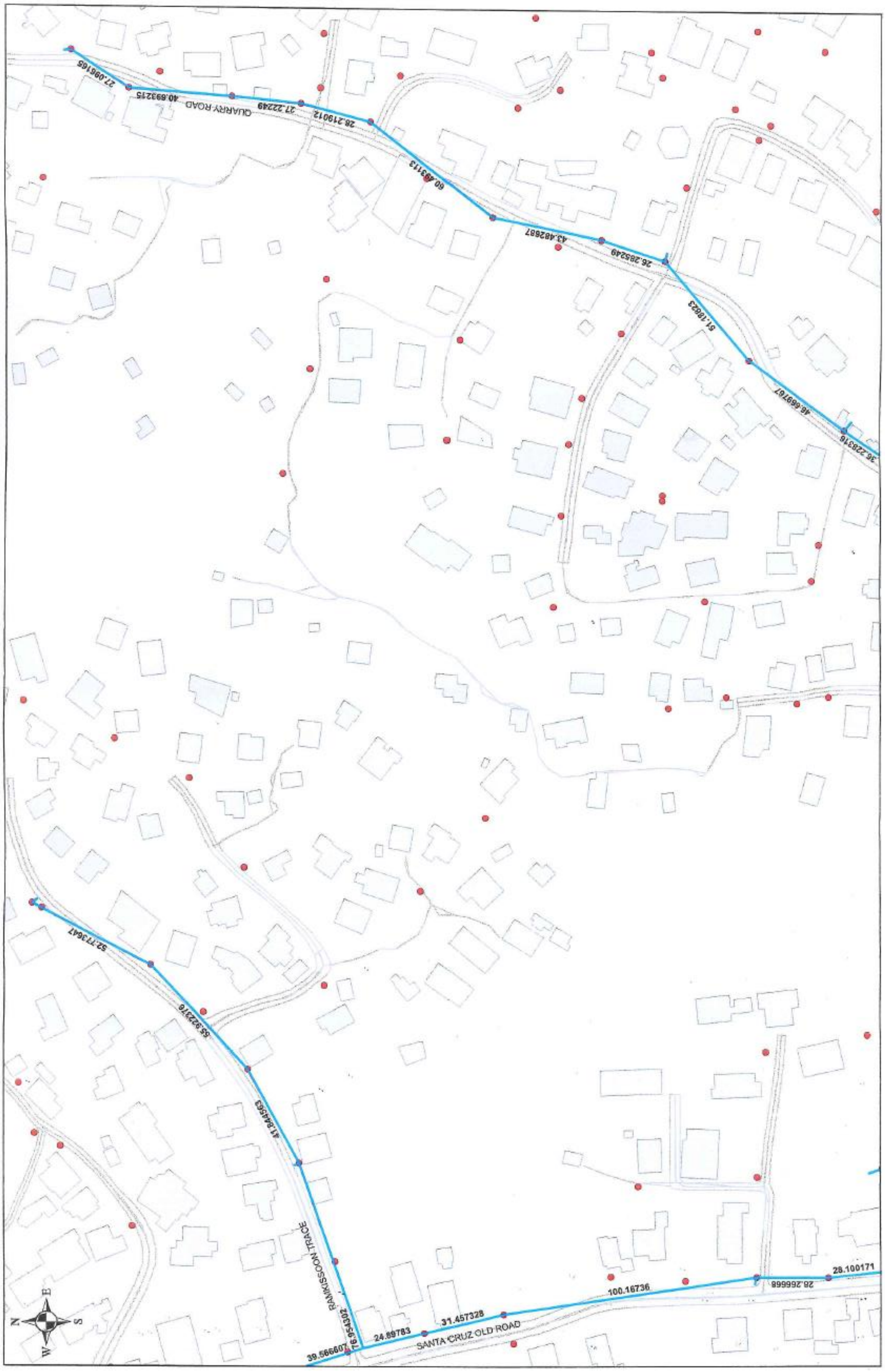

27.096165
40.693215
QUARRY ROAD
27.22249
28.219012
60.493113
43.482687
26.285249
51.18623
46.669767
36.228316
52.773647
55.922376
41.844563
RAMKISSOON TRACE
76.954302
39.566607
24.89783
31.457328
SANTA CRUZ OLD ROAD
100.16736
28.266668
28.100171
N
E
S
W

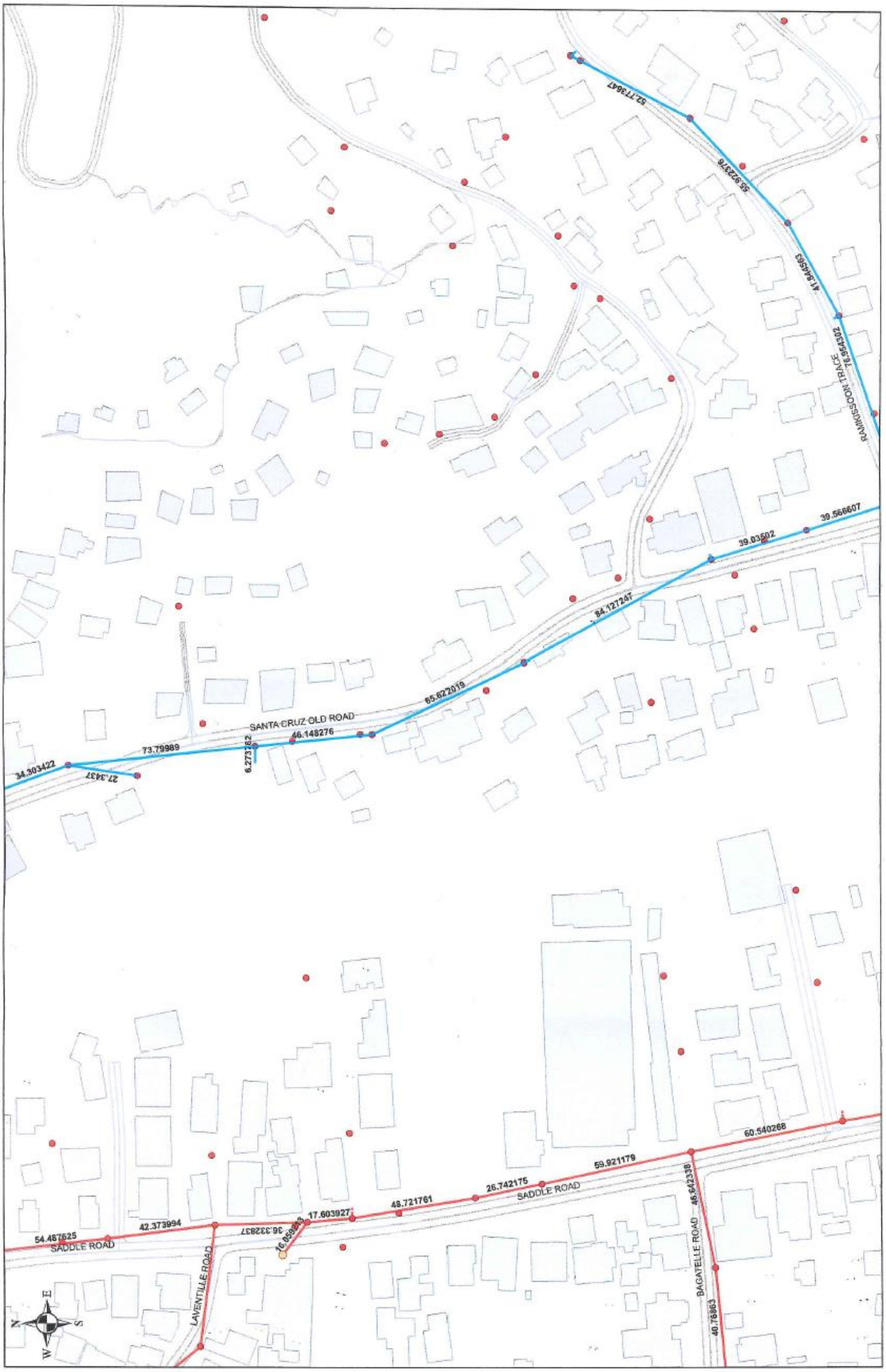

52.773647
55.923276
41.845563
76.9554302
RAMKISSOON TRACE
39.566607
39.03502
84.127247
65.622019
SANTA CRUZ OLD ROAD
46.148276
6.273282
73.79989
34.303422
27.3437
60.540268
59.921179
26.742175
SADDLE ROAD
48.721761
17.603927
36.332837
42.373994
54.487625
SADDLE ROAD
46.642338
BAGATELLE ROAD
LAVENTILLE ROAD
40.76863
N
E
S
W

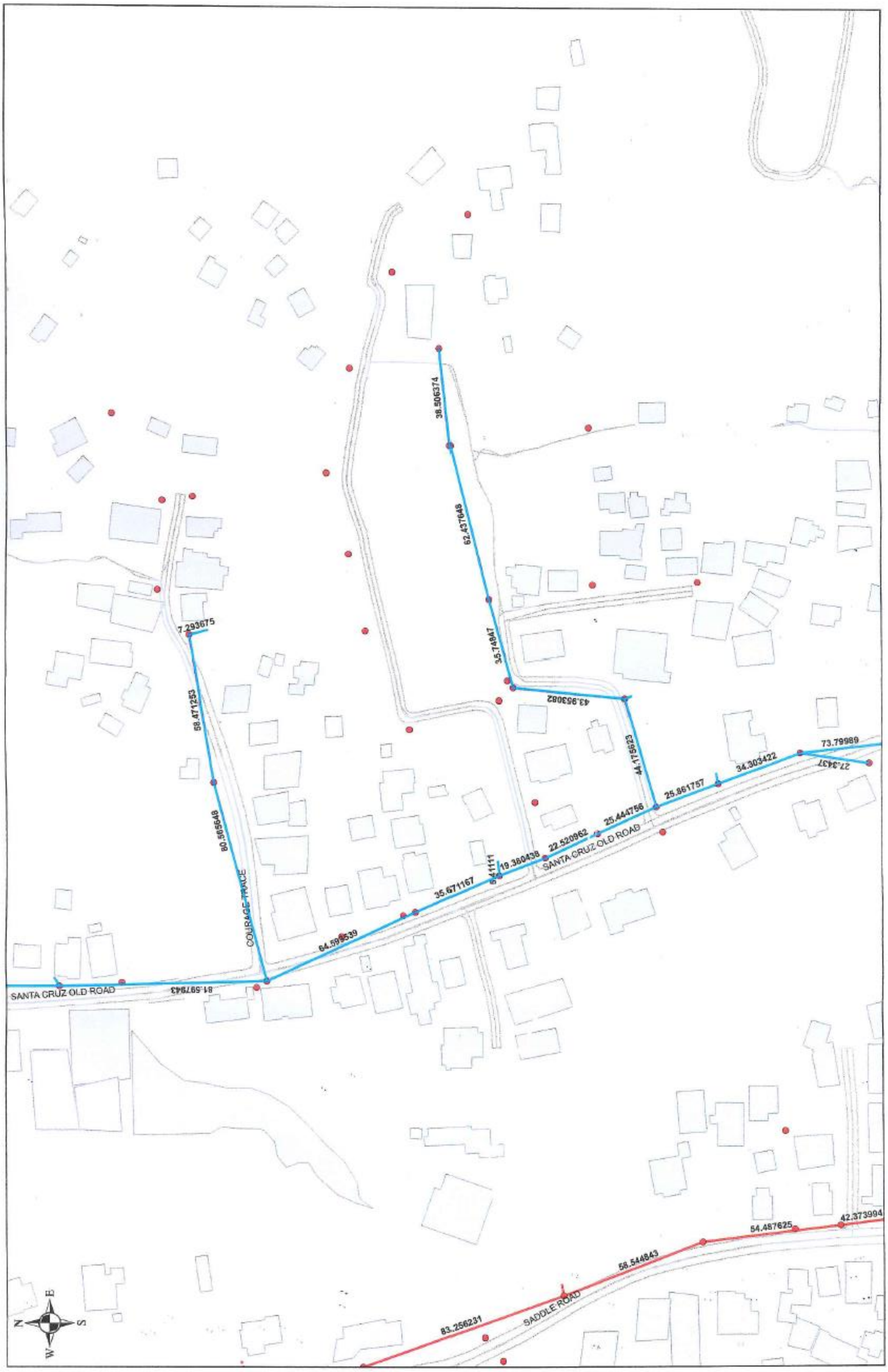

38.506374
62.437648
35.74847
43.953082
44.175623
7.293675
58.471253
80.565648
COURAGE TRACE
35.671167
19.380438
22.520962
25.444756
25.861757
34.303422
73.79989
27.3437
SANTA CRUZ OLD ROAD
SANTA CRUZ OLD ROAD
81.597643
54.487625
42.373994
58.544843
83.256231
SADDLE ROAD
N
E
S
W

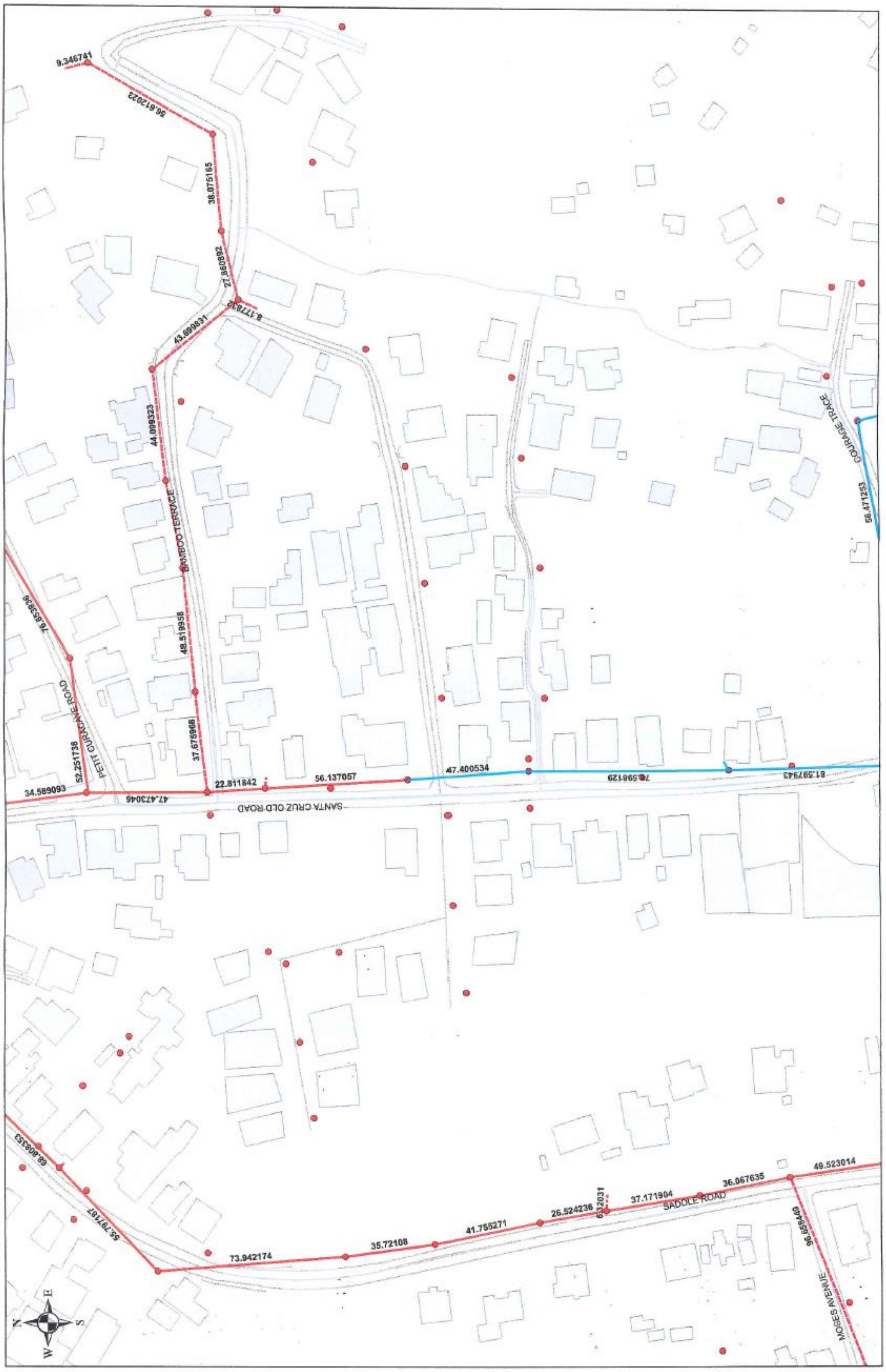
9.346741
56.612022
38.075165
27.860892
8.177832
43.699831
44.099323
BAMBOO TERRACE
49.519958
37.675968
PETIT CURUCAYE ROAD
52.251738
34.589093
47.473046
22.811842
56.137057
47.400534
81.597943
SANTA CRUZ OLD ROAD
COURAGE TRACE
58.471253
49.523014
36.067635
37.171904
SADDLE ROAD
26.524236
41.755271
35.72108
73.942174
96.658449
MOSES AVENUE
N
E
S
W

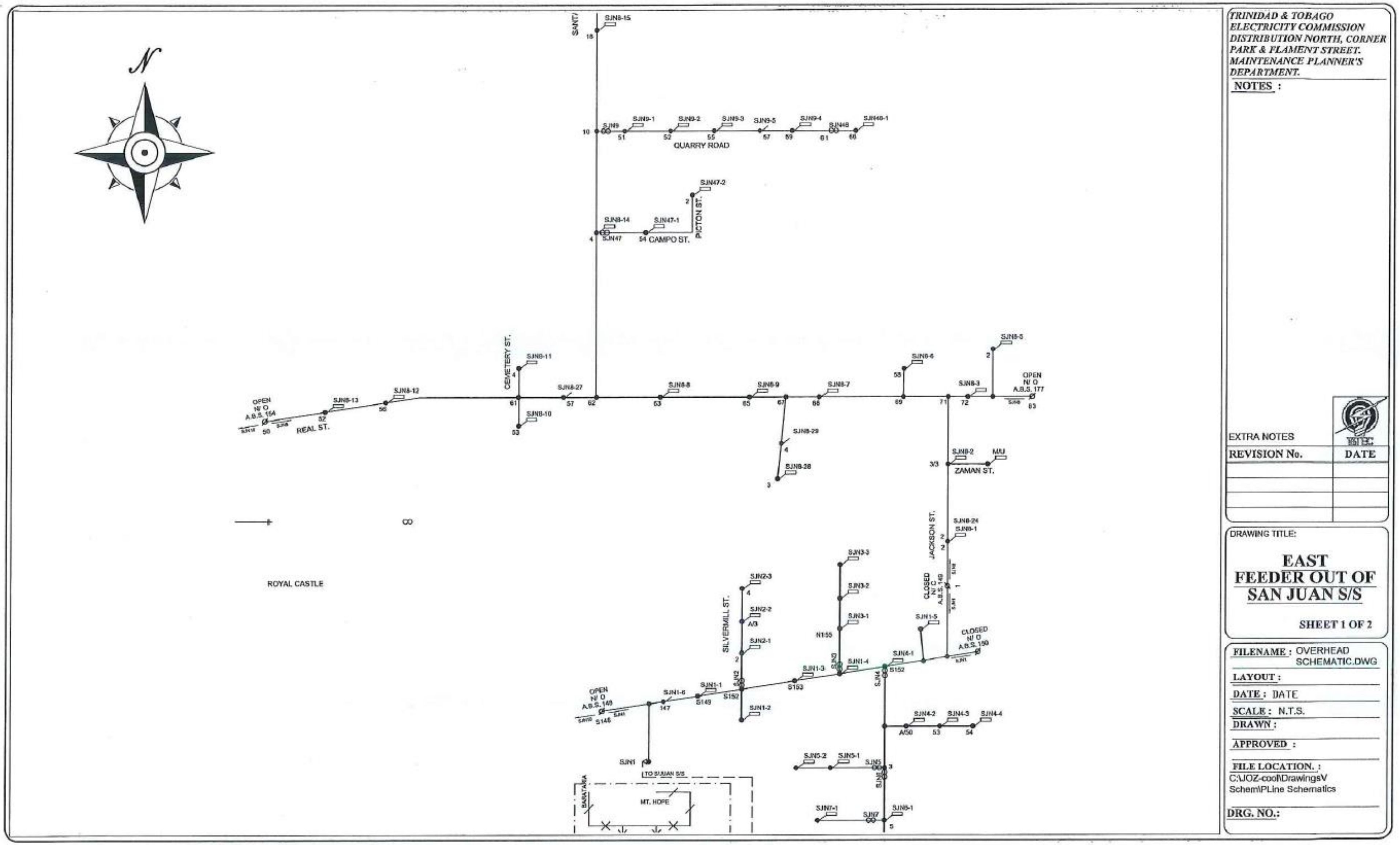
TRINIDAD & TOBAGO ELECTRICITY COMMISSION DISTRIBUTION NORTH, CORNER PARK & FLAMENT STREET. MAINTENANCE PLANNER'S DEPARTMENT.
NOTES :
EXTRA NOTES
REVISION No.
DATE
DRAWING TITLE:
EAST FEEDER OUT OF SAN JUAN S/S
SHEET 1 OF 2
FILENAME : OVERHEAD SCHEMATIC.DWG
LAYOUT :
DATE : DATE
SCALE : N.T.S.
DRAWN :
APPROVED :
FILE LOCATION. : C:\JOZ-cool\DrawingsV Schem\PLine Schematics
DRG. NO.:
QUARRY ROAD
PICTON ST.
CAMPO ST.
CEMETERY ST.
REAL ST.
ZAMAN ST.
JACKSON ST.
SILVERMILL ST.
MT. HOPE
BARATARIA
ROYAL CASTLE

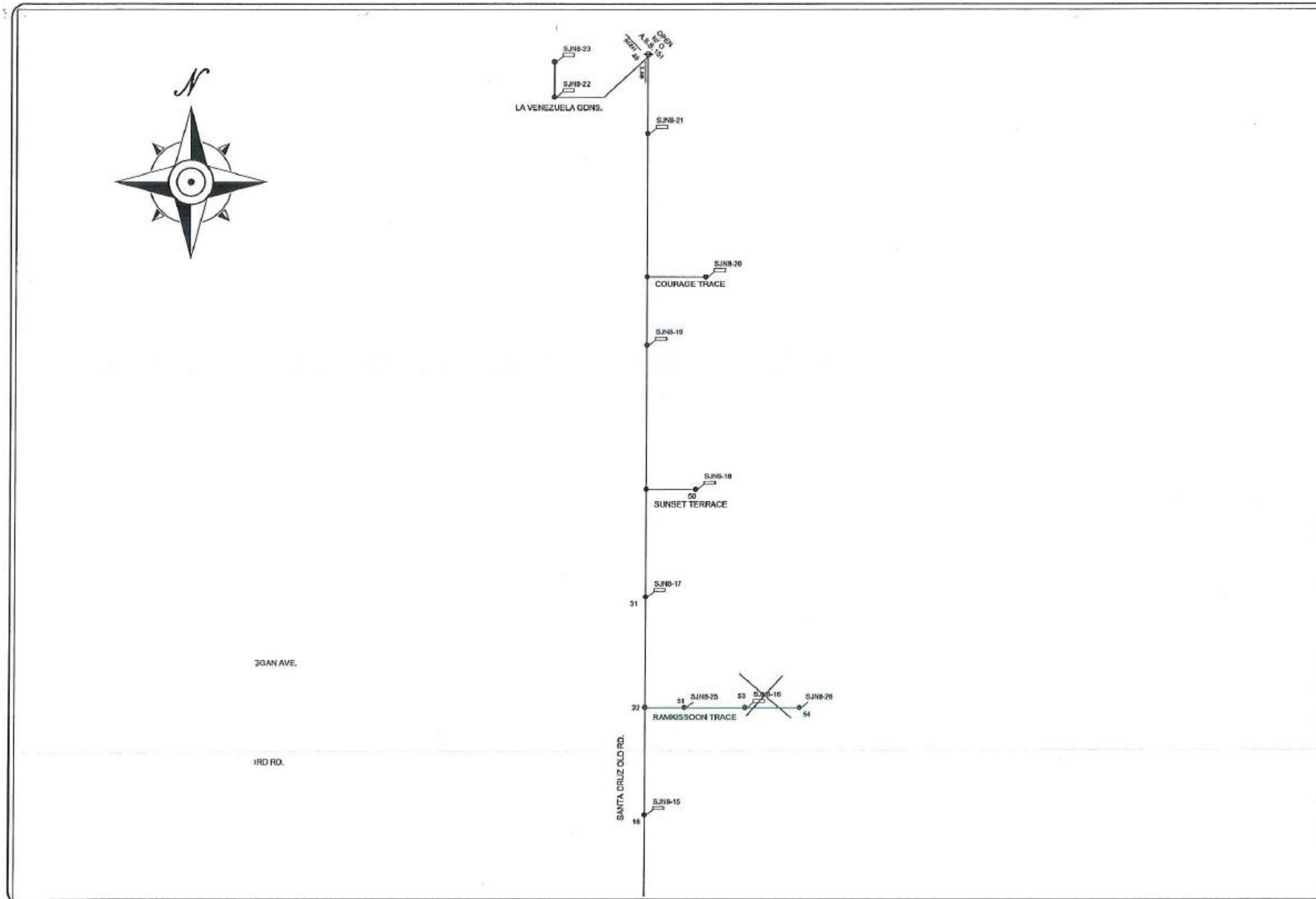

TRINIDAD & TOBAGO ELECTRICITY COMMISSION
DISTRIBUTION NORTH, CORNER PARK & FLAMENT STREET.
MAINTENANCE PLANNER'S DEPARTMENT.

NOTES :

EXTRA NOTES

REVISION No.	DATE

DRAWING TITLE:

EAST FEEDER OUT OF SAN JUAN S/S

SHEET 2 OF 2

FILENAME : OVERHEAD SCHEMATIC.DWG

LAYOUT :

DATE : DATE

SCALE : N.T.S.

DRAWN :

APPROVED :

FILE LOCATION. : C:\JOZ-cool\Drawings\ Schem\PLine Schematics

DRG. NO.: